Modified Spiegler-Kedem Model to Predict the Rejection and Flux of Nanofiltration Processes at High NaCl Concentrations

by

Farah Naz Ahmed

A thesis submitted to the Faculty of Graduate and Post-Doctoral Studies in partial fulfillment of the requirements for the degree of

Masters of Applied Science

Department of Civil Engineering

University of Ottawa

EVG 7999

November 2013

ABSTRACT

Current nanofiltration (NF) models are based on the "diluted solution" assumption and cannot successfully predict permeate fluxes at high salt concentrations. The reasons behind the strong differences between the predicted and observed fluxes are still not fully understood. In this work, it is proposed that these deviations are possibly caused by the electrical charges inside the membrane pores. At a nanoscale level, the complex electrostatic interactions between the highly confined charged solutes and the charges inside membrane pores contribute to flow retardation and this phenomena can be characterized using an additional resistance factor, which is defined as the electric resistance factor in this study. To this extent, experiments were carried out with aqueous sodium chloride (NaCl) solutions in a wide range of concentrations (0.05 – 1.96 M) using two commercial membranes (NF270 and Desal-5 DL). Salt retention was fitted and analysed by means of the classical Spiegler-Kedem model (SK). The model has been modified to include the proposed empirical electric resistance factor, R_{elec}, to account for this additional hydrodynamic flow resistance. The modified Spiegler-Kedem model (MSK) was verified by fitting experimental data at relatively low salt concentration to obtain model parameters and then comparing the model prediction with experimental data at higher concentrations. A mathematical equation was developed to describe the dependence of an important model parameter, reflection coefficient (σ), on operational conditions such as pressure and bulk salt concentration. The thesis also discussed the mechanisms of NF separation, highlighting the electrostatic interaction between the co-ions and the membrane charges in the confined nano-environment inside the NF membrane pores.

RÉSUMÉ

Les modèles actuels de nanofiltration (NF) sont basés sur l'hypothèse de la "solution diluée" et ne peuvent pas prédire avec succès l'écoulement d'une solution à haute teneur en sel. Les raisons derrière les importantes différences entre les prévisions et les flux observées ne sont pas encore complètement élucider. Dans ce travail, il est proposé que ces divisions sont causées par les charges électriques dans les pores de la membrane. À une échelle nanométrique, la complexité des interactions électrostatiques, due à la proximité des charges dans les solutés et les charges à l'intérieur des pores de la membrane, contribuent au retard de débit. Dans cette étude, ce phénomène est caractérisé en utilisant le facteur de résistance électrique. Dans cette mesure, des expériences ont été menées avec des solutions aqueuses de chlorure de sodium (NaCl) dans une large gamme de concentrations (0,05 - 1,96 M) à l'aide de deux membranes commerciales (NF270 et Desal-5 DL). La rétention de sel a été adaptée et analysée à l'aide du modèle classique de Spiegler-Kedem (SK). Ce modèle a été modifié pour inclure le facteur empirique de résistance électrique, R_{elec}, afin de tenir compte de cette résistance hydrodynamique supplémentaire au débit. La modification du modèle Spiegler-Kedem (MSK) a été vérifiée par la comparaison de données expérimentales de solution aqueuse à faible concentration de sel pour obtenir les paramètres du modèle, puis en comparant ce modèle de prédiction avec des données expérimentales à des concentrations élevées. Une équation mathématique a été développée pour décrire la dépendance vis-à-vis d'un paramètre important du modèle, le coefficient de réflexion (σ), sur les conditions de fonctionnement, telles que la pression et la concentration élevée de sel. La thèse discute également des mécanismes de séparation par NF et met en évidence les interactions électrostatiques entre les co-ions et les charges de la membrane confinés dans le nano-environnement à l'intérieur des pores de la membrane de NF.

ACKNOWLEDGEMENTS

My heartfelt thanks to my supervisor, Dr. Christopher Lan, for providing me the opportunity to work with nanofiltration membranes. Thank you for your time, guidance, and continuous support during this research project.

I would like to thank Dr. Dipak Rana for his scientific input and valuable discussions. Without his expertise in membranes, this thesis would not have been possible.

Technical support provided by Louis Tremblay and Franco Ziroldo is also greatly appreciated.

Many thanks also go to Jiannan Liu, Jeffrey Chen, and Shuaibo Yu for their assistance in the lab.

I gratefully acknowledge financial support for this project from Natural Sciences and Engineering Research Council of Canada (NSERC).

Special thanks go to my new husband who has been extremely supportive and encouraging during the chaotic latter days of this work.

To my parents and my brother and sister, thank you so much for your love and endless support. To my mother and father, I dedicate this work: thank you so much for everything.

TABLE OF CONTENTS

LIST OF FIGURES

LIST OF TABLES

ABBREVIATIONS

AFM	Atomic Force Microscopy
BOD	Biochemical Oxygen Demand
CFD	Computational Fluid Dynamics
CFSK	Combined Film theory/Spiegler Kedem
COD	Chemical Oxygen Demand
CP	Concentration Polarization
CPP	Compressed Phase Precipitation
DBP	Disinfection By-Products
DSPM	Donnan-Steric Pore Model
DSPM & DE	Donnan Steric Pore Model & Dielectric Exclusion
EDC	Endocrine Disrupting
EDL	Electrical Double Layer
ENP	Extended Nernst-Planck
EP	Electro-polymerization
ES	Electrostatic and Steric-hindrance
HAA	Haloacetic Acids
IEP	Isoelectric Point
IP	Interfacial Polymerization
IT	Irreversible Thermodynamics
LPP	Liquid Phase Precipitation
MBR	Membrane Bioreactor
MF	Microfiltration
MSF	Multistage Flash
MSK	Modified Spiegler-Kedem
MWCO	Molecular Weight Cut Off
NF	Nanofiltration
NOM	Natural Organic Matter
OSN	Organic Solvent Nanofiltration
PF	Pore-Flow
PPCP	Pharmaceuticals and Personal Care Products
PVDF	Polyvinylidene Fluoride
PWP	Pure Water Permeability
RO	Reverse Osmosis
SC	Space-Charge
SD	Solution-Diffusion
SEDE	Steric, Electric, Dielectric Exclusion
SHP	Steric-hindrance Pore
SK	Spiegler-Kedem
SMP	Soluble Microbial Product
SWCC	Saline Water Conversion Corporation
SWRO	Seawater Reverse Osmosis
TDS	Total Dissolved Solids
TFC	Thin Film Composite
TMS	Teorell-Meyer-Sievers

UF	Ultrafiltration

NOMENCLATURE

A	ratio of $1-\sigma$ and P_s
A_m	membrane area (m^2)
C_b	bulk/feed solute concentration (M)
C_m	solute concentration at feed-membrane interface (M)
C_p	permeate solute concentration (M)
D	diffusion coefficient ($m^2\ h^{-1}$)
F	flow parameter
F_w, F_s	generalized forces
J_s	solute flux (mol $m^{-2}\ h^{-1}$)
J_{sol}	solution flux (L $m^{-2}\ h^{-1}$)
J_v	volumetric flux of permeate solution (L $m^{-2}\ h^{-1}$)
J_w	pure water flux (L $m^{-2}\ h^{-1}$)
k	mass transfer coefficient (L $m^{-2}\ h^{-1}$)
L_{ij}	phenomenological coefficients
L_p	membrane hydraulic permeability (L $m^{-2}\ h^{-1}\ bar^{-1}$)
$L_{p,w}$	pure water permeability of membrane (L $m^{-2}\ h^{-1}\ bar^{-1}$, $m^3\ m^{-2}\ s^{-1}\ kPa^{-1}$)
P_s	solute permeability (L $m^{-2}\ h^{-1}$)
R	intrinsic rejection (%)
R_{elec}	hydraulic resistance correction factor due to electrostatic interactions
R_g	universal gas constant (0.083145 L bar $K^{-1}\ mol^{-1}$)
R_m	intrinsic membrane resistance (m^{-1})
R_{obs}	observed solute rejection (%)
r_p	effective pore radius (nm)
T	absolute temperature (K)
t	time of permeate sample collection (s)
v	dimensionless Van't Hoff factor
V_p	volume of the permeate (mL)
X_d	effective membrane charge density (M, mol m^{-3})
ΔP	applied pressure difference (psi, bar, kPa)
ΔP_e	effective pressure driving force ($\Delta P - \Delta\pi$) (psi, bar, kPa)
Δx	effective membrane thickness (μm)
$\Delta x/A_k$	effective thickness over porosity (μm)

Greek letters

δ	thickness of CP layer (mm)
$\Delta\pi$	osmotic pressure differences (psi, bar)
λ	Debye length (nm)
μ	solvent viscosity (cP, Pa·s)
μ_s	viscosity of water (cP, Pa·s)
μ_w	viscosity of salt solution (cP, Pa·s)
ξ	normalized charge density

σ	reflection coefficient
χ	volumetric charge density (M)

Chapter 1: Introduction

Nanofiltration (NF) membranes are playing an increasingly important role in many separation and purification applications such as seawater and brackish water desalination [1-3], industrial wastewater treatment [4-6], and food and pharmaceutical industries [7-9]. These pressure-driven membranes can reject ions that are much smaller than the membrane pores, owing to the presence of fixed charges on the membrane surface. NF membranes also allow higher fluxes and operation at lower pressures than reverse osmosis (RO) membranes [10], which functions solely on size exclusion mechanism, thereby providing much-needed cost-reduction and energy-saving benefits. Furthermore, NF membranes can selectively reject multivalent electrolytes based on their much larger electrostatic interaction with membrane charges in comparison to monovalent electrolytes, finding them important applications such as desulfation in chlor-alkali industry [11-12].

It is crucial to develop practical and reliable models to better predict the flux and rejection of a membrane process in order to optimize their performance and scale up laboratory and pilot-scale results. However, research efforts have shown that modelling NF performance is made complicated by the interaction between the electric charges on ions and membranes. Today, it is believed that ion exclusion in NF processes is governed by three main effects: steric, Donnan, and dielectric [13]. The relevant contribution of each mechanism depends on several factors, namely, ion size and charge, solution concentration and pH, and membrane characteristics.

Currently, the predominant mechanistic approaches to NF modelling use the extended Nernst-Planck (ENP) equation, which incorporates contributions from diffusion, convection, and electrical migration, to model ion transport across the membrane. The Donnan-Steric

Pore model (DSPM) and the Steric, Electric and Dielectric Exclusion (SEDE) model are examples of the approaches based on the ENP equation. These models have been shown to be reasonably successful in predicting ion retentions in dilute solutions of both single and multi-ionic solutions [14-17]. However, they have failed to a great extent in predicting the performance of NF at high salt concentrations. This is because these models were developed using a "diluted solution" assumption.

It goes without saying that these numerous theoretical studies dealing with the matter of solute transport mechanisms [14-19] provide an in-depth insight into the complex ion exclusion phenomena in NF membranes, thereby increasingly advancing our comprehension of the underlying thermodynamics. However, the mathematical complexity of these models coupled with our insufficient knowledge of the complex phenomena involving ion and membrane interaction as well as of membrane morphology and characteristics mean that complete predictive calculations are unlikely in the near future [13]. The aforementioned models can be termed semi-predictive at best.

Traditionally, the primary objective of these models has been to predict the solute retention while permeate flux prediction has been largely overlooked. This practice is quite acceptable when dealing with low concentration solutions, where osmotic pressure effects can be considered negligible and permeate fluxes do not deviate significantly from those of pure water. However, many applications of NF such as desalination of seawater and desulfation in chlor-alkali industry require the treatment of brine with very high salt concentration and neglecting the effects of the large osmotic pressure of the brine on permeate fluxes is not an option. Numerous attempts have been made to apply different variants of these models through which researchers have noted the limitations of these

current models when dealing with high salt feed concentrations, especially in permeate flux prediction [1,20,21].

Classic Hagen-Poiseuille-type relationships, commonly used for aqueous systems permeation through porous media, are also utilized for description of permeate flux in NF processes [15,20]. In the case of NF of aqueous solutions, these studies demonstrated a considerable overestimation of the permeate fluxes. It has been observed that this deviation between the predicted and observed fluxes cannot be attributed solely to driving force reduction as a result of osmotic pressure.

Several explanations for the flux reduction with increased salt concentration, which is not accounted for by the current models, have been proposed in the literature. Rodrigues et al. [20] showed that the use of the pure water permeability and hence, pure water viscosity, contributed to these deviations. Incorporation of the feed solution viscosity greatly improved the flux predictions [20]. Freger et al. [21] suggested membrane swelling to be a possible cause while other researchers proposed that inaccurate determination of the concentration polarization phenomena to be an important factor [1,22]. However, the reasons behind the strong differences between the predicted and observed fluxes are still not fully understood.

Researchers have so far failed to establish models that can predict both rejection and flux of NF processes dealing with highly concentrated electrolyte solutions. This is somewhat ironic since some of the most important NF applications including processes such as seawater desalination and chlor-alkali desulfination, deal with brines where feed ionic concentrations are very high (0.5 M or above). Evidently, it is advantageous to have a predictive model capable of estimating the permeate flux for high feed concentrations, especially at the early stages of process design [23]. Therefore, given the industrial importance of the current and potential applications, the extension of NF theory to highly

concentrated brines are now considered to be major open problems in this on-going field of research and development [24].

In this study, we propose to modify the Spiegler-Kedem (SK) equation by introducing an electric resistance factor, which is demonstrated to be able to effectively correct the universally observed overestimation of flux by researchers using current NF models. It is hypothesized that these deviations are caused by primarily the resistance of electrical charges inside the membrane pores to anions passing these pores. At a nano-scale level, the complex electrostatic interactions between the highly confined charged solutes and the charged membrane contribute to flow retardation and this phenomenon can be characterized using an additional correction factor. To this end, the modified SK model (MSK) includes an empirical charge resistance factor, R_{elec}, to account for this additional hydrodynamic flow resistance. This modification is added on top of the improvements based on the incorporation of solution viscosity in to the model [20] and the inclusion of the concentration polarization phenomenon in the calculation of osmotic pressure of solution.

Experimentally, pure sodium chloride (NaCl) solution was used in this study for demonstrating both the challenges faced by the classical SK model and the applicability of the MSK model for the following reasons: (1) high NaCl concentrations are commonly encountered in most industrial applications of NF, and (2) availability of extensive literature data allows for model comparison and verification. Two commercial membranes, NF270 and Desal-5 DL, were utilized as they are both important NF membranes that have found applications in a variety of different industries and for the same reason that a large number of scientific literature data are available on them. The SK model has been frequently used to describe the transport mechanism of ions through RO and NF membranes. It is a “black-box” model that substantially reduces numerical complexity and computation efforts.

The objectives of the present work are threefold: (1) develop a model based on the SK equation which enables simultaneous prediction of permeate flux and salt rejection of NF at both low and high salt concentration, (2) investigate the concentration dependency of both the NF membrane performance and MSK model parameters, (3) through the analysis of experimental and modelling data, elucidate an important NF ion rejection mechanism, retention of co-ions by intrapore membrane charges, which is enhanced by the fact that the nano-channels of NF through which the ions have to pass through to escape into the permeate has a radius only marginally larger than the ions themselves.

The thesis consists of seven chapters: Chapter 1, introduction, which provides a brief account of the background of the project; Chapter 2 presents a comprehensive literature review in NF modelling and applications; Chapter 3 lays out the development of the modified SK model and the numerical procedure for prediction of NF performance; Chapter 4 describes the experimental setup and methodologies employed in this study; Chapter 5 is dedicated to results and discussions. In Chapter 6, the physical significance of the hydraulic resistance due to charge effects is discussed in detail. Finally, conclusions and future works related to this study are summarized in Chapter 7.

References

1. V. Silva, V. Geraldes, A.M. Brites Alves, L. Palacio, P. Prádanos, A. Hernández, Multi-ionic nanofiltration of highly concentrated salt mixtures in the seawater range, Desalination 277 (2011) 29-39.
2. N. Hilal, H. Al-Zoubi, N.A. Darwish and A.W. Mohammad, Performance of nanofiltration membranes in the treatment of synthetic and real seawater, Separation Science and Technology 42 (2007) 493-515.
3. K. Walha, R.B. Amar, L. Firdaous, F. Quéméneur and P. Jaouen, Brackish groundwater treatment by nanofiltration, reverse osmosis and electrodialysis in Tunisia: performance and cost comparison, Desalination 207 (2007) 95–106.
4. A. Bes-Pia, B. Cuastas-Uribe, J.A. Mendoza-Roca, M.I. Alcaina-Miranda, Study of the behaviour of different NF membranes for the reclamation of a secondary textile effluent in rinsing processes, Journal of Hazardous Materials 178 (2010) 341-348.
5. A. Aouni, C. Fersi, B. Cuartas-Uribe, A. Bes-Pia, M.I. Alcaina-Miranda and M. Dhahbi, Reactive dyes rejection and textile effluent treatment study using ultrafiltration and nanofiltration processes, Desalination 297 (2012) 87-96.
6. Z. Ji, Y. He and G. Zhang, Treatment of wastewater during the production of reactive dyestuff using a spiral nanofiltration membrane system, Desalination 201 (2006) 255–266.
7. K.Y. Wang and T.-S. Chung, The characterization of flat composite nanofiltration membranes and their applications in the separation of Cephalexin, Journal of Membrane Science 247 (2005) 37–50.
8. B. Cuartas-Uribe, M.C. Vincent-Vela, S. Alvarez-Blanco, M.I. Alcaina-Miranda, E. Soriano-Costa, Nanofiltration of sweet whey and prediction of lactose retention as a function of permeate flux using the Kedem-Spiegler and Donnan Steric Partioning models, Separation and Purification Technology 56 (2007) 38-46.
9. A. Bes-Pia, B. Cuastas-Uribe, JA Mendoza-Roca, M.V. Galiana-Aleixandre, M.I. Iborra-Clar, M.I. Alcaina-Miranda, Pickling wastewater reclamation by means of nanofiltration, Desalination 221 (2008) 225-233.

10. N. Hilal, H. Al-Zoubi, N.A. Darwish, A.W. Mohammad and M. Abu Arabi, A comprehensive review of nanofiltration membranes: treatment, pretreatment, modeling, and atomic force microscopy, Desalination 170 (2004) 281–308
11. L. Meihong, Y. Sanchuan, Z. Yong and G. Congjie, Study on the thin-film composite nanofiltration membrane for the removal of sulfate from concentrated salt aqueous: Preparation and performance, Journal of Membrane Science 310 (2008) 289–295.
12. S.S. Madaeni and V. Kazemi, Treatment of saturated brine in chlor-alkali process using membranes, Separation and Purification Technology 61 (2008) 68–74.
13. S. Bason, O. Kedem, V. Freger, Determination of concentration-dependent transport coefficients in nanofiltration: Experimental evaluation of coefficients, Journal of Membrane Science 326 (2009) 197-204.
14. A. Santafé-Moros, J.M. Gozálvez-Zafrilla and J. Lora-García, Applicability of the DSPM with dielectric exclusion to a high rejection nanofiltration membrane in the separation of nitrate solutions, Desalination 221 (2008) 268–276.
15. W.R. Bowen and J.S. Welfoot, Modelling the performance of membrane nanofiltration-critical assessment and model development, Chemical Engineering Science 57 (2002) 1121-1137.
16. A. Szymczyk and P. Fievet, Ion transport through nanofiltration membranes: the steric, electric and dielectric exclusion model, Desalination 200 (2006) 122–124.
17. A. Szymczyk and P. Fievet, Investigating transport properties of nanofiltration membranes by means of a steric, electric and dielectric exclusion model, Journal of Membrane Science 252 (2005) 77–88.
18. J. Garcia-Aleman and J. M. Dickson, Mathematical modeling of nanofiltration membranes with mixed electrolyte solutions, Journal of Membrane Science 235 (2004) 1–13.
19. A.E. Yaroshchuk, Recent progress in the transport characterization of nanofiltration membranes, Desalination 149 (2002) 423-428.
20. C. Rodrigues, A.I. Cavaco Morão, M.N. de Pinho, V. Geraldes, On the prediction of permeate flux for nanofiltration of concentrated aqueous solutions with thin-film composite polyamide membranes, Journal of Membrane Science 346 (2010) 1-7.

21. V. Freger, T.C. Arnot, J.A. Howell, Separation of concentrated organic/inorganic salt mixtures by nanofiltration, Journal of Membrane Science 178 (2000) 185-193.
22. W.B.S. de Lint, P.M. Biesheuvel and H. Verweij, Application of the charge regulation model to transport of ions through hydrophilic membranes: one-dimensional transport model for narrow pores (nanofiltration), Journal of Colloid and Interface Science 251 (2002) 131–142.
23. R. Wang, Y. Li, J. Wang, G. You, C. Cai, B. H. Chen, Modeling the permeate flux and rejection of nanofiltration membrane separation with high concentration uncharged aqueous solutions, Desalination 299 (2012) 44-49.
24. X. Lefebvre, J. Palmeri, P. David, Nanofiltration theory: An analytical approach for single salts, Journal of Physical Chemistry B 108 (2004) 16811-16824.

Chapter 2: Literature Review

2.1 Introduction

The utilization of membrane based separation technologies can be dated back to the late 1960s when they were gradually being considered as replacements for more conventional processes like distillation, extraction, and evaporation in industrial settings [1]. It is not surprising that the advent of membrane-based filtration processes coincide with the significant developments made in the field of polymer chemistry. Membrane processes are classified and categorized based on the required driving force and separation mechanisms. Application of a driving force such as pressure, temperature, chemical, or electrical potential is the most crucial step to achieving separation.

Pressure driven membranes include reverse osmosis (RO), microfiltration (MF), ultrafiltration (UF), and nanofiltration (NF) with the latter being the most recent one that has been developed. The history of NF membranes, or "loose RO" membranes as they are so frequently termed for exhibiting properties intermediate between RO and UF membranes, dates back to the late 1970s when the need for a lower energy consumption and lower cost (compared to RO processes) was apparent in the industry. Low operation pressure, high flux, and selective rejection of multivalent ions are some of the many advantages offered by NF membranes. In 1978, the first industrial application of NF membranes was for the desalination of dyes and brighteners [2]. NF is now commonplace in seawater and wastewater, dairy, dye production, pulp and paper, textile, and pharmaceutical industries.

NF is used when liquid-phase separations of monovalent ions from multivalent salts or low molecular weight organic solutes such as glucose and sucrose are desired. NF is almost always operated in the tangential or cross-flow mode as opposed to the dead-end

mode, to reduce the build up of solid filter cake on membrane surface. NF membranes are characterized by 0.5-3 nm pore sizes corresponding to a nominal molecular weight cut off (MWCO) of approximately 200-1000 Dalton. The presence of distinct pores in NF and RO membranes has been a constant source of debate in the scientific community as of lately, however, recent Atomic Force Microscopy (AFM) studies suggest that pores can be viewed in NF membranes and pore size is being used as a parameter to describe membrane morphology in NF transport models [3].

The purpose of this review can be outlined as follows: to review (1) NF membrane materials, preparation and module configurations, (2) transport phenomenon, separation mechanisms and process modelling in aqueous media, and (3) major applications of NF processes. This review seeks to clearly and concisely summarize the current literature on the above stated aspects of NF membranes.

2.2 NF membranes: Materials, Preparation and Configurations

2.2.1 Materials and Preparation

Membranes can be categorized into symmetric and asymmetric membranes; the former consisting of a thick, uniform film with defined pores and composed entirely from one material [5]. Asymmetric structures consist of an ultra-thin active layer (toplayer) supported by a thicker porous sublayer (substrate), which is often a porous UF membrane. If the two layers are composed of different polymeric materials so as to optimize each layer separately, the membrane is termed ‘composite’, which is distinguished from ‘integral asymmetric’ membranes consisting of the same material for both layers [6]. Virtually all NF membranes are composite or thin-film composite (TFC).

Several methods are used to prepare NF membranes: phase inversion, interfacial polymerization, solution coating, hot-melt spinning, leaching, track-etching, sintering, and sol-gel techniques [7]. Phase inversion is most commonly used for 'integral' asymmetric membranes, while interfacial polymerization (IP) is used for TFCs. Recently, Gloukhovski et al. [8] reported a novel approach to fabricate TFC NF membranes via electropolymerization (EP). The technique involves the EP deposition of a thin film (instead of an IP one) on top of a conductively and asymmetrically porous support. This innovative technique has several advantages over the more traditional IP technique, which are specified in greater detail in the article [8].

Nearly all NF membranes in current use are polymeric. Some common polymeric materials used in the manufacturing of NF membranes are organic polymers such as cellulose derivatives (e.g. cellulose acetate), polysulfone, polyethersulfone, polyacrylonitrile, polyamide, polycarbonate, polypropylene, and fluorinated polymers [2,7]. However, these organic membranes have proven to be unstable and ineffective in aggressive environments, such as high pH and temperatures, and organic solvents. The need for membranes with long term chemical and mechanical stability led to the search for new materials and the development of inorganic membranes such as ceramic membranes [9]. Much research today focuses on a deeper understanding of ceramic membranes. Metal oxides such as alpha (or gamma) alumina (Al_2O_3), zirconia (ZrO_2), and titania (TiO_2) are common materials for ceramic membranes [9].

Several researchers have investigated the preparation techniques, characterization (determination of pore size, porosity, charge, and filtration layer thickness), and applications of ceramic NF membranes [10-16]. These researchers reported the amphoteric behaviour of ceramic membranes (caused by hydroxyl groups) via zeta potential measurements and as a

consequence, the dependency of the membrane electric surface charge on the pH of the filtering solution. Tests conducted using electrolyte solutions demonstrated that operating conditions such as the salt concentration and solution pH play an important role in the retention characteristics of the membrane. Generally, a ceramic membrane performs ion separation (higher ion retentions) best at pH values further from the isoelectric point (IEP), when the zeta potential is higher. For divalent sulphate ions, retention values as high as 90% (and higher) were observed in the alkaline pH region [15,16]. At the IEP, minimal retention is almost always observed since the negligible membrane charge corresponds to retention via size exclusion only. These trends are also prevalent in most polymeric NF membranes.

The suitability of ceramic NF membranes for the removal of dyes/colouring agents in the treatment of textile wastewaters has been studied by several researchers. Benfer et al. [17] and Weber et al. [18] found that the rejection of dyes (such as Direct Red, SAC_{436}, SAC_{525}, SAC_{620}) was as high as 99%. Lee and Cho [19] tested two TiO_2 ceramic membranes and two polyamide TFC membranes for the removal of natural organic matter (NOM) and disinfection by-products (DBP) precursors such as haloacetic acids (HAA) from drinking water sources. The ceramic membranes were found to more effectively remove DBP precursors and produce higher permeability rates than the polymeric ones.

Virtually all ceramic membranes are multilayered, consisting of a membrane support, interlayer(s), and a toplayer, and developed via the sol-gel procedure [11,14,15]. The interlayers are usually mesoporous (pore diameter > 2 nm) and prepared by colloidal sol-gel process, which is then deposited on a macroporous membrane support. The final step involves the synthesis and deposition of a thin, usually microporous (pore diameter < 2nm) toplayer. This is typically done using the polymeric sol gel technique.

It should be noted that although originally intended for use in non-aqueous media, relatively few researchers have investigated the use of ceramic NF membranes in organic solvents, despite the several advantages offered by this membrane. Van Gestel et al. [20] suggested that the highly hydrophilic nature of ceramic membrane materials could be one reason and hence, proposed a method to modify the hydrophilic behaviour of a γ-Al_2O_3/anatase-TiO_2 by a silane treatment (use of an organo-silane coupling reagent for surface modification). Conversion of the hydrophilic nature of ceramic membranes have become lately of particular interest to scientists. To assess the effect of the silane treatment, Van Gestel et al. [20] measured the hexane/water permeability ratio. They concluded that the membrane pore structure was crucial to the efficacy of the silane treatment. A microporous anatase-TiO_2 toplayer remained hydrophilic, however, a (partly) mesoporous anatase-TiO_2 toplayer exhibited a complete hydrophobic behaviour. Kujawski et al. [21] also successfully changed the hydrophilic character of mesoporous ceramic alumina and titania NF membranes into a hydrophobic one by grafting them with perfluoroalkylsilane, an organo-silane coupling reagent, different from the one used by Van Gestel. To deal with non aqueous solvents, Tsuru et al. [22] modified a silica-zirconia ceramic membrane with another organo-silane compound, trimethylchorosilane, to produce an organic-inorganic hybrid NF membrane, and tested its separation performance of alcohol and alkane solutes in ethanol solvents. In a more recent study, Van Gestel et al. [23] prepared a corrosion-resistant ceramic NF membrane. Their all ZrO_2 layers membrane demonstrated high stability in several corrosion tests with feed solution pH of 1, 2, and 13 and has been recommended for applications in NF involving acidic or alkaline feed.

Nevertheless, ceramic membranes are still less frequently considered for NF applications than polymeric ones due to their inherent high costs. Therefore, the development

of polymeric organic solvent nanofiltration (OSN) membranes is an emerging field with potentially wide applications [24-28]. Most aqueous NF membranes use supports that are either polysulfone or polyethersulfone, polymers that present little to no stability in organic solvents. Much research has focussed on the fabrication of solvent resistant supports [29,30]. Very recently, Kosaraju and Sirkar [30] fabricated TFC organic solvent NF membrane using porous microfiltration (instead of the conventional UF) polypropylene supports. The resultant membrane was found to withstand significantly high pressures (up to 1241 kPa) and proved to be resistant to alcohols and aromatics hydrocarbon. In addition, See Toh et al. [31] prepared an OSN membrane using chemical cross linking strategies, which proved to be chemically stable in organic including polar aprotic solvents (such as methylene chloride and tetrahydrofuran) and temperatures below 100^{o}C. The search for improved materials and preparation methods for membranes is still ongoing.

2.2.2 Configurations

Membranes are usually packed in small units called modules to provide support and protection against operating pressures and the production environment [32]. When a feed inlet stream is passed through the module, it is separated into (a) permeate stream (fluid passing through the membrane), and (b) retentate stream (the fluid retained or rejected) by the membrane. The most common configurations are flat sheet/plate, tubular, hollow-fibre, capillary, and spiral wound. Tubular, hollow-fibre, and capillary are types of cylindrical membranes with differing dimensions (tubular with diameter > 10 mm, hollow-fibres with diameter < 0.5 mm, and capillary with intermediate dimensions) [33]. Numerous sources describe the construction, operating conditions, fouling tendencies and economic considerations of each configuration [32-35]. NF membranes are mostly packed in spiral wound elements due to the availability of high packing density and low cost. However,

because this module is susceptible to plugging with suspended particles, NF membranes in flat sheet, tubular, and hollow-fibre are also made available.

2.3 Transport and Separation Mechanism: Modelling of NF membranes

2.3.1 Transport and Separation Phenomena

Given the diversity of NF applications, to fully understand the potential and predict the performance of NF membranes in different circumstances, it is important to gain a deeper understanding of the basic mechanisms responsible for separation and transport. However, the combination of nanoscale pore dimensions and electrically charged membrane surfaces makes the transport and partitioning mechanisms of electrolytes highly complex.

An excellent comprehensive review by Hilal et al. [36] detailed the distribution mechanisms of ionic species and organic solutes in aqueous media. Scientists today agree that a combination of steric hindrance and Donnan exclusion forms the basis of ion partitioning and selectivity in NF membranes. The distribution of neutral solutes at the NF membrane interface depends on steric or size exclusion, in which the solute size and shape are the predominant factors [2]. For charged solutes, Donnan equilibrium, resulting from the charged nature of NF membranes serves as an additional partitioning effect [1]. A simple consequence of the Donnan equilibrium is that solutes with the same charge (co-ions) as the membrane surface are repelled while those with opposite charge (counter-ions) are attracted [37]. Moreover, membranes display a higher rejection to multivalent co-ions than monovalent co-ions, whereas less rejection to multivalent counter-ions than monovalent counter-ions [37].

Wang et al. [38] observed the following rejection trend of a negatively charged NF45 membrane for neutral organic solutes and inorganic electrolytes:

$$R(raffinose) > R(Na_2SO_4) > R(MgSO_4) > R(sucrose)$$

$$> R(glucose) >> R(KCl) = R(NaCl) > R(MgCl_2) > R(glycerine)$$

It can be clearly seen that the rejection of charged salts is in accordance with the Donnan principle whereas the neutral organics are rejected based on the steric exclusion (raffinose, sucrose, glucose, and glycerine are in the order of decreasing molar mass). In their studies Schaep et al. [39] obtained similar results with a negatively charged NTR7450 membrane: $R(Na_2SO_4) > R(MgSO_4) > R(NaCl) > R(MgCl_2)$. However, for a negatively charged NF40 membrane, a different trend was observed: $R(Na_2SO_4) > R(MgCl_2) > R(NaCl)$. This discrepancy was hypothetically explained as a result of the ratio of ion radius to pore size being close to 1 for a NF40 membrane, causing steric effects to be more dominant than the Donnan effect and diffusive flow more dominant than convective flow. Hydrated ionic radii of Mg^{2+} ion is larger than that of Na^+ and the diffusion coefficient of Na^+ is greater than that of Mg^{2+} (more sodium ions will diffuse through the membrane, causing lower retention).

All these studies and others frequently report the decrease in salt retention with increasing salt concentration [40,41]. Tanninen et al. [42] and Schaep and Vandecasteele [43] showed that with increasing salt concentration, the effect of the membrane charge on separation decreases to a minimal due to a decrease in the electrical double layer (neutralizing excess of counter-ions near a charged surface), causing steric hindrance and salt diffusion to play a more prominent role. Numerous other studies have focused on the role of pH [44-47] or temperature [48] on salt separations with NF membranes. A fair amount of literature also deals with the separation of mixed electrolyte solutions, such as of NaCl and Na_2SO_4 [42,49]. Lately, it has been realized that Donnan effect cannot solely account for experimental observations using various ionic species, and it is necessary to include a second

partitioning effect, the dielectric exclusion (DE). The concept of DE shall be presented in greater detail later on in this paper.

2.3.2 Modelling of NF membranes

In order to predict and optimize the NF membrane performance, it is necessary to incorporate the above phenomena into a mathematical transport model. However, if one were to focus solely on existing literature dedicated to the modelling of membranes, it would become clear that the staggering number of such models would make it an impossible feat to cover them all. This paper will briefly review some of the well-known earlier models and provide more detailed discussions of the more well-known recent ones.

Perhaps the earliest known models are the pore-flow model [50-52] used to describe the principles of ultrafiltration and the solution-diffusion model used for modelling gas permeation and later for RO and pervaporation. In the solution-diffusion model, permeants diffuse through the membrane down a concentration gradient while the pressure is assumed to remain constant within the membrane itself [53]. On the other hand, pore-flow model assumes the permeants convectively flow through tiny pores down a pressure gradient, while the solvent and solute concentration stay uniform within the membrane [53]. Most literature models are now categorized into mechanism-independent or mechanism-dependant models. Initial transport models belonged to the former category based mostly on non-equilibrium or irreversible thermodynamics (IT). Spiegler and Kedem [54] and Kedem and Katchalsky [55] were the first ones to use this “black-box” approach to study RO membranes. The “black-box” approach was so named since the authors make the assumption that the membrane acts as a black box with no inclusion of any separation or membrane characteristics. These models are often criticized for providing little insight into the physicochemical processes involved in transport mechanisms across a membrane. Several authors have developed (or

improved upon) models based on the Spiegler-Kedem model or the combined Spiegler, Kedem, Katchalsky (SKK) model and used them to study the separation of (a) water soluble organic solutes from NaCl [56,57], (b) aqueous dye salt solutions [58,59], (c) organic solutes from water [60]. By incorporating the Donnan effect and effect of salt concentration, these authors have successfully predicted separation performance using the IT approach.

Mechanistic models use structure-related membrane parameters and model equations to account for the separation mechanisms. These models also integrate the physical and chemical factors of both the membrane and the solution to deliver a complete picture of the interactions between the filtering solution and the membrane. Early mechanistic models include the previously mentioned pore-flow and solution-diffusion models, Teorell-Meyer-Sievers (TMS) model [61,62], and the space-charge (SC) model by Osterle and co-workers. [63,64]. The TMS model assumes a uniform distribution of fixed charge, mobile ions, and electric potential and provides a simplified mathematical analysis for ionic transport [65]. The SC model, which describes electrolyte transport through charged capillaries, is a more rigorous and mathematically complicated approach [66]. Several authors have proposed models for NF derived from either the TMS or SC model with additional phenomena; of which Tsuru and co-workers [67,68,69], and Bowen and co-workers [70,71] have made the most contributions. Nakao and Kimura [72] developed the steric-hindrance pore (SHP) model in 1982, from which the pore-wall correction factors of the original pore-flow model were eliminated. Later in 1997, Wang et al. [69] combined the SHP and the TMS model to form the electrostatic and steric-hindrance (ES) model. The ES model was used to predict the transport performance of organic electrolytes in the presence of NaCl through NF membranes and was found to be in good agreement with the experimental results.

It should be noted that the most widely adopted models today and some of the previously mentioned models [67-71] use the extended Nernst-Planck (ENP) equation to depict mass transfer in membranes. This equation describes the three most important mechanisms of mass transfer in membranes: diffusion, electromigration, and convection, which are caused by concentration, electropotential, and pressure gradients across the membrane. All model descriptions that follow use the ENP equation as a starting point, unless otherwise stated.

Probably the most recent NF model to gain wide popularity is the "Donnan-steric-pore model" (DSPM) developed by Bowen et al. [71]. The ENP equation was modified to include hindrance effects for diffusion and convection, and equilibrium partitioning was assumed to be a result of electrical (Donnan) and sieving (steric) effects. The NF membrane was characterized using the effective pore radius (r_p), effective thickness over porosity ($\Delta x/A_k$), and the effective membrane charge density (X_d). A series of studies by various researchers were conducted to test the validity of the DSPM model. Bowen and coworkers [73,74] used DSPM to model a diafiltration process, involving a mixture of dye and NaCl. It was found that the prediction of the rejections of Cl^- and Na^+ were in good agreement with the experimental results if the effective charge density (X_d) was assumed to be dependent on the total concentration of negative charges present in the solution. Schaep et al. [75] measured the retentions of several ionic compounds (NaCl, Na_2SO_4, $MgCl_2$, $MgSO_4$, and $LaCl_3$) using different commercial NF membranes and showed that the DSPM model was a good predictor of rejection of single salt solutions. It was also shown that the membrane charge density is not constant, but dependent on salt type and concentration. Moreover, the presence of $MgCl_2$, $MgSO_4$, and $LaCl_3$ caused some of the membranes to change the sign of their original charge (from negative to positive) and this was hypothesized to be a result of

ion adsorption at the membrane surface. Similar studies by Labbez et al. [76,77] on a commercial titania NF membrane demonstrated the effectiveness of using DSPM as a tool for membrane charge characterization and confirmed the dependency of the membrane charge on salt type, concentration, pH and specific adsorption of ions on the membrane material [76]. Cuartas-Uribe et al. [78] compared the rejection of charged and uncharged solutes across NF membranes using the DSPM and Spiegler-Kedem models and concluded that although models were in good agreement with the experimental observations, the DSPM model made better predictions due to its consideration of more transport phenomena.

However, it was quickly realized that the DSPM model proved to be a less efficient predictor in studies involving multivalent cations and mixtures of electrolytes and therefore, Bowen and Welfoot [79,80] made some modifications to the original DSPM model. It was found that the success of the DSPM model was a direct consequence of using an arbitrary fitting parameter, $\Delta x/A_k$, and unrealistically high values of the membrane charge (X_d) [77,80]. Bowen and Welfoot [80] developed a two-parameter model using just r_p and X_d (since rejection was found to be independent of membrane thickness) and incorporating more complex separation phenomena (effect of pressure on chemical potential, pore radius dependant viscosity and dielectric exclusion) without increasing the complexity of calculations or number of undefined parameters. The end result was a model that was in good agreement with the experimental data, although not so as the original DSPM model, but with membrane parameters more in conformity with actual membrane properties. A different work by Bowen and Welfoot [81] outline the steps required to develop a predictive model that can be applied to industrial applications.

To deal with the shortcomings of the DSPM model, several authors have proposed more sophisticated modifications to this model or newer models of their own. Some of the

more preferred and frequently used models will be discussed here. Bandini and Vezzani [82] presented the DSPM & DE model, an extension of the DSPM model by simply taking the dielectric exclusion phenomenon into account. According to the Donnan theory and as predicted by the DSPM model, a negatively charged NF membrane leads to lower retention of multivalent cations such as Ca^{2+} or Mg^{2+}. However, experimental values tend to be higher than those predicted by the Donnan theory. This difference is believed to be caused by the dielectric exclusion (DE), which serves as an additional rejection mechanism of paramount importance. Extensive research devoted to the dielectric exclusion of ions in membranes has been submitted by Yaroshchuk [83-85]. Two aspects of DE have been noted: (1) production of "image forces" resulting from the difference in dielectric constant of an aqueous solution and the membrane matrix [82-84], and (2) differences in the structure and properties of a solvent in a confined geometry (membrane pores) and in the bulk (outside pores) resulting in excess solvation energy [82,84-86]. In the first case, ions in the solution interact with the polarization charges that they themselves induce at the boundary between the two dielectric media. These polarization charges, having the same sign as the inducing ions, do not distinguish between co-ions and counter-ions, but repel them both from the membrane pores [82-86]. This is the accompanying rejection mechanism that is overlooked by the original DSPM model. In the second case, the greater spatial and orientation order of a solvent in the confined membrane pores (caused by decreased mobility) lowers the dielectric constant of the solvent inside the pore when compared to the bulk values [86]. In the DSPM & DE model, all the above phenomena are included, the membrane is characterized by three parameters (average pore radius (r_p), the effective membrane thickness ($\Delta x/A_k$), and volumetric charge density (χ)), and the excess solvation energy is calculated using the Born formula. The model successfully predicted the experimental behaviour of all the salt

mixtures investigated with a negatively charged membrane, in particular, the rejection of divalent counter-ions, Ca^{2+} and Mg^{2+}. However, it was noticed that DE did not play a prominent role in the case of mixtures with various co-ions, such as NaCl + Na_2SO_4.

Very recently, Mohammad et al. [87] used the DSPM & DE model to predict permeate fluxes and rejections of highly concentrated salt solutions (NaCl, KCl, Na_2SO_4, $MgCl_2$, $MgSO_4$, Na_2CO_3, and $CaSO_4$) in a NF90 membrane. Given the high concentrations (typical seawater concentrations) of the solutions, the DSPM & DE model was slightly modified to include osmotic pressure, calculated using the Van't Hoff equation. The model provided good predictions for the rejections and fluxes of the following salts: NaCl, Na_2SO_4, $MgSO_4$, and $CaSO_4$. Another study by Santafe-Moros et al. [88] discussed the applicability of the DSPM & DE model for nitrate rejection and the limitations of this model in high feed concentrations and varying pH scenarios. Both the DSPM and DSPM & DE models were used by Hussain et al. [89,90] to study the effect of ion size on charged solute rejection in NF membranes. The ion radius was determined from Stokes-Einstein relationship (Stokes radius), Born's effective radius, and the Pauling radius. It was found that ionic hydration has strong influence on ion diffusion properties, and consequently ion rejections.

Another very recent model to gain wide attention is the steric, electric, and dielectric exclusion (SEDE) model by Szymczyk and Fievet [91]. The SEDE model, while similar to the DSPM & DE model in the sense that it takes into account the steric hindrance effects, the Donnan exclusion, and the two parts to the dielectric exclusion (Born dielectric effect and image forces), and incorporates the dielectric constant of the pore solution, ε_p, as an additional parameter along with r_p, $\Delta x/A_k$, and χ. The Born dielectric effect is accounted for by means of the modified Born formula proposed by Rashin and Honig [92]. The SEDE model showed good agreement between experimental and theoretical values when used to

assess the rejection rate using symmetric and asymmetric salts of a polyamide NF membrane, whose volume charge density was determined using tangential streaming potential measurements [93]. Rouge et al. [94] used the SEDE model to assess the relative influence of steric, Donnan, and dielectric mechanisms in the retention properties of a polyamide NF membrane in the presence of both single and mixed inorganic salts. The importance of including DE was established in a study of transport of metallic salts ($CuCl_2$, $ZnCl_2$, $NiCl_2$, $CaCl_2$) through polyamide NF membrane by Szymczyk et al. [95] when the classic NF theory (sans DE) failed to describe the experimental rejection data ($CuCl_2 > ZnCl_2 \approx NiCl_2 > CaCl_2$), as opposed to the SEDE model. The analysis indicated membrane efficiency decreased as volume charge density increased, contradictory to the classical theory that predicts rejection rate increases monotonously with the volume charge density.

A unique one-dimensional mathematical model by Garcia-Aleman and Dickson [96] combines the extended Nernst-Planck equation and the Donnan equilibrium theory with the Gouy-Chapman theory of electrical double layers; and characterizes membranes using three fitting parameters: pure water permeability (L_p), pore radius (r_p), and surface electrical potential (φ). The Gouy-Chapman equation was solved for both flat and cylindrical pore surface approximations, with the results indicating that the cylindrical surface approximation was better than the flat one in most cases, but especially at lower feed concentrations when the double layer effects are most important. Satisfactory agreement was found between the model and experimental data when commercial NF membranes were tested in mixed electrolyte solutions.

Although the use of ENP-based models is more well-known, Straatsma et al. [97] had developed a NF membrane filtration model based on the Maxwell-Stefan equations to describe transport mechanisms and a Freundlich equation to describe membrane charge by

means of adsorption of ions. The permeate flux and rejections of multi-component liquid feeds were calculated as a function of membrane properties (mean pore size, porosity, thickness, surface charge) and feed pressure. The model fitted the experimental flux-rejection curves reasonably well.

Several researchers have also incorporated the concentration polarization (CP) effect into their models. This phenomena, caused as a result of particles/solute accumulation in a mass transfer boundary layer adjacent to the membrane surface [98], is a serious problem intrinsic to membranes that reduces the membrane flux and restricts the full exploitation of membrane capacity [99]. Most of the previously discussed models either do not account for CP or operate NF modules at sub-critical flux conditions or sufficiently high cross-flow velocities so that CP becomes negligible. Geraldes et al. [100-104] and Geraldes and Afonso [105,106] have used innovative modeling tools (such as computational fluid dynamics or CFD) to analyze the CP phenomenon, flow structure, and solute concentration distribution in NF membranes, especially NF spiral wound modules with ladder type spacers [100-102]. Other authors developed models that incorporated membrane fouling due to natural organic matter [99,107], bacteria and their soluble microbial product (SMP) accumulation [108], and $CaSO_4$ scaling [109,110]. A thorough discussion of these models and others incorporating CP is however, beyond the scope of this review paper.

2.4 Applications of NF membranes: Water treatment

As mentioned in the introduction, there are a tremendous number of industrial applications of NF membranes. Nevertheless, the treatment of water from any source (groundwater, surface water, brackish water, seawater, or wastewater from various chemical industries) is undeniably, the primary application of NF. Not surprisingly, the major focus of

this review shall be the use of NF membranes in water treatment. It should be noted that this review shall report only the most important literature work relevant to each section.

2.4.1 Wastewater and industrial effluent treatment

NF has been found suitable for the treatment of wastewater generated in many chemical industries. The principal concern of wastewater treatment is the water recovery rate, which should be as high as possible, preferably close to 100%, so as to avoid water loss through discharge. To find a solution, researchers have investigated the potential of integrated membrane systems [111-113]. Rautenbach et al. [111] introduced the concept of combining RO, high-pressure RO, and NF processes to treat contaminated wastewaters. They found that the newly developed integrated systems achieved average water recovery rate of greater than 95% at relatively low energy consumption.

The textile industry being one such industry where large amounts of water are consumed, have led many researchers to investigate the potential application of NF membranes in dye removal, both BOD (biochemical oxygen demand) and COD (chemical oxygen demand) reduction, and salt reduction [34]. In a recent study by Kim et al. [114], the optimal operating conditions for COD, colour, and salt rejections were examined using a combined NF-RO process. By only using NF membrane, the rejection of COD and colour was greater than 96% and the salt rejections of two different reactive dyes, reactive yellow 145 and reactive black 5, were 51.7% and 21.2% respectively. The combined membrane processes of RO and NF showed a very slight improvement for COD and color rejections but a huge improvement in the salt rejections of the two reactive dyes (R.Y.145: 96.6% and R.B.5: 53.2%). It was also suggested that the high quality of the treated wastewater recovered by means of combined RO/NF process could be reused as cooling or washing water. Another work by Qin et al. [115] showed that NF membranes allowed 99% dye-

removal efficiency, along with a 70% water recovery from the Max Textile dyeing facility in Singapore. Schoeberl et al. [116] also found that the use of a membrane bioreactor (MBR), followed by NF as an additional post-treatment, was the best method for producing high quality effluents from wastewater produced in a polyester finishing factory. Kopecky and Mikulasek [117] focussed on the optimal operating conditions for the separation of reactive dye/salt mixture using commercially available NF membranes. Newly developed polyvinylidene fluoride (PVDF) membranes, PF45 and PF45psm, were prepared by Buonomenna et al. [118] and used to test the removal of two dyes (congo red and methylene blue) from aqueous solutions. 'Methylene blue' was retained 100% by PF45psm and 'congo red' was retained 100% by PF45. Other researchers have also conducted studies in this field [119-125].

Produced water, or wastewater generated from oil production fields, is of major environmental concern. Produced water is characterized by inorganic salts, process chemicals, heavy metals, and toxic hydrocarbons [126]. A study by Cakmakci et al. [127] compared the best membrane technologies (MF, UF, NF, RO) for treatment of produced water from oil fields in the Trakya region of Turkey, and determined the best pre- and final treatment methods. It was found that for final treatment units (NF vs. RO); the highest permeate flux with NF membranes, with no flux decline over time. Visvanathan et al. [128] suggested that using NF as a pre-treatment to RO process significantly reduced the amount of dissolved organic matter and other pollutants in produced water.

The removal of heavy metals from wastewater using NF membranes have also been studied, especially since these toxic contaminants are produced in metal finishing, battery manufacturing, and mining industries. Qdais and Moussa [129] showed that NF membranes can be very successful in the removal of copper and cadmium ions from the wastewater

streams. Khedr [130] also compared the use of NF membranes and conventional methods, such as chelating ion exchange resins, for the separation of trace heavy metal cations (HMC, Cd^{2+}, Ag^{2+}, and Hg^{2+}) from mixture salt solutions. The NF membrane achieved 98% separation at water recovery of above 90% and also enabled the optimum recycling of permeate for reuse as process water. The performance of NF and RO membranes in treating the toxic metal effluent from a metallurgical industry was also studied [131], and it was shown that while RO offered higher rejections for the metal ions (95% vs. 78.9%) and a lower COD value in the permeate stream (10 mg/L vs. 35 mg/L) than NF, NF was still found to be more suitable in large-scale industrial operations due to a significantly higher permeate flux at low pressures.

Another problematic class of contaminants found in wastewater (especially municipal wastewater effluents) include pharmaceuticals and personal care products (PPCPs), and endocrine disrupting chemicals (EDCs). These compounds, EDCs in particular, have had adverse biological effects (e.g. reproductive abnormalities) in aquatic organisms. Quite a few researchers have studied the removal of these compounds using membrane technology [132-137]. Kim et al. [134] found that standard water treatment processes like coagulation and filtration were inefficient in the removal of pharmaceuticals, hormones, and other pollutants commonly found in wastewater effluents in South Korea. Since both RO and NF membranes showed excellent removal rates (>95%) for all pollutants, it was recommended using a MBR, followed by either RO or NF, for best results. Yoon et al. [135,136] showed that EDC/PPCPs were better retained by NF than UF due to both hydrophobic adsorption and size exclusion mechanisms in NF, as opposed to just hydrophobic adsorption in UF membranes. Kosutic et al. [137] found the removal of antibiotics from artificially prepared wastewater (composition similar to pharmaceutical plant effluent) by a RO and a tight NF membrane was

exceptionally high (>98.5%), with the tight NF membrane showing the optimal performance in terms of higher permeate flux, lower operating pressures, and lower energy consumption.

The use of membrane technology in the dairy industry dates back to the 1970s, when RO and UF membranes were used to recover and purify proteins from whey. Dairy industries usually generate large volumes of water that contain diluted amounts of dairy matter such as milk proteins and lactose. Research scientists have investigated the use of membrane technology to recover these milk constituents and lower water consumption by recycling and reusing the purified water [138-143]. In a recent study by Vourch et al. [144], model dairy plant process waters were treated using single-stage (RO) and two-stage (NF+RO and RO+RO) membrane operations. It was shown that although a RO+RO treatment produced the highest quality of purified water, purified water from RO or NF+RO operations was good enough to be reused for cleaning, heating, or cooling purposes. It was also concluded that factors like heat treatment, fat content, or whey/milk ratio do not significantly affect the membrane performances. A similar work by Atra et al. [145] utilized a combination of UF and NF membranes, where the filtrate from UF was fed to the NF membrane, to concentrate milk, whey protein, and lactose. The NF filtrate, containing only 0.1-0.3% lactose was found to be suitable for reuse and recycle. Koyuncu et al. [146] demonstrated that apart from excellent rejections for COD and heavy metals and a 90% water recovery, the NF membranes used for treating dairy plant effluents did not suffer from any serious membrane fouling.

2.4.2 Ground and surface water treatment

Ground and surface waters have been used for agricultural and industrial purposes for centuries and as a source of drinking water. To make these waters fit for agricultural/industrial applications or safe for human consumption; they may have to undergo

various treatments, such as removal of hardness and other dissolved ions, natural organic matter, pesticides, bacteria and viruses, and any other pollutants. Groundwater [147-150] and surface water [151-153] treatments using NF membranes have been studied extensively by many researchers in the late 1990s. As already stated many times, the objective of this review paper is to report the more recent research findings. It is important to note that NF is, at present, the best technology for treating brackish groundwater [154].

The presence of arsenic in ground and surface water is a major concern because it can lead to a number of health problems (e.g. arsenic poisoning, cancer, etc.). The two most common oxidation states of Arsenic in groundwater are As(III) and As(V). Recently, Nguyen et al. [155] compared three different technologies for arsenic removal: iron coated sponge (IOCSp) adsorbent, iron coated sand (IOCS-2) adsorbent, and low pressure NF. Although, the highest percentage of the arsenic was removed by NF (94%), the water recovery rate was quite low. Therefore, the NF method was found to be feasible only when a high quality effluent is needed. Other authors have focussed on the effect of operating conditions (pressure, concentration, cross-flow velocity, and pH), and the study of relevant transport and ion-partitioning mechanisms involved in arsenic removal via NF membranes [156-158].

Problems associated with using hard water are not new to the industrial world. The softening of ground and surface water prior to their utilization in chemical industries is therefore, of paramount importance. Schafer and Richards [159] tested NF performance in groundwater (sample from an Australian park site) hardness removal and found that calcium carbonate and other multivalent ions (sulphate, magnesium, calcium, manganese) were retained higher than 98% and surprisingly, the retention was independent of pressure. These

high rejection values for multivalent ions have been reported by several other authors as well [160-162].

Considerable amount of work has been also done on the removal of fluoride ions [163-165], nitrate ions [166,167] and NOM [168-170] from ground and surface water resources. Recently, Hu and Dickson [171] developed a mathematical model based on the ENP and Grahame equations and the Donnan exclusion theory to interpret NF membrane performance at different fluoride contents. At high fluoride concentrations (1000 and 2000 ppm), the model was in agreement with the experimental values but hugely overestimated the rejection at lower concentrations (20 and 100 ppm). A possible explanation put forward is that the model ignores the reduction of effective pore diameter when ions are adsorbed on to the membrane pore surface. A decrease in ion adsorption at lower concentrations, increases the effective pore size, and simultaneously increases the effective diffusivity across the membrane, resulting in rejections lower than predicted.

A recent article by Teixeira and Rosa [172] study the impact of pH and calcium hardness ions on the removal of NOM (especially humic acids) by a negatively charged NF membrane. NOM rejection in varying pH environment was explained satisfactorily by the classical size exclusion and electrostatic repulsion theory. Membrane performance in the presence of calcium ions was influenced by adsorption of calcium ions onto the membrane surface and formation of complexes with carboxylic groups of humic substances. Van der Bruggen et al. [160] showed the rejections of pesticides (atrazine, simazine, diuron, and isoproturon) from groundwater using NF were in the 90-95% range and these rejections could be explained by the combined effects of size and dipole moment. Van der Bruggen and Vandecasteele [173] have also compiled an excellent overview of possible applications of NF in the drinking water industry: namely, ground and surface water treatment.

2.4.3 Desalination of seawater and brine solutions

The high salt concentration makes seawater unsuitable for direct use in many chemical processes. Desalination processes like RO, vacuum evaporators, and multi-stage flash evaporators require extensive pretreatment to reduce fouling and scale formation and ensure long-term performance of the process elements [174]. Conventional treatments to reduce hardness, total dissolved solids (TDS), turbidity, alkalinity, and biological impurities in seawater include coagulation, flocculation, acid treatment, pH control, disinfection, and addition of antiscalants [175]. The major drawbacks of using these pretreatment methods have been noted by Van Hoof et al. [175] and Al-Ahmad and Aleem [176]. The use of pressure-driven membrane processes (MF and UF) as feed pretreatment has been thoroughly studied by many [176-180].

At the 1997 IDA World Congress in Madrid, Hassan et al. [181] introduced the possibility of using NF as pretreatment for seawater reverse osmosis (SWRO) and multistage flash (MSF) desalination processes. The NF unit removed (1) very fine turbidity, (2) residual bacteria, (3) total hardness by 93.3%, and reduced (4) TDS by 57.7%. The fully integrated NF-SWRO and NF-MSF desalination systems lowered energy consumption by 25-30%. Following their promising breakthrough in seawater desalination, the Research & Development Centre of Saline Water Conversion Corporation (SWCC) in Saudi Arabia, built a NF-SWRO demonstration plant (six spiral-wound NF modules followed by three SWRO elements) that confirmed the previously obtained results [182]. The next logical step being the evaluation of this new configuration on a commercial scale, a single SWRO plant in Umm Lujj, Saudi Arabia, was converted to a dual NF-SWRO desalination plant and [183] with the benefit of a 42% increase in the permeate flow. In a recent paper, Hamed [184] provides an overview of research endeavours carried out by the R&D centre to develop

hybrid desalination systems: NF/MSF and NF/SWRO/MSF. Turek and Dydo [185] noted that hybrid NF/RO/MSF crystallization system also offered a promising possibility for desalination because of the high water recovery and low water costs. The emerging role of NF in pretreatment procedures has driven researchers to test commercially available NF membranes against seawater, enabling them to better predict NF performance and realize the full potential of NF membranes for seawater desalination purposes [186-189].

Chloralkali industries produce sodium hydroxide and chlorine gas from the electrolysis of sodium chloride brine. This process uses seawater or saturated brine solutions as a source of sodium chloride. These sources often contain impurities, namely sodium sulphate, magnesium, and calcium cations, the accumulation of which has a detrimental effect on the ion-exchange membranes used for electrolysis [190]. Since 1992 when the idea was first conceived, NF membranes have been extensively studies and proven to be quite effective and economical in sulphate removal from brine streams [191-193]. Laboratory tests carried out by Kvaerner Chemetics showed that SO_4^{2-} rejection remained high while Cl^- rejection remained low over a wide range of NaCl concentrations, preventing any significant loss of the feed salt [193]. Very recently, Madaeni and Kazemi [194] tested the ability of seven commercial polymeric (both RO and NF) membranes in Mg^{2+}, Ca^{2+}, Fe^{2+}, and SO_4^{2-} removal from saturated brine. Hydrophilic polyethylene terphetalate PVD membrane was recommended for use in chloralkali processes for exhibiting highest Mg^{2+} and Ca^{2+} removal and minimum NaCl rejection. Asymmetric PBI NF hollow-fibre membranes developed by Wang et al. [195] exhibited high sulphate and chromate rejection and low chloride rejection under high alkalinity and high pressure environments. Both studies concluded that ionic rejection was mainly dependant on size differences between hydrated ion and membrane pore [194,195].

In oil and gas industries, seawater is commonly injected into offshore oil wells to displace oil [196]. It goes without saying that the high sulphate content in seawater will cause scale formation in the injection wells. Bader has done extensive work in this field, including highlighting sulphate scale problems inherent in seawater injection operations [197], investigating the possibility of integrating NF or RO processes with compressed phase precipitation (CPP) and liquid-phase precipitation (LPP) to solve these problems [198,199], and providing modeling tools for ion rejection prediction in conjunction with scaling tendency and concentration polarization effects [200-202].

Other applications of NF include purification and separation of pharmaceuticals from fermentation broths [203], recovery and concentration of antibiotics [204-206], enzymes and amino acids [207-209], separation of heavy metals from acidic solutions [210,211], and removal of dissolved solids from pulp and paper industries [212-214]. A detailed presentation of these applications is beyond the scope of this paper.

2.5 Conclusions

As one of most recent development in membrane technologies, NF has found important applications in numerous industries, owing to its ability in selectively rejecting electrolytes that are small than the pore size of NF membranes. The complexity of NF separation mechanisms, which roots in the steric and electric interaction between ions, hydrated ions, and the charged membrane surface and membrane pores, makes the theoretical analysis and modelling of NF processes particularly challenging. Although a large variety of different models have been proposed for the simulation of NF processes as a result of extensive investigations by a numbers of best scientists in the field, all of the existing models are valid only for applications at low salt concentrations. Ironically, some of the most

important applications of NF, including seawater desalination and desulfination in chlor-alkali industry, deal with brines of very high salt concentration. The failure in establishing mathematical models that can accurately describe the NF process indicates the lack of precise understanding to the separation mechanisms involved in NF and warrantees systematic studies in well-controlled systems.

References

1. J.M.K. Timmer, Properties of nanofiltration membranes; model development and industrial application, Eindhoven: Technische Universiteit Eindhoven, 2001.
2. H. Yacubowicz and J. Yacubowicz, Nanofiltration: properties and uses, Filtration & Separation, 42 (2005) 16-21.
3. A.T. Hubbard, Encyclopedia of Surface and Colloid Science, New York: Marcel Dekker, 2002.
4. S. Sourirajan, T.Matsuura, Reverse Osmosis/Ultrafiltration Principles, National Research Council of Canada, Ottawa, Canada, 1985.
5. C.A.Patterson, Membrane Processing: State of the Art Technology, Technology Watch 2 (2005), 1-12.
6. M. Mulder, Basic Principles of Membrane Technology, Dordrecht: Kluwer Academic Publishers, 1997.
7. M. Gagliardi, Nanofiltration: Industry Report, BCC Research, September 2007.
8. R. Gloukhovski, Y. Oren, C. Linder and V. Freger, Thin-film composite nanofiltration membranes prepared by electropolymerization, Journal of Applied Electrochemistry 38 (2008) 759-766.
9. R. Sondhi, R. Bhave and G. Jung, Applications and benefits of ceramic membranes, Membrane Technology 2003 (2003) 5-8.
10. S. Condom, A. Larbot, S. A. Younssi and M. Persin, Use of ultra- and nanofiltration ceramic membranes for desalination, Desalination 168 (2004) 207-213.
11. T. Van Gestel, C. Vandecasteele, A. Buekenhoudt, C. Dotremont, J. Luyten, R. Leysen, B. Van der Bruggen and G. Maes, Alumina and titania multilayer membranes for nanofiltration: preparation, characterization and chemical stability, Journal of Membrane Science 207 (2002) 73–89.
12. C. Combe, C. Guizard, E. Aamar and V. Sanchez, Experimental determination of four characteristics used to predict the retention of a ceramic nanofiltration membrane, Journal of Membrane Science 129 (1997) 147-160.

13. W.B. Samuel de Lint, T. Zivkovic, N. E. Benes, H. J.M. Bouwmeestera and D.H.A. Blank, Electrolyte retention of supported bi-layered nanofiltration membranes, Journal of Membrane Science 277 (2006) 18–27
14. S. Benfer, P. Arki and G. Tomandl, Ceramic membranes for filtration applications – preparation and characterization, Advanced Engineering Materials 6 (2004) 495-500.
15. T. Van Gestel, C. Vandecasteele, A. Buekenhoudt, C. Dotremont, J. Luyten, R. Leysen , B. Van der Bruggen and G. Maes, Salt retention in nanofiltration with multilayer ceramic TiO2 membranes, Journal of Membrane Science 209 (2002) 379–389.
16. P. Puhlfürß, A. Voigt, R. Weber and M. Morbé, Microporous TiO2 membranes with a cut off <500 Da, Journal of Membrane Science 174 (2000) 123–133.
17. S. Benfer, U. Popp, H. Richter, C. Siewert and G. Tomandl, Development and characterization of ceramic nanofiltration membranes, Separation and Purification Technology 22-23 (2001) 231–237.
18. R. Weber, H. Chmiel and V. Mavrov, Characteristics and application of new ceramic nanofiltration membranes, Desalination 157 (2003) 113-125.
19. S. Lee and J. Cho, Comparison of ceramic and polymeric membranes for natural organic matter (NOM) removal, Desalination 160 (2004) 223-232.
20. T. Van Gestel, B. Van der Bruggen, A. Buekenhoudt, C. Dotremont, J. Luyten, R. Leysen , C. Vandecasteele and G. Maes, Surface modification of γ-Al2O3/TiO2 multilayer membranes for applications in non-polar organic solvents, Journal of Membrane Science 224 (2003) 3–10.
21. W. Kujawski, S. Krajewskaa, M. Kujawski, L. Gazagnes, A. Larbot and Michel Persin, Pervaporation properties of fluoroalkylsilane (FAS) grafted ceramic membranes, Desalination 205 (2007) 75–86.
22. T. Tsuru, M. Miyawaki, H. Kondo, T. Yoshioka and M. Asaeda, Inorganic porous membranes for nanofiltration of nonaqueous solutions, Separation and Purification Technology 32 (2003) 105-109.
23. T. Van Gestel, H. Kruidhof, D.H.A. Blank and H.J.M. Bouwmeester, ZrO2 and TiO2 membranes for nanofiltration and pervaporation: Part 1. Preparation and

characterization of a corrosion-resistant ZrO2 nanofiltration membrane with a MWCO< 300, Journal of Membrane Science 284 (2006) 128–136.

24. Y.H. See Toh, X.X. Loh, K. Li, A. Bismarck and A.G. Livingston, In search of a standard method for the characterization of organic solvent nanofiltration membranes, Journal of Membrane Science 291 (2007) 120–125.
25. L. S. White, Development of large-scale applications in organic solvent nanofiltration and pervaporation for chemical and refining processes, Journal of Membrane Science 286 (2006) 26–35.
26. D.A. Musale and A. Kumar, Solvent and pH resistance of surface crosslinked chitosan/poly(acrylonitrile) composite nanofiltration membranes, Journal of Applied Polymer Science 77 (2000) 1782–1793.
27. B.V. Bruggen, J. Geens and C. Vandecasteele, Influence of organic solvents on the performance of polymeric nanofiltration membranes, Separation and Purification Technology 37 (2002) 783–797.
28. P. Silva, S.J. Han and A.G. Livingston, Solvent transport in organic solvent nanofiltration membranes, Journal of Membrane Science 262 (2005) 49.
29. A.P. Korikov, P.B. Kosaraju and K.K. Sirkar, Interfacially polymerized hydrophilic microporous thin film composite membranes on porous polypropylene hollowfibers and flat films, Journal of Membrane Science 279 (2006) 588–600.
30. P.B. Kosaraju and K.K. Sirkar, Interfacially polymerized thin film composite membranes on microporous polypropylene supports for solvent-resistant nanofiltration, Journal of Membrane Science 321 (2008) 155–161.
31. Y.H. See Toh, F.W. Limb and A.G. Livingston, Polymeric membranes for nanofiltration in polar aprotic solvents, Journal of Membrane Science 301 (2007) 3–10.
32. A.S. Grandison and M.J. Lewis, Separation processes in the food and biotechnology industries: principles and applications, Cambridge: Woodhead Publishing Ltd., 1996.
33. I. F. J. Vankelecom, Polymeric Membranes in Catalytic Reactors, Chemical Reviews 102 (2002) 3779 -3810.
34. D. Woerner, Membrane technology in textile operations, Koch Membrane Systems, Massachusetts, USA.

35. R. Ahmad, S. Begum, E. M.V. Hoek, T. Karanfil, E. A. Genceli, A. Yadav, P. Trivedi and C. Zhang, Physico-chemical processes, Water Environment Research 76 (2004) 829-1002.
36. N. Hilal, H. Al-Zoubi, N.A. Darwish, A.W. Mohammad and M. Abu Arabi, A comprehensive review of nanofiltration membranes: treatment, pretreatment, modeling, and atomic force microscopy, Desalination 170 (2004) 281–308.
37. F.G. Donnan, Theory of membrane equilibria and membrane potentials in the presence of non-dialysing electrolytes. A contribution to physical-chemical physiology, Journal of Membrane Science 100 (1995) 45-55.
38. X. Wang, C. Zhang and P. Ouyang, The possibility of separating saccharides from a NaC1 solution by using nanofiltration in diafiltration mode, Journal of Membrane Science 204 (2002) 271-281.
39. J. Schaep, B. Van der Bruggen, C. Vandecasteele and D. Wilms, Influence of ion size and charge in nanofiltration, Separ. Purif. Technol., 14 (1998) 155-162.
40. D. Wang, M. Su, Z. Yu, X. Wang, M. Ando and T. Shintani, Separation performance of a nanofiltration membrane influenced by species and concentration of ions, Desalination 175 (2005) 219-225.
41. X.L. Wang, W.N. Wang and D.X. Wang, Experimental investigation on separation performance of nanofiltration membranes for inorganic electrolyte solutions, Desalination 145 (2002) 115-122.
42. J. Tanninen, M. Mänttäri and M. Nyström, Effect of salt mixture concentration on fractionation with NF membranes, Journal of Membrane Science 283 (2006) 57–64.
43. J. Schaep and C. Vandecasteele, Evaluating the charge of nanofiltration membranes, Journal of Membrane Science 188 (2001) 129-136.
44. S. Szoke, G. Patzay and L. Weiser, Characteristics of thin-film nanofiltration membranes at various pH-values, Desalination 151 (2002) 123-129.
45. J. Tanninen, S. Platt, A. Weis and M. Nyström, Long-term acid resistance and selectivity of NF membranes in very acidic conditions, Journal of Membrane Science 240 (2004) 11–18.
46. M. R. Teixeira, M. J. Rosa and M. Nystrom, The role of membrane charge on nanofiltration performance, Journal of Membrane Science 265 (2005) 160–166.

47. K. Boussu, Y. Zhang, J. Cocquyt, P. Van der Meeren, A. Volodin, C. Van Haesendonck, J.A. Martens and B. Van der Bruggen, Characterization of polymeric membranes for systematic analysis of membrane performance, Journal of Membrane Science 278 (2006) 418–427.
48. R. R. Sharma and S. Chellam, Temperature and concentration effects on electrolyte transport across porous thin-film composite nanofiltration membranes: Pore transport mechanisms and energetics of permeation, Journal of Colloid and Interface Science 298 (2006) 327–340.
49. D. Wang, X. Wang, Y. Tomi, M. Ando and T. Shintani, Modeling the separation performance of nanofiltration membranes for the mixed salts solution, Journal of Membrane Science 280 (2006) 734–743.
50. J. D. Ferry, Statistical evaluation of sieve constants in ultrafiltration, Journal of General Physiology 20 (1936) 95-104.
51. J. R. Pappenheimer, E.M. Renkin and L.M. Borrero, Filtration, diffusion and molecular sieving though peripheral capillary membranes. A contribution to the pore theory of capillary permeability, American Journal of Physiology 167 (1951) 13-46.
52. E.M. Renkin, Filtration, diffusion, and molecular sieving through porous cellulose membranes, Journal of General Physiology 38 (1954) 225-243.
53. J.G. Wijmans and R.W. Baker, The solution-diffusion model: a review, Journal of Membrane Science 107 (1995) 1-21.
54. K. S. Spiegler and O. Kedem, Thermodynamics of hyperfiltration (reverse osmosis): Criteria for efficient membranes, Desalination 1 (1966) 311-326.
55. O. Kedem and A. Katchalsky, Permeability of composite membranes. Part 1. – Electric current, volume flow and flow of solute through membranes, Transactions of the Faraday Society 59 (1963) 1918-1930.
56. M. Perry and C. Linder, Intermediate reverse osmosis ultrafiltration (RO UF) membranes for concentration and desalting of low molecular weight organic solutes, Desalination 71 (1989) 233-245.
57. X. Xu and H. G. Spencer, Dye-salt separations by nanofiltration using weak acid polyelectrolyte membranes, Desalination 114 (1997) 129-137.

58. P. Schirg and F. Widmer, Characterisation of nanofiltration membranes for the separation of aqueous dye-salt solutions, Desalination 89 (1992) 89-107.
59. R. Levenstein, D. Hasson and R. Semiat, Utilization of the Donnan effect for improving electrolyte separation with nanofiltration membranes, Journal of Membrane Science 116 (1996) 77-92.
60. B. Van der Bruggen and C. Vandecasteele, Modelling of the retention of uncharged molecules with nanofiltration, Water Research 36 (2002) 1360–1368.
61. K. Meyer, J. Sievers, La Permeabilite des membranes 1. Theorie del a Permeabilite Ionique, Helv. Chim. Acta 19 (1936) 649-664.
62. T. Teorell, Transport processes and electrical phenomena in ionic membranes, Prog. Biophys. 3 (1953) 305.
63. F.A. Morrisson, J.F. Osterle, Electrokinetic energy conversion in ultrafine capillaries, J. Chem. Phys. 43 (1965) 2111-2115.
64. R.J. Gross, J.F. Osterle, Membrane transport characteristics of ultrafine capillaries, J. Chem. Phys. 49 (1968) 228-234.
65. X. L. Wang, T. Tsuru, S. Nakao and Shoji Kimura, Electrolyte transport through nanofiltration membranes by the space-charge model and the comparison with Teorell-Meyer-Sievers model, Journal of Membrane Science 103 (1995) 117-133.
66. A. Szymczyk, P. Fievet, B. Aoubiza, C. Simon and J. Pagetti, An application of the space charge model to the electrolyte conductivity inside a charged microporous membrane, Journal of Membrane Science 161 (1999) 275-285.
67. T. Tsuru, S. Nakao and S. Kimura, Calculation of ion rejection by extended Nernst-Planck equation with charged reverse osmosis membranes for single and mixed electrolyte solutions, J. Chem. Eng. Japan 24 (1991) 511-517.
68. X.L. Wang, T. Tsuru, M. Togoh, S. Nakao and S. Kimura, Transport of organic electrolytes with electrostatic and steric- hindrance effects through nanofiltration membranes, J. Chem. Eng. Japan 28 (1995) 372-380.
69. X.L. Wang, T. Tsuru, S. Nakao and S. Kimura, The electrostatic and steric-hindrance model for the transport of charged solutes through nanofiltration membranes, J. Membr. Sci. 135 (1997) 19-32.

70. W. R. Bowen and H. Mukhtar, Characterisation and prediction of separation performance of nanofiltration membranes, J. Membr. Sci. 112 (1996) 263-274.
71. W.R. Bowen, A. Mohammad and N. Hilal, Characterization of nanofiltration membranes for predictive purposes use of salts, uncharged solutes and atomic force microscopy, J. Membr. Sci. 126 (1997) 91-105.
72. S. Nakao and S. Kimura, Models of membrane transport phenomena and their applications for ultrafiltration data, J. Chem. Eng. Japan 15 (1982) 200–205.
73. W. R. Bowen and A. W. Mohammad, Diafiltration by nanofiltration: prediction and optimization, AIChE Journal 44 (1998) 1799–1812.
74. W.R. Bowen, A. Mohammad and N. Hilal, Characterisation of nanofiltration membranes for predictive purposes use of salts, uncharged solutes and atomic force microscopy, J. Membr. Sci. 126 (1997) 91-105.
75. J. Schaep, C. Vandecasteele, A.W. Mohammad and W.R. Bowen, Evaluation of the salt retention of nanofiltration membranes using the Dorman and steric partitioning model, Separ. Sci. Technol. 34 (15) (1999) 3009-3030.
76. C. Labbez, P. Fievet, A. Szymczyk, A. Vidonne, A. Foissy and J. Pagetti, Analysis of the salt retention of a titania membrane using the "DSPM" model: effect of pH, salt concentration and nature, Journal of Membrane Science 208 (2002) 315–329.
77. C. Labbez, P. Fievet, F. Thomas, A. Szymczyk, A. Vidonne, A. Foissy and J. Pagetti, Evaluation of the "DSPM" model on a titania membrane: measurements of charged and uncharged solute retention, electrokinetic charge, pore size, and water permeability, Journal of Colloid and Interface Science 262 (2003) 200–211.
78. B. Cuartas-Uribe, M.C. Vincent-Vela, S. Alvarez-Blanco, M.I. Alcaina-Miranda and E. Soriano-Costa, Prediction of solute rejection in nanofiltration processes using different mathematical models, Desalination 200 (2006) 144-145.
79. W. Bowen and J. Welfoot, Modelling of membrane nanofiltration -- pore size distribution effects, Chem. Engin. Sci. 57 (2002) 1393-1407.
80. W.R. Bowen and J.S. Welfoot, Modelling the performance of membrane nanofiltration-critical assessment and model development, Chem. Engin. Sci. 57 (2002) 1121-1137.

81. W.R. Bowen and J.S. Welfoot, Predictive modelling of nanofiltration: membrane specification and process optimisation, Desalination 147 (2002) 97-203.
82. S. Bandini and D. Vezzani, Nanofiltration modeling: the role of dielectric exclusion in membrane characterization, Chem. Engin. Sci. 58 (2003) 3303-3326.
83. A. E. Yaroshchuk, Recent progress in the transport characterization of nanofiltration membranes, Desalination 149 (2002) 423-428.
84. A. E. Yaroshchuk, Dielectric exclusion of ions from membranes, Advances in Colloid and Interface Science 85 (2000) 193-230.
85. A. E. Yaroshchuk, Non-steric mechanisms of nanofiltration: superposition of Donnan and dielectric exclusion, Separation and Purification Technology 22-23 (2001) 143–158.
86. A. Szymczyk, P. Fievet and C. Ramseyer, Dielectric constant of electrolyte solutions confined in a charged nanofiltration membrane, Desalination 200 (2006) 125-126.
87. A.W. Mohammad, N. Hilal, H. Al-Zoubi and N.A. Darwish, Prediction of permeate fluxes and rejections of highly concentrated salts in nanofiltration membranes, Journal of membrane science 289 (2007) 40-50.
88. A. Santafé-Moros, J.M. Gozálvez-Zafrilla and J. Lora-García, Applicability of the DSPM with dielectric exclusion to a high rejection nanofiltration membrane in the separation of nitrate solutions, Desalination 221 (2008) 268–276.
89. A.A. Hussain, M.E.E. Abashar and I.S. Al-Mutaz, Effect of ion sizes on separation characteristics of nanofiltration membrane systems, Journal of King Saud university (Engineering Sciences) 19 (2006) 1-19.
90. A.A. Hussain, M.E.E. Abashar and I.S. Al-Mutaz, Influence of ion size on the prediction of nanofiltration membrane systems, Desalination 214 (2007) 150–166.
91. A. Szymczyk and P. Fievet, Investigating transport properties of nanofiltration membranes by means of a steric, electric and dielectric exclusion model, Journal of Membrane Science 252 (2005) 77–88.
92. A.A. Rashin and B. Honig, Reevaluation of the Born model of ion hydration, J. Phys. Chem. 89 (1985) 5588–5593.
93. A. Szymczyk and P. Fievet, Ion transport through nanofiltration membranes: the steric, electric and dielectric exclusion model, Desalination 200 (2006) 122–124.

94. N. Fatin-Rouge, A. Szymczyk, E. Ozdemir, A. Vidonne and P. Fievet, Retention of single and mixed inorganic electrolytes by a polyamide nanofiltration membrane, Desalination 200 (2006) 133–134.
95. A. Szymczyk, N. Fatin-Rouge, P. Fievet, C. Ramseyer and A. Vidonne, Identification of dielectric effects in nanofiltration of metallic salts, Journal of Membrane Science 287 (2007) 102–110.
96. J. Garcia-Aleman and J. M. Dickson, Mathematical modeling of nanofiltration membranes with mixed electrolyte solutions, Journal of Membrane Science 235 (2004) 1–13.
97. J. Straatsma, G. Bargeman, H.C. van der Horst and J.A.Wesselingh, Can nanofiltration be fully predicted by a model? J. Membr. Sci. 198 (2002) 273-284.
98. P. Bacchin, P. Aimar and R.W. Field, Critical and sustainable fluxes: Theory, experiments and applications, J. Membr. Sci. 281 (2006) 42-69.
99. T. Thorsen, Concentration polarisation by natural organic matter (NOM) in NF and UF, Journal of Membrane Science 233 (2004) 79–91.
100. V. Geraldes, V. Semião and M.N de Pinho, Concentration polarisation and flow structure within nanofiltration spiral-wound modules with ladder-type spacers, Computers and Structures 82 (2004) 1561–1568.
101. V. Geraldes, V. Semião and M.N de Pinho, Hydrodynamics and concentration polarization in NF/RO spiral-wound modules with ladder-type spacers, Desalination 157 (2003) 395-402.
102. V. Geraldes, V. Semião and M.N de Pinho, The effect of the ladder-type spacers configuration in NF spiral-wound modules on the concentration boundary layers disruption, Desalination 146 (2002) 187-194.
103. M.N. de Pinho, V. Semião and V. Geraldes, Integrated modeling of transport processes in fluid/ nanofiltration membrane systems, J. Membr. Sci., 195 (2002) 1-12.
104. V. Geraldes, V. Semião and M.N de Pinho, Flow and mass transfer modelling of nanofiltration, J. Membr. Sci. 191 (2001) 109-128.

105. V. Geraldes and M.D. Afonso, Prediction of the concentration polarization in the nanofiltration/reverse osmosis of dilute multi-ionic solutions, Journal of Membrane Science 300 (2007) 20–27.
106. V. Geraldes and M.D. Afonso, Generalized mass-transfer correction factor for nanofiltration and reverse osmosis, AIChE Journal 52 (2006) 3353-3362.
107. S.-C. Tu, V. Ravindran and M. Pirbazari, A pore diffusion transport model for forecasting the performance of membrane processes, Journal of Membrane Science 265 (2005) 29–50.
108. N. Park, B. Kwon, I. S. Kim and J. Cho, Biofouling potential of various NF membranes with respect to bacteria and their soluble microbial products (SMP): Characterizations, flux decline, and transport parameters, Journal of Membrane Science 258 (2005) 43–54.
109. S. Bhattacharjee and G. M. Johnston, A model of membrane fouling by salt precipitation from multicomponent ionic mixtures in crossflow nanofiltration, Environmental Engineering Science 19 (2002) 399–412.
110. C.-J. Lin, S. Shirazi and P. Rao, Mechanistic model for CaSO4 fouling on nanofiltration membrane, Journal of Environmental Engineering 131 (2005) 1387–1392.
111. R. Rautenbach and Th. Linn, High pressure reverse osmosis and nanofiltration, a "zero discharge" process combination for the treatment of waste water with severe fouling/sealing potential, Desalination, 105 (1996) 63-70.
112. R. Rautenbach, Th. Linn and L. Eilers, Treatment of severely contaminated waste water by a combination of RO, high-pressure RO and NF - potential and limits of the process, J. Membr. Sci. 174 (2000) 231-241.
113. V. Geraldes and M. de Pinho, Process water recovery from pulp bleaching effluents by an NF/ED hybrid process, J. Membr. Sci. 102 (1995) 209-221.
114. T.-H. Kim, C. Park and S. Kim, Water recycling from desalination and purification process of reactive dye manufacturing industry by combined membrane filtration, Journal of Cleaner Production 13 (2005) 779-786.

115. J.-J. Qin, M. H. Oo and K. A. Kekre, Nanofiltration for recovering wastewater from a specific dyeing facility, Separation and Purification Technology 56 (2007) 199–203.

116. P. Schoeberl, M. Brik, R. Braun and W. Fuchs, Treatment and recycling of textile wastewater - case study and development of a recycling concept, Desalination 171 (2004) 173-183.

117. V. Kopecký and P. Mikulášek, Desalination of reactive yellow 85 by Nanofiltration, Environment Protection Engineering 31 (2005) 187-198.

118. M.G. Buonomenna, L.C. Lopez, P. Favia, R. d'Agostino, A. Gordano and E. Drioli, New PVDF membranes: The effect of plasma surface modification on retention in nanofiltration of aqueous solution containing organic compounds, Water Research 41 (2007) 4309-4316.

119. I. Koyuncu, Influence of dyes, salts and auxiliary chemicals on the nanofiltration of reactive dye baths: experimental observations and model verification, Desalination 154 (2003) 79-88.

120. Z. Ji, Y. He and G. Zhang, Treatment of wastewater during the production of reactive dyestuff using a spiral nanofiltration membrane system, Desalination 201 (2006) 255–266.

121. M. Marcucci, G. Nosenzo, G. Capannelli, I. Ciabatti, D. Corrieri and G. Ciardelli, Treatment and reuse of textile effluents based on new ultrafiltration and other membrane technologies, Desalination 138 (2001) 75-82.

122. R. Żyłła, J. Sójka-Ledakowicz, E. Stelmach and S. Ledakowciz, Coupling of membrane filtration with biological methods for textile wastewater treatment, Desalination 198 (2006) 316–325.

123. I.-C. Kim and K.-H. Lee, Dyeing process wastewater treatment using fouling resistant nanofiltration and reverse osmosis membranes, Desalination 192 (2006) 246–251.

124. C. Allègre, P. Moulin, M. Maisseu and F. Charbit, Treatment and reuse of reactive dyeing effluents, Journal of Membrane Science 269 (2006) 15–34.

125. I. Voigt, M. Stahn, St. Wöhner, A. Junghans, J. Rost and W. Voigt, Integrated cleaning of coloured waste water by ceramic NF membranes, Sep. Purifi. Technol. 25 (2001) 509-512.
126. G.T. Tellez, N. Nirmalakhandan and J.L. Gardea-Torresdey, Evaluation of biokinetic coefficients in degradation of oilfield produced water under varying salt concentrations, Water Research 29 (1995) 1711–1718.
127. M. Çakmakcı, N. Kayaalp and I. Koyuncu, Desalination of produced water from oil production fields by membrane processes, Desalination 222 (2008) 176–186.
128. C. Visvanathan, P. Svenstrup and P. Ariyamethee, Volume reduction of produced water generated from natural gas production process using membrane technology, Water Science and Technology 41 (2000) 117-123.
129. H.A. Qdaisa and H. Moussa, Removal of heavy metals from wastewater by membrane processes: a comparative study, Desalination 164 (2004) 105-110.
130. M.G. Khedr, Membrane methods in tailoring simpler, more efficient, and cost effective wastewater treatment alternatives, Desalination 222 (2008) 135–145.
131. L. Feini, Z. Guoliang, M. Qin and Z. Hongzi, Performance of Nanofiltration and Reverse Osmosis Membranes in Metal Effluent Treatment, Chinese Journal of Chemical Engineering 16 (2008) 441-445.
132. K. Kimura, G. Amy, J. E. Drewes, T. Heberer, T.-U. Kim and Y. Watanabe, Rejection of organic micropollutants (disinfection by-products, endocrine disrupting compounds, and pharmaceutically active compounds) by NF/RO membranes, Journal of Membrane Science 227 (2003) 113–121.
133. S. A. Snyder, S. Adham, A. M. Redding, F.S. Cannon, J. DeCarolis, J. Oppenheimer, E.C. Wert and Y. Yoon, Role of membranes and activated carbon in the removal of endocrine disruptors and pharmaceuticals, Desalination 202 (2007) 156–181.
134. S. D. Kim, J. Cho, I. S. Kim, B. J. Vanderford and S. A. Snyder, Occurrence and removal of pharmaceuticals and endocrine disruptors in South Korean surface, drinking, and waste waters, Water Research 41 (2007) 1013-1021.
135. Y. Yoon, P. Westerhoff, S. A. Snyder, E. C. Wert and J. Yoon, Removal of endocrine disrupting compounds and pharmaceuticals by nanofiltration and ultrafiltration membranes, Desalination 202 (2007) 16–23.

136. Y. Yoon, P. Westerhoff, S. A. Snyder and E. C. Wert, Nanofiltration and ultrafiltration of endocrine disrupting compounds, pharmaceuticals and personal care products, Journal of Membrane Science 270 (2006) 88–100.
137. K. Košutić, D. Dolar, D. Ašperger and B. Kunst, Removal of antibiotics from a model wastewater by RO/NF membranes, Separation and Purification Technology 53 (2007) 244–249.
138. M. Frappart, O. Akoum, L. H. Ding and M. Y. Jaffrin, Treatment of dairy process waters modelled by diluted milk using dynamic nanofiltration with a rotating disk module, Journal of Membrane Science 282 (2006) 465–472.
139. B. Balannec, M. Vourch, M. Rabiller-Baudry and B. Chaufer, Comparative study of different nanofiltration and reverse osmosis membranes for dairy effluent treatment by dead-end filtration, Separation and Purification Technology 42 (2005) 195–200.
140. M. Turan, Influence of filtration conditions on the performance of nanofiltration and reverse osmosis membranes in dairy wastewater treatment, Desalination 170 (2004) 83-90.
141. B. Balannec, G. Gésan-Guiziou, B. Chaufer, M. Rabiller-Baudry and G. Daufin, Treatment of dairy process waters by membrane operations for water reuse and milk constituents concentration, Desalination 147 (2002) 89-94.
142. M. Nguyen, N. Reynolds and S. Vigneswaran, By-product recovery from cottage cheese production by nanofiltration, Journal of Cleaner Production 11 (2003) 803–807.
143. V. Mavrov and E. Bélières, Reduction of water consumption and wastewater quantities in the food industry by water recycling using membrane processes, Desalination 131 (2000) 75-86.
144. M. Vourch, B. Balannec, B. Chaufer and G. Dorange, Nanofiltration and reverse osmosis of model process waters from the dairy industry to produce water for reuse, Desalination 172 (2005) 245-256.
145. R. Atra, G. Vatai, E. Bekassy-Molnar and A. Balint, Investigation of ultra- and nanofiltration for utilization of whey protein and lactose, Journal of Food Engineering 67 (2005) 325–332.

146. I. Koyuncu, M. Turan, D. Topacik and A. Ates, Application of low pressure nanofiltration membranes for the recovery and reuse of dairy industry effluents, Water Science and Technology 41 (2000) 213-221.

147. J. Schaep, B. Van der Bruggen, S. Uytterhoeven, R. Croux, C. Vandecasteele, D. Wilms, E. Van Houtte and F. Vanlerberghe, Removal of hardness from groundwater by nanofiltration, Desalination 119 (1998) 295-302.

148. H.D.M Sombekke, D.K. Voorhoeve and P. Hiemstra, Environmental impact assessment of groundwater treatment with nanofiltration, Desalination, 113 (1997) 293-296.

149. B. Van der Bruggen, J. Schaep, W. Maes, D. Wilms and C. Vandecasteele, Nanofiltration as a treatment method for the removal of pesticides from ground waters, Desalination 117 (1998) 139-147.

150. M. Alborzfar, K. Escande and S.J. Allen, Removal of natural organic matter from two types of humic ground waters by nanofiltration, Water Res., 32 (1998) 2970-2983.

151. C Reiss, J. Taylor and C. Robert, Surface water treatment using nanofiltration--pilot testing results and design considerations, Desalination, 125 (1999) 97-112.

152. J. De Witte, Surface water potabilisation by means of a novel nanofiltration element, Desalination 108 (1997) 153-157.

153. M. Thanuttamavong, K. Yamamotob, J. Oh, K. Chood and S. Choi, Rejection characteristics of organic and inorganic pollutants by ultra low- pressure nanofiltration of surface water for drinking water treatment, Desalination 145 (2002) 257-264.

154. M. D. Afonso, J.O. Jaber and M.S. Mohsen, Brackish groundwater treatment by reverse osmosis in Jordan, Desalination 164 (2004) 157-171.

155. T. V. Nguyen, S. Vigneswaran, H. H. Ngo, D. Pokhrel and T. Viraraghavan, Specific treatment technologies for removing arsenic from water, Eng. Life Sci. 6 (2006) 86-90.

156. K. Košutić, L. Furač, L. Sipos and B. Kunst, Removal of arsenic and pesticides from drinking water by nanofiltration membranes, Separation and Purification Technology 42 (2005) 137–144.

157. J.-I. Oh, S.-H. Lee and K. Yamamoto, Relationship between molar volume and rejection of arsenic species in groundwater by low-pressure nanofiltration process, Journal of Membrane Science 234 (2004) 167–175.
158. H. Saitúa, M. Campderrós, S. Cerutti and A. P. Padilla, Effect of operating conditions in removal of arsenic from water by nanofiltration membrane, Desalination 172 (2005) 173-180.
159. A.I. Schäfer and B.S. Richards, Testing of a hybrid membrane system for groundwater desalination in an Australian national park, Desalination 183 (2005) 55–62.
160. B. Van der Bruggen, K. Everaert, D. Wilms and C. Vandecasteele, Application of nanofiltration for removal of pesticides, nitrate and hardness from ground water: rejection properties and economic evaluation, Journal of Membrane Science 193 (2001) 239–248.
161. K. Walha, R.B. Amar, L. Firdaous, F. Quéméneur and P. Jaouen, Brackish groundwater treatment by nanofiltration, reverse osmosis and electrodialysis in Tunisia: performance and cost comparison, Desalination 207 (2007) 95–106.
162. K. Košutić, I. Novak, L. Sipos and B. Kunst, Removal of sulfates and other inorganics from potable water by nanofiltration membranes of characterized porosity, Separation and Purification Technology 37 (2004) 177–185.
163. M. Tahaikt, R. El Habbani, A. Ait Haddou, I. Achary, Z. Amor, M. Taky, A. Alami, A. Boughriba, M. Hafsi and A. Elmidaoui, Fluoride removal from groundwater by nanofiltration, Desalination 212 (2007) 46–53.
164. M. Pontié, H. Dach, J. Leparc, M. Hafsi and A. Lhassani, Novel approach combining physico-chemical characterizations and mass transfer modelling of nanofiltration and low pressure reverse osmosis membranes for brackish water desalination intensification, Desalination 221 (2008) 174–191.
165. K. Hu and J. M. Dickson, Nanofiltration membrane performance on fluoride removal from water, Journal of Membrane Science 279 (2006) 529–538.
166. B. Van der Bruggen, K. Everaert, D. Wilms and C. Vandecasteele, Application of nanofiltration for removal of pesticides, nitrate and hardness from ground water:

rejection properties and economic evaluation, Journal of Membrane Science 193 (2001) 239–248.

167. A. Santafé-Moros, J.M. Gozálvez-Zafrilla and J. Lora-García, Performance of commercial nanofiltration membranes in the removal of nitrate ions, Desalination 185 (2005) 281–287.

168. A. Greenfly, D. Velázquez-Pardon and F.H. Frame, Nanofiltration of a German groundwater of high hardness and NOM content: performance and costs, Desalination 15 1 (2002) 253-265.

169. S. Lee and C.-H. Lee, Effect of membrane properties and pretreatment on flux and NOM rejection in surface water nanofiltration, Separation and Purification Technology 56 (2007) 1–8.

170. M.D. Petala and A.I. Zouboulis, Vibratory shear enhanced processing membrane filtration applied for the removal of natural organic matter from surface waters, Journal of Membrane Science 269 (2006) 1–14.

171. K. Hu and J. M. Dickson, Nanofiltration membrane performance on fluoride removal from water, Journal of Membrane Science 279 (2006) 529–538.

172. M. R. Teixeira and M. J. Rosa, The impact of the water background inorganic matrix on the natural organic matter removal by nanofiltration, Journal of Membrane Science 279 (2006) 513–520.

173. B. Van der Bruggen and C. Vandecasteele, Removal of pollutants from surface water and groundwater by nanofiltration: overview of possible applications in the drinking water industry, Environmental Pollution 122 (2003) 435–445.

174. T. Peters, D. Pintó and E. Pintó, Improved seawater intake and pre-treatment system based on Neodren technology, Desalination 203 (2007) 134–140.

175. S.C.J.M. van Hoof, J.G. Minnery and B. Mack, Dead-end ultrafiltration as alternative pre-treatment to reverse osmosis in seawater desalination: a case study, Desalination 139 (2001) 161-168.

176. M. AI-Ahmad and F. Abdul Aleem, Scale formation and fouling problems effect on the performance of MSF and RO desalination, plants in Saudi Arabia, Desalination 93 (1993) 287-310.

177. S. Bou-Hamad, M. Abdel-Jawad, S. Ebrahim, M. AI-Mansour and A. A1-Hijji, Performance evaluation of three different pretreatment systems for seawater reverse osmosis technique, Desalination 110 (1997) 85-92.
178. S.C.J.M. van Hoof, A. Hashim and A.J. Kordes, The effect of ultrafiltration as pretreatment to reverse osmosis in wastewater reuse and seawater desalination applications, Desalination, 124 (1999) 231-242.
179. J.A. Redondo, Brackish-, sea- and wastewater desalination, Desalination 138 (2001) 29-40.
180. A. Brehant, V. Bonnelye and M. Perez, Comparison of MF/UF pretreatment with conventional filtration prior to RO membranes for surface seawater desalination, Desalination 144 (2002) 353-360.
181. A. Hassan, M. A1-Sofi, A. A1-Amoudi, A. Jamaluddin, A. Farooque, A. Rowaili, A. Dalvi, N. Kither, G. Mustafa and I. AI-Tisan, A new approach to thermal seawater desalination processes using nanofiltration membranes (Part 1), Desalination 118 (1998) 35-51.
182. A. Hassan, A. Farooque, A. Jamaluddin, A. A1-Amoudi, M. A1-Sofi, A. AI-Rubaian, N. Kither, I. Al.-Tisan and A. Rowaili, A demonstration plant based on the new NF-SWRO process, Desalination 131 (2000) 157-171.
183. A.S. A1-Amoudi and A.M. Farooque, Performance restoration and autopsy of NF membranes used in seawater pretreatment, Desalination 178 (2005) 261-271.
184. O.A. Hamed, Overview of hybrid desalination systems – current status and future prospects, Desalination 186 (2005) 207-214.
185. M. Turek and P. Dydo, Hybrid membrane - thermal versus simple membrane system, Desalination 157 (2003) 51-56.
186. C.J. Harrison, Y.A. Le Gouellec, R.C. Cheng and A.E. Childress, Bench-Scale testing of nanofiltration for seawater desalination, Journal of Environmental Engineering 133 (2007) 1004-1014.
187. N. Hilal, H. Al-Zoubi, N.A. Darwish and A.W. Mohammad, Performance of nanofiltration membranes in the treatment of synthetic and real seawater, Separation Science and Technology 42 (2007) 493-515.

188. N. Hilal, H. Al-Zoubi, A.W. Mohammad and , N.A. Darwish, Nanofiltration of highly concentrated salt solutions up to seawater salinity, Desalination 184 (2005) 315–326.
189. M. Pontié, A. Lhassani, C.K. Diawara, A. Elana, C. Innocent, D. Aureau, M. Rumeau, J.P. Croue, H. Buisson, and P. Hemery, Seawater nanofiltration for the elaboration of usable salty waters, Desalination 167 (2004) 347-355.
190. D. Bessarabov and Z. Twardowski, Industrial application of nanofiltration – new perspectives, Membrane Technology 2002 (2002) 6-9.
191. L. Meihong, Y. Sanchuan, Z. Yong and G. Congjie, Study on the thin-film composite nanofiltration membrane for the removal of sulfate from concentrated salt aqueous: Preparation and performance, Journal of Membrane Science 310 (2008) 289–295.
192. H.M. Krieg, S.J. Modise, K. Keizer and H.W.J.P. Neomagus, Salt rejection in nanofiltration for single and binary salt mixtures in view of sulphate removal, Desalination 171 (2004) 205-215.
193. A. Barr, Sulphate removal by nanofiltration, Filtration & Separation 38 (2001) 18-20.
194. S.S. Madaeni and V. Kazemi, Treatment of saturated brine in chlor-alkali process using membranes, Separation and Purification Technology 61 (2008) 68–74.
195. K.Y. Wang, T.-S. Chung and R. Rajagopalan, Novel Polybenzimidazole (PBI) Nanofiltration Membranes for the Separation of Sulfate and Chromate from High Alkalinity Brine To Facilitate the Chlor-Alkali Process, Ind. Eng. Chem. Res. 46 (2007) 1572-1577.
196. M. Yuan, A.C. Todd and K. S. Sorbie, Sulphate scale precipitation arising from seawater injection: a prediction study, Marine and Petroleum Geology , 11 (1994) 24-30.
197. M.S.H. Bader, Sulfate scale problems in oil fields water injection operations, Desalination 201 (2006) 100–105.
198. M.S.H. Bader, Innovative technologies to solve oil-fields water injection sulfate problems, Desalination 201 (2006) 121–129.

199. M.S.H. Bader, Sulfate removal technologies for oil fields seawater injection operations, Journal of Petroleum Science and Engineering 55 (2007) 93–110.
200. M.S.H. Bader, Analysis of the Paradox Valley brine desulfation by nanofiltration, Desalination 229 (2008) 33–51.
201. M.S.H. Bader, Nanofiltration for oil-fields water injection operations: analysis of osmotic pressure and scale tendency, Desalination 201 (2006) 114–120.
202. M.S.H. Bader, Nanofiltration for oil-fields water injection operations: analysis of concentration polarization, Desalination 201 (2006) 106–113.
203. C. Christy and S. Vermant, The state-of-the-art of filtration in recovery processes for biopharmaceutical production, Desalination 147 (2002) 1-4.
204. J.P. Sheth, Y.J. Qin, K.K. Sirkar and B.C. Baltzis, Nanofiltration-based diafiltration process for solvent exchange in pharmaceutical manufacturing, J. Membr. Sci. 211 (2003) 251-261.
205. W. Zhang, G.H. He, P. Gao and G.H. Chen, Development and characterization of composite nanofiltration membranes and their application in concentration of antibiotics, Sep. Purif. Technol. 30 (2003) 27-35.
206. K.Y. Wang and T.-S. Chung, The characterization of flat composite nanofiltration membranes and their applications in the separation of Cephalexin, Journal of Membrane Science 247 (2005) 37–50.
207. T. Tsuru, T. Shutou, S.I. Nakao and S. Kimura, Peptide and amino acid separation with nanofiltration membranes, Sep. Sci. Technol. 29 (1994) 971-984.
208. S.L. Li, C. Li, Y.S. Liu, X.L. Wang and Z.A. Cao, Separation of l-glutamine from fermentation broth by nanofiltration, J. Membr. Sci. 222 (2003) 191-201.
209. A. Garem, G. Daufin, J.L. Maubois, B. Chaufer and J. Leonil, Selective separation of amino acids with a charged inorganic nanofiltration membrane: effect of physicochemical parameters on selectivity, Biotech. Bioeng. 54 (1997) 291-302.
210. D. Jakobs and G. Baumgarten, Nanofiltration of nitric acidic solutions from Picture Tube production, Desalination 145 (2002) 65-68.
211. M. Wengel and G. Gleixner, Preparative isolation and characterization of heavy metal complexes from acid mine drainage and surface wastewater, Acta hydrochim. hydrobiol. 34 (2006) 568 – 578.

212. M. Mänttäri, T. Pekuri and M. Nyström, NF270, a new membrane having promising characteristics and being suitable for treatment of dilute effluents from the paper industry, Journal of Membrane Science 242 (2004) 107–116.
213. M. Mänttäri, K. Viitikko and M. Nyström, Nanofiltration of biologically treated effluents from the pulp and paper industry, Journal of Membrane Science 272 (2006) 152–160.
214. M. Mänttäri and M. Nyström, Ultrafiltration and nanofiltration in the pulp and paper industry using cross-rotational (CR) filters, Water Science & Technology 50 (2004) 229–238.

Chapter 3: Modified SK model for prediction of the flux and rejection of NF separation of concentrated NaCl solution: theories and model development

3.1 Introduction

Until recently, most of the research literature in NF performance and modelling published within the last 40 years or so dealt with low concentration salt solutions (< 0.1 M). This is understandable given that the majority of the modelling efforts reviewed in Section 2.3 were developed based on the assumption of "diluted solution". However, as evident from Table 3.1, concentrated aqueous solutions are commonly involved in many important industrial separation processes.

Table 3.1 Applications of NF dealing with high salt concentrations

Application	Typical feedwater characteristics (NaCl)	
	($g\ L^{-1}$)	(M)
Chlor-alkali process	~180 - 250	~3 - 4
Organic synthesis & food processes	~ 200	~3
Coal-mine brines purification	~100 - 125	~2
Seawater desalination	~ 25	~0.4 - 0.5

Thus, the prevalence of high electrolyte concentrations in real industrial applications demands NF transport models capable of carrying out reliable plant design simulations. It has been widely observed that filtration operations of concentrated salt solutions considerably degrade the performance (reduced rejections and decreased volumetric fluxes) of NF membranes. The following approach of Kedem and Katchalsky [1], based on

irreversible thermodynamics, is commonly applied for the determination of volumetric flux, J_v, for NF of aqueous solutions.

$$J_v = L_p(\Delta P - \sigma\Delta\pi) \qquad [3.1]$$

where L_p is the hydraulic permeability of the membrane, ΔP is the trans-membrane pressure, σ is the reflection coefficient, and $\Delta\pi$ is the osmotic pressure. In most cases, when the solute is almost completely rejected, $\sigma \to 1$, the above equation can be simplified as follows:

$$J_v = L_p\Delta P_e \qquad [3.2]$$

where $\Delta P_e = \Delta P - \Delta\pi$, is the effective pressure driving force.

Several authors have related the hydraulic permeability (L_p) to the solvent viscosity (μ) and the effective membrane thickness, Δx by means of a Hagen-Poiseuille-type relationship [2]:

$$L_p = \frac{r_p^2}{8\mu\Delta x} \qquad [3.3]$$

where r_p is the average membrane pore radius.

Since AFM measurements now indicate that most NF membranes have a porous structure with pore dimensions ~ 1 nm, the use of a Hagen-Poiseuille-type equation is justified.

Nyström et al. [3] attributed the significant reduction in the permeate flux with salt concentration to the osmotic pressure difference. Conversely, Braghetta et al. [4] noted that osmotic pressure alone could not account for the 10% decrease in permeate flux observed in their experiments with sodium chloride. Similarly, Freger et al. [5] proposed that an additional cause besides trans-membrane pressure reduction and viscosity correction was responsible for the observed flux reduction in single salt experiments.

A widely accepted explanation for the gradual attenuation of permeate flux with salt concentration is the increased shielding of the membrane charge at high ionic strengths. In

the case of NaCl solutions, the mechanism of charge screening and decreased electrostatic double layer can be sufficiently applied to explain the decrease in salt retention with increasing concentration. The reduced membrane charge implies that steric hindrance remains the only exclusion factor, thereby, allowing more co-ions to penetrate the membrane. However, the influence of the charge screening mechanism on the permeate flux remains unclear and inadequately explained in the literature.

Lint et al. [6] theoretically investigated ion retention and solvent flow through a charged NF membrane using a charge regulation model combined with the Hagen-Poiseuille equation. Their simulations predicted that at sufficiently high salt concentrations, the potential gradient across the membrane vanishes since the membrane becomes uncharged and the solvent velocity approaches a maximum, contrary to what is observed in experiments with NF membranes.

Boussu et al. [7] hypothesized that shielding of the membrane charge at high NaCl concentrations resulted in reduced ion repulsion from the pores and hence, increased pore blocking and lower fluxes. On the other hand, Braghetta et al. [4] explained that the reduced charge of the membrane matrix at high ionic concentrations resulted in membrane compaction (membrane polymers coming close to one another) and a reduced interstitial pore volume and hence, lower permeability.

Alternative explanations for the loss of flux with increasing ionic strength can also be found in literature. According to Bargeman et al. [8], the electrostatic effect was enhanced by increased salt concentration i.e. membrane charge was in fact increased. The increased membrane charge density and consequently, increased friction between the components in the membrane, results in lower fluxes at high concentrations. However, this explanation is often criticized for contradicting the charge-screening concept at high concentrations.

Membrane swelling has also been cited by several works as a cause for the flux decline [5,9]. However, the mechanism of membrane swelling (increase in membrane pore size and/or membrane thickness) remains controversial and not yet clearly understood.

Several researchers proposed electroviscous effects as an additional flux reducing mechanism when dealing with salt separations [10-12]. Electroviscous effects arise when liquid is forced through a charged micro- or nano-channel under an applied hydrostatic pressure [13]. In the case of salt separations using a negatively charged membrane, the pressure-driven flow carries counterions towards the downstream end whereas the generated streaming potential acts to drive these ions in the opposite direction, resulting in an increased apparent viscosity and reduced flow rate [13]. Lefebvre et al. [11] included electroviscous effects in their permeate flux simulations and concluded that this electrokinetic phenomenon can be sufficiently important when predicting the productivity of industrial NF plants. Bowen and Welfoot [2], on the other hand, showed that increase in viscosity due to the electroviscous effect was, in most cases, less than 5%, and therefore, not significant. Conversely, these authors assumed that solvent viscosity due to confinement within the nanopore increases by a factor of almost 8.3, which will drastically underpredict the volumetric flux at all NaCl concentrations. However, neither of these works [2,11] verified their model predictions using experimental data. Rodrigues et al. [14] demonstrated that replacing the pure water viscosity with the bulk solution viscosity in Eq. (3.3) significantly improved the flux predictions of NF separation of sodium sulfate solutions, however, indicated that the model must be used with caution for design purposes as permeate fluxes were still overpredicted.

Recent studies by Merdaw et al. [15,16] attempted to produce an empirical model based on a combination of two well-known RO models, the solution-diffusion (SD) and the

pore-flow (PF) model to determine water permeability across pressure-driven membranes. After accounting for CP, the developed model failed to adequately represent the experimental results obtained with NF of aqueous solutions of NaCl and $MgSO_4$. The authors postulated that the deviations of their model from the actual experimental values were due to the existence of several resistances besides CP, such as electrostatic forces between the feed solution and membrane. Given that the origins of these deviations were unclear, the additional resistances were lumped into a new dynamic resistance (Ω^*) correction factor that was incorporated into their model.

Nevertheless, despite the numerous contradicting theories proposed in the literature, researchers have yet to incorporate these explanations into a practical, modelling tool that is capable of predicting the observed phenomena at high salt concentrations. Moreover, a thorough survey of the current literature reveals a distinct lack of NF modelling studies that enable simultaneous prediction of both permeate flux and salt rejection at high concentrations. Majority of the reviewed works can be loosely classified into three broad categories based on their modelling efforts: (1) those that deal with very low salt concentrations (< 0.1 M) so that fluxes are essentially equal to that of pure water, (2) those that focus on ion rejection and either ignore modelling of permeate fluxes or explain the observed flux reductions qualitatively and, (3) those that simulate permeate fluxes but do not validate their model using experimental data.

3.2 NF theory background and model development

3.2.1 Spiegler-Kedem model

The classical Spiegler-Kedem (SK) model, based on irreversible thermodynamics, provides a simple framework for description of solute transport in both RO and NF

processes. In the SK approach, the membrane is regarded as a "black-box" that can be characterized in terms of two coefficients: the solute permeability (P_s) and the reflection coefficient (σ). Unlike the traditional solution-diffusion model, which is based on the primary assumption that the solute and solvent flux are independent of each other, the SK model considers convective coupling of solute and solvent species. Solute transport in RO membranes occur predominantly via diffusion, however, for "looser" membranes such as NF, both the convective and diffusive contributions to the solute flux are important and cannot be ignored [17]. The SK model has been successfully used to model solute retention in various NF applications, such as desalination of saline and brackish waters, demineralization, etc. [18].

For the derivation of the SK model, the starting point is the assumption that the water flux (J_w) and the solute flux (J_s) are driven by forces F_w and F_s, respectively [19]. These generalized forces are due to chemical potential gradients across the membrane, namely, the pressure gradient and the concentration gradient.

$$J_w = L_{11}F_w + L_{12}F_s \qquad [3.4]$$

$$J_s = L_{21}F_w + L_{22}F_s \qquad [3.5]$$

where L_{ij} are phenomenological coefficients.

The final working equations of the nonlinear SK model for permeate flux and intrinsic rejection (R) are:

$$J_v = L_p(\Delta P - \sigma\Delta\pi) \qquad [3.1]$$

$$R = 1 - \frac{C_P}{C_m} = \frac{\sigma(1-F)}{1-\sigma F} \qquad [3.6]$$

where C_m is the solute concentration at the feed-membrane interface, C_p is the permeate solute concentration, and F is the flow parameter defined as follows:

$$F = exp\left(-\frac{(1-\sigma)J_v}{P_s}\right) \qquad [3.7]$$

The two transport parameters (σ and P_s) for a single salt system can be obtained by the fitting of the experimentally obtained rejection/permeation data to the analytical solution of the SK equation considering constant coefficients. The fitted coefficients are then said to represent the values of the transport coefficients for the given feed salt composition and concentration dependence is assessed by fitting the data for different feed concentrations [20].

3.2.2 Film theory based concentration polarization

Concentration polarization (CP) is a reversible phenomenon that occurs when the rejected solutes accumulate at the membrane surface creating a local concentration, C_m, much higher than of the feed solution, C_b (Fig. 3.1). Such a concentration build-up will generate diffusive flow back to the bulk solution. At steady state conditions, the convective transport of the solute to the membranes surface will be balanced by the diffusive back-transport plus that which passes with the permeate flow [21]. This phenomenon has adverse effects on the membrane performance, namely, lower separation efficiency, flux reduction, and increase of the rate of membrane fouling [22].

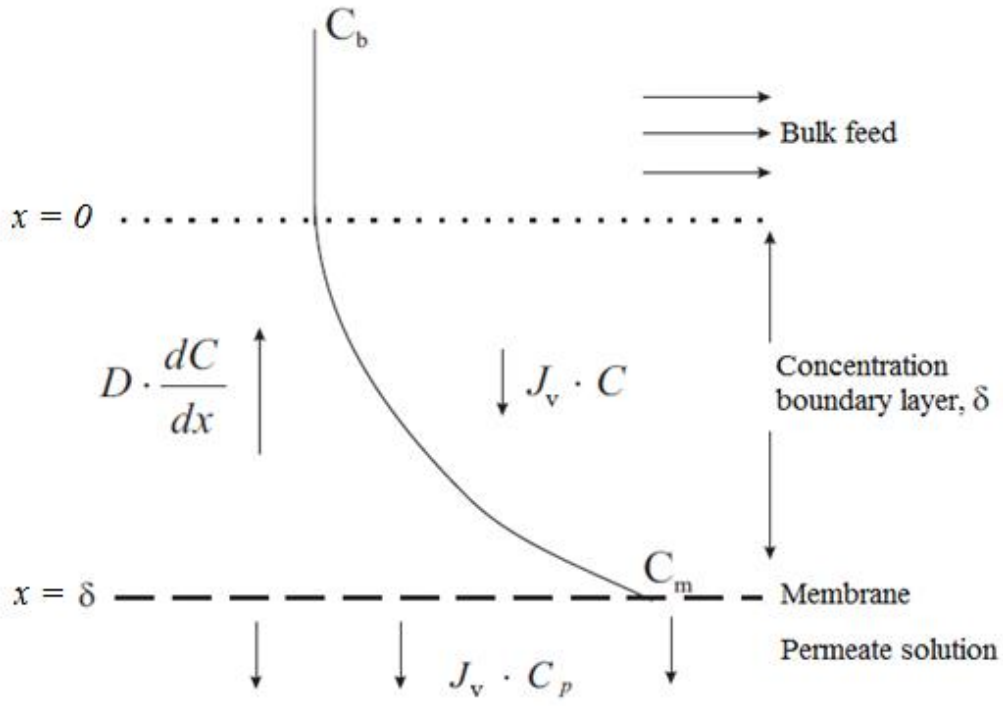

Fig. 3.1 Concentration polarization. Mass transfer and concentration profile under steady-state conditions [23].

From Fig. 3.1, a solute mass balance in the concentration boundary layer gives the following equation:

$$J_v C - D\frac{dC}{dx} = J_v C_p \qquad [3.8]$$

where C_p is the solute concentration in the permeate and D is the diffusion coefficient. Rearranging and integrating the above equation with the following boundary conditions gives the well-known film model of CP i.e. Eq. (3.11):

$$x = 0, C = C_b \qquad [3.9]$$

$$x = \delta, C = C_m \qquad [3.10]$$

$$\frac{C_m - C_p}{C_b - C_p} = exp\left(\frac{J_v}{k}\right) \qquad [3.11]$$

where C_b is the bulk concentration, δ is the thickness of the concentration boundary layer, and k is the mass transfer coefficient:

$$k = \frac{D}{\delta} \qquad [3.12]$$

CP and thus, k, depends on the membrane properties and configuration, feed solution hydrodynamics, and solute properties [24]. The presented simplified approach for CP assumes one-dimensional concentration profile and absence of turbulence within the film [16]. To incorporate CP phenomena, Murthy and Gupta [25] have suggested the use of a combined SK and film theory model to simultaneously enable the estimation of the mass transfer coefficient, k, and σ and P_s:

$$\frac{R_{obs}}{1 - R_{obs}} = \left(\frac{\sigma}{1 - \sigma}\right)\left(1 - exp\left(-\frac{(1 - \sigma)J_v}{P_s}\right)\right)\left(exp\left(\frac{-J_v}{k}\right)\right) \qquad [3.13]$$

where R_{obs} is the observed salt rejection.

The combined three-parameter model above allows the estimation of P_s, σ, and k by using a nonlinear parameter estimation method. Murthy and Gupta [25] showed that in the absence of any other reliable techniques, this combined SK/film theory approach to k determination can be quite useful, especially where NF membranes with reflection coefficients far from unity are concerned.

3.2.3 The reflection coefficient

According to the classical SK model, the imperfections present in a semipermeable membrane are commonly characterized by the so-called "reflection" coefficient, σ. When an osmotic difference, $\Delta\pi$, across an imperfect semipermeable membrane is compensated by an applied pressure, ΔP, so that the volume flow, J_v, is zero, ΔP will be smaller than $\Delta\pi$ [19]. Traditionally, σ was defined as the ratio of these two differences:

$$\sigma = \left(\frac{\Delta P}{\Delta \pi}\right)_{J_v \to 0} \qquad [3.14]$$

Thus, the reflection coefficient is seen as a measure of the degree of selectivity of the membrane. If σ=1, the membrane is ideally semipermeable and there is no solute transport, whereas, if σ=0, the membrane is entirely unselective and no separation takes place.

In this work, an alternative expression for determining σ has been proposed. At a given concentration of the feed salt solution, an analytical expression for the reflection coefficient as a function of the trans-membrane pressure can be derived by considering the NF membrane to be composed of a parallel arrangement of perfectly semipermeable (A) and entirely non-selective (B) regions (Fig. 3.2). In the context of this work, perfectly semipermeable regions (A) represent 100% solute rejection whereas non-selective areas (B) denote 0% solute rejection.

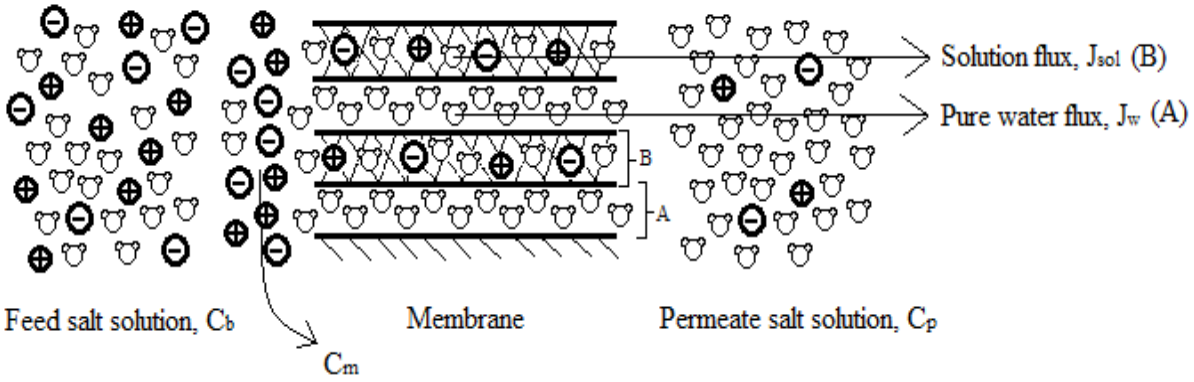

Fig. 3.2 Schematic representation of a NF membrane. Membrane is divided into parallel segments of perfectly semipermeable (A) and entirely non-selective areas (B).

The total volumetric flux (J_v) caused by the applied hydrostatic pressure (ΔP) is the sum of the flows through the perfect (J_w) and non-prefect (J_{sol}) regions:

Total volumetric flux = Pure water flux + Solution flux

$$J_v = J_w + J_{sol} \qquad [3.15]$$

In terms of the respective hydraulic permeabilities (L_p) of the two areas, the corresponding fluxes can be written as follows:

$$J_w = L_p^A(\Delta P - \Delta\pi) \qquad [3.16]$$

$$J_{sol} = L_p^B(\Delta P) \qquad [3.17]$$

where in the perfect region of the membrane (A), the water flux is proportional to the effective trans-membrane pressure (difference between applied and osmotic pressure across the membrane), whereas in the non-ideal portion (B), the solution flux is simply proportional to the applied pressure, according to Darcy's law [19].

It can be seen that Eq. (3.15) can be written in the following manner by combining Eqs. (3.16) and (3.17):

$$J_v = \left(L_p^A + L_p^B\right)\left(\Delta P - \frac{L_p^A}{L_p^A + L_p^B}\Delta\pi\right) = L_p(\Delta P - \sigma\Delta\pi) \qquad [3.18]$$

where L_p is the membrane hydraulic permeability and

$$L_p = \left(L_p^A + L_p^B\right) \qquad [3.19]$$

and

$$\sigma = \frac{L_p^A}{L_p^A + L_p^B} \qquad [3.20]$$

From the above equation, it can be seen that the reflection coefficient, σ, can be considered as the fractional contribution of the ideal portion of the membrane to the total volumetric flow.

Eqs. (3.16) and (3.17) can also be rewritten to include the reflection coefficient:

$$J_w = \sigma L_p(\Delta P - \Delta\pi) \qquad [3.21]$$

$$J_{sol} = (1 - \sigma)L_p\Delta P \qquad [3.22]$$

A solute material balance across the membrane, gives the following equation for the solute flux, J_s:

$$J_s = J_v C_p \qquad [3.23]$$

However, J_s can also be written as follows:

$$J_s = J_{sol} C_m \qquad [3.24]$$

where C_m is higher than C_b due to the CP phenomena (Fig. 3.1).

Equating Eqs. [3.23] and [3.24] and substituting Eqs. [3.18] and [3.22] for the respective volume fluxes, an analytical expression for σ can be derived as follows:

$$\frac{J_{sol}}{J_v} = \frac{C_p}{C_m} \qquad [3.25]$$

$$\frac{J_{sol}}{J_v} = \frac{(1-\sigma)L_p\Delta P}{L_p(\Delta P - \sigma\Delta\pi)} = \frac{C_p}{C_m} \qquad [3.26]$$

Rearranging for σ gives:

$$\sigma = \frac{\Delta P(1-\frac{C_p}{C_m})}{(\Delta P - \Delta\pi\frac{C_p}{C_m})} \qquad [3.27]$$

3.2.4 Modified Spiegler-Kedem (MSK) model

Numerous studies have shown that the selective separation of electrolytes by NF membranes depends on the synergistic effect of steric hindrance (sieving effect) and electrostatic repulsion (charge effect). NF membranes typically have an average pore diameter in the range of 1 to 2 nm, which is of the same order of magnitude as the size of most inorganic ions of interest to NF processes. These ions include but are not limited to Na^+, Mg^{2+}, Ca^{2+}, Cl^-, and SO_4^{2-} (Table 3.2). However, size rejection alone would not be able to retain any of these ions. As mentioned previously, most commercial NF membranes carry a fixed negative charge and these charges in combination with the nano-length pores play a major role as a mechanism for selective electrolyte separation.

Table 3.2 Stokes-Einstein and hydrated radii of some common ions

Ion	Stokes-Einstein radius (nm)	Hydrated radius (nm)
Na^{+}	0.184	0.36
Ca^{2+}	0.309	0.41
Mg^{2+}	0.341	-
Cl^{-}	0.121	0.33
SO_4^{2-}	0.23	-

It becomes clear then that for any anions to pass the pores of the membrane from the feed side to the permeate side, they must overcome the resistance rooting in the expelling force due to the electric interaction between the negative charges located inside the membrane pores and the negative charges on the surface of the anion. Since the pore size of NF membrane is in the range of 1-2 nm, the distance between the membrane charges and the ionic charges would be no more than that at the closest distance, i.e., when an anion passing over the in-pore membrane charge. The electric interaction would be significant owing to the nanoscale distance since the Coulombic force of attraction between two charges is proportional to the reciprocal of the squared distance between them.

For a given pair of NF membrane and anions, the magnitude of this electric force is dependent on the following factors: 1) the size distribution and morphorlogy of the membrane pores; 2) the radius of anions passing the pores; 3) the charge density inside membrane pores; and 4) the charge density of anions.

In addition to the increased retention of anions by NF membrane, the electric resistance generated by the expelling of anions by the negative charges in membrane pores would also serve as resistance to slow down anion diffusion inside the pores. First of all, the anions that do pass the charge barriers inside the nanopore would approach the barrier at a greatly reduced speed due to the repelling force imposed on them by the negative intrapore

charges. Secondly, the rejection of anions in the nanopores would accumulate in the nanopores to create a nano-environment that has a significantly higher anion concentration than on the membrane surface or in the bulk solution, resulting in high local viscosity that would slow down the diffusion of particles, including water molecules, cations, and anions, through the pores. Thirdly, given the fact that the anions are only slightly smaller than the nanopores, high concentration of anions would cause significantly steric hindrance to the movement of other particles inside the nanopore and therefore slow down the overall permeate flux across the membrane. This resistance derived from the electric interaction, however, is not included in the original equations for permeate solution flux i.e. Eqs. (3.1) and (3.3). Consequently, during flux predictions when L_p is represented by the pure water permeability in Eq. (3.1), it should, in fact, be corrected as follows to account for the charge resistance.

$$J_v = \frac{L_p}{R_{elec}}(\Delta P - \sigma\Delta\pi) \quad [3.28]$$

where R_{elec} is the additional hydrodynamic resistance due to electrostatic interactions between the charged nanopore and the ions passing through these pores. Since hydraulic resistance is the reciprocal of permeability, R_{elec} can be essentially interpreted as an empirical factor that corrects the intrinsic membrane resistance (R_m) at high salt concentrations:

$$J_v = \frac{1}{\mu R_m R_{elec}}(\Delta P - \sigma\Delta\pi) \quad [3.29]$$

The physical significance of R_{elec} and the rationale behind its introduction are discussed in greater detail in Chapter 6.

3.2.5 Determination of osmotic pressure

In the case of electrolyte solutions, osmotic pressure across the membrane results in a decrease of the available pressure driving force and cannot be neglected in the prediction of

permeate flux. The Van't Hoff equation is commonly applied for osmotic pressure estimations due to its simplicity and ease of calculation.

$$\Delta\pi = vR_gT(C_m - C_p) \qquad [3.30]$$

where v is the dimensionless Van't Hoff factor, R_g is the universal gas constant, and T is the absolute temperature.

However, in the case of highly concentrated electrolyte solutions, the Pitzer equation has been shown to be more suitable than the above equation for osmotic pressure determination. The Pitzer equation is able to predict the osmotic pressure within experimental error from dilute solutions up to an ionic strength of 6 M, which is the maximum solubility of NaCl in water at 25°C [26]. In Fig. 3.3, the relative difference between the osmotic pressure values for a wide range of NaCl concentrations as predicted by both the Van't Hoff (π_v) and Pitzer (π_p) theories are shown.

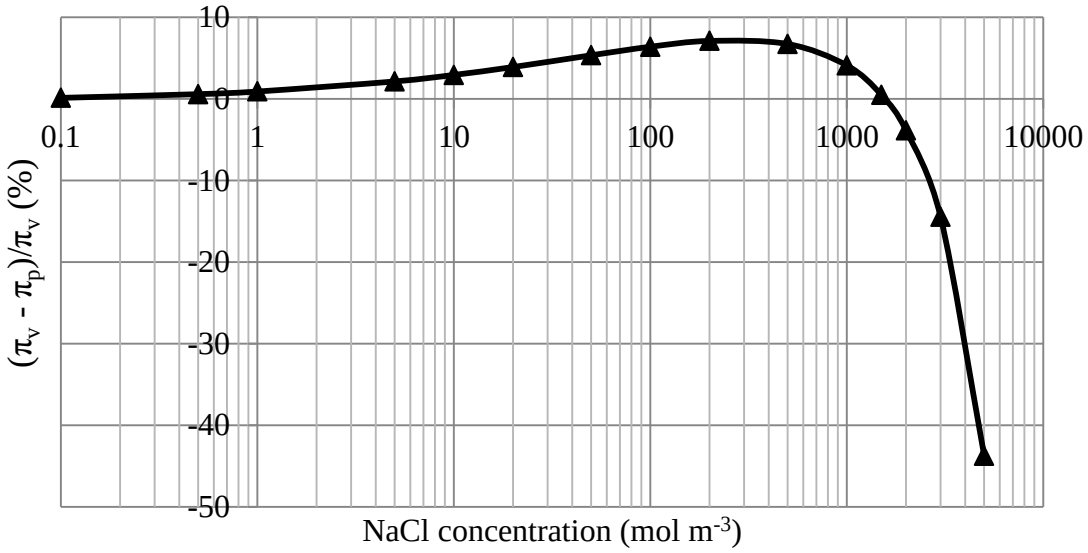

Fig. 3.3 Percentage relative difference between Van't Hoff and Pitzer models for osmotic pressure calculations.

From Fig. 3.3, it is evident that for NaCl concentrations below 2 M (2000 mol/m^3), the difference between the two models is below 7%, however, for higher concentrations, the differences increase rapidly and the Pitzer equation predicts higher osmotic pressure values than the Van't Hoff theory. Since concentrations studied in this work are below 2 M, Fig. 3.3 shows that the Van't Hoff model is suitably sufficient for osmotic pressure calculations in permeate flux predictions.

3.2.6 Determination of solution viscosity

As mentioned by several researchers, the assumption of bulk solvent properties may not be valid within nanopores of NF membranes and may likely overestimate the water permeability [2, 27]. Although there is sufficient evidence that nanoconfinement effects result in an increase in viscosity with decreasing pore size, this actual increase in magnitude remains difficult to quantify [2]. As noted in Section 3.1, studies have also incorporated electroviscous effects to account for this change in viscosity, however, the presence of this phenomena in NF pores has not be substantiated using experimental results. In this work, we have implemented the approach recommended by Rodrigues et al. [14] of replacing the pure water viscosity in Eq. (3.29) with the solution viscosity. A correction to the hydraulic permeability can be made using the following expression:

$$L_p = L_{p,w}\frac{\mu_w}{\mu_s} \qquad [3.31]$$

where $L_{p,w}$ is the pure water permeability (PWP), μ_w is the water viscosity, and μ_s is the solution viscosity. Since μ_s is a function of the salt concentration, correlations for the dynamic viscosity of NaCl aqueous solutions from Aleksandrov et al. [28] were used in this work.

3.3 Determination of transport parameters

For the different feed NaCl concentrations studied in this work, the transport parameters, P_s and σ, and the mass transfer coefficient, k, were determined by fitting Eq. [3.13] to the experimentally obtained, R_{obs}. Standard nonlinear parameter estimation routines of MATLAB were used for the fitting problem. A least-squares-based objective function for n data points was used for the criterion minimization:

Objective function = $\min \sum_{i=1}^{n} (R_{i,exp} - R_{i,calc})^2$ [3.32]

The objective function was subjected to the following two constraints:

(1) $0 < \sigma < 1$

where the reflection coefficient was bounded between a lower value of 0 and upper value of 1, and

(2) $\left| \frac{\sigma_{fit} - \sigma_{calc}}{\sigma_{fit}} \right| \leq 0.01$

where σ_{calc} was determined using Eq. (3.27) as follows:

$$\sigma_{calc} = \frac{\sum_{i=1}^{n} \left[\frac{\Delta P_i (1 - \frac{C_{p,i}}{C_{m,i}})}{(\Delta P_i - \Delta \pi_i \frac{C_{p,i}}{C_{m,i}})} \right]}{n} \qquad [3.33]$$

It can be seen that σ_{calc} is, in essence, the arithmetic mean of the reflection coefficients calculated at different applied pressures for a given feed NaCl concentration. The second constraint is thus, the normalized absolute deviation of the fitted and the calculated reflection coefficients. In this case, an arbitrary tolerance limit of 0.01 was chosen. In essence, this additional constraint during parameter estimation allows us to place restrictions on the possible values of σ based on our newly derived mathematical expression for σ. To the best

of our knowledge, this additional restriction imposed in our parameter estimation approach is a novel concept that has not been proposed in existing literature.

At a given feed concentration, the resistance due to electrical charge, R_{elec}, was determined by fitting the calculated applied pressure to the experimental data.

$$\Delta P_{calc} = \frac{J_v}{L_p/R_{elec}} + \sigma v R_g T\left(C_b - C_p\right)\exp(\frac{J_v}{k}) \qquad [3.34]$$

where L_p was corrected using the solution viscosity (Eq. 3.31).

The objective function, in this case, was

Objective function = $\min \sum_{i=1}^{n}(\Delta P_{i,exp} - \Delta P_{i,calc})^2$ [3.35]

For the straightforward case above, the Solver routine of MS Excel was used for minimizing the objective function and determining R_{elec}.

The transport parameters, σ and P_s, the mass transfer coefficient, k, and the resistance due to charge interaction, R_{elec}, were obtained for a wide range of NaCl feed concentrations, and their concentration dependency were assessed by plotting the parameters against C_b.

3.4 Numerical solution for modelling of NF of concentrated NaCl solutions using the modified SK (MSK) model

A numerical computational procedure based on the modified SK model was developed to determine R_{obs} and J_v for NF of concentrated NaCl solutions. The numerical solution was programmed using Excel VBA (visual basic for applications) 2007.

Eq. (3.6) can be rearranged to give the following equation:

$$\frac{C_p}{C_m} = \frac{1-\sigma}{1-\sigma F} \qquad [3.6b]$$

where F was given by Eq. (3.7) previously.

Rearranging and dividing both sides of Eq. (3.11) by C_m gives the following equation for C_m as a function of J_v, k, and C_p/C_m:

$$C_m = \frac{C_b exp\left(\frac{J_v}{k}\right)}{1+\frac{C_p}{C_m}\left(exp\left(\frac{J_v}{k}\right)-1\right)} \qquad [3.11b]$$

For a membrane previously characterized by the following transport parameters: σ, P_s, k, and R_{elec}, the following steps were taken to predict R_{obs} and J_v at higher C_b.

1. An initial value of J_v was guessed
2. Using σ, P_s, and the guessed value of J_v the value of F was calculated using Eq. (3.7)
3. Using σ and F, C_p/C_m was determined using Eq. (3.6b)
4. Using C_b and k, the guessed value of J_v, and the calculated value of C_p/C_m from Step 3, the value of C_m was found
5. C_p was obtained from the calculated values of C_m and C_p/C_m using the equation $C_p = C_m*(C_p/C_m)$
6. Using Eq. (3.28), a new value of J_v was found by first calculating osmotic pressure from Eq. (3.30)
7. If *abs* $(J_{v,guess} - J_{v,new}) > 0.001$, Steps 1 to 6 were repeated with $J_{v,new}$ as the initial guess value until the stop criteria was met
8. When iteration terminated, J_v and R_{obs} were determined using the final obtained values

It should be stressed that the values of σ, P_s, k, and R_{elec} used in the above procedure for model prediction were not the fitted values but the calculated values from empirical correlations.

The computation procedure for the modelling approach is briefly summarized in Fig. 3.4 in a flow diagram format.

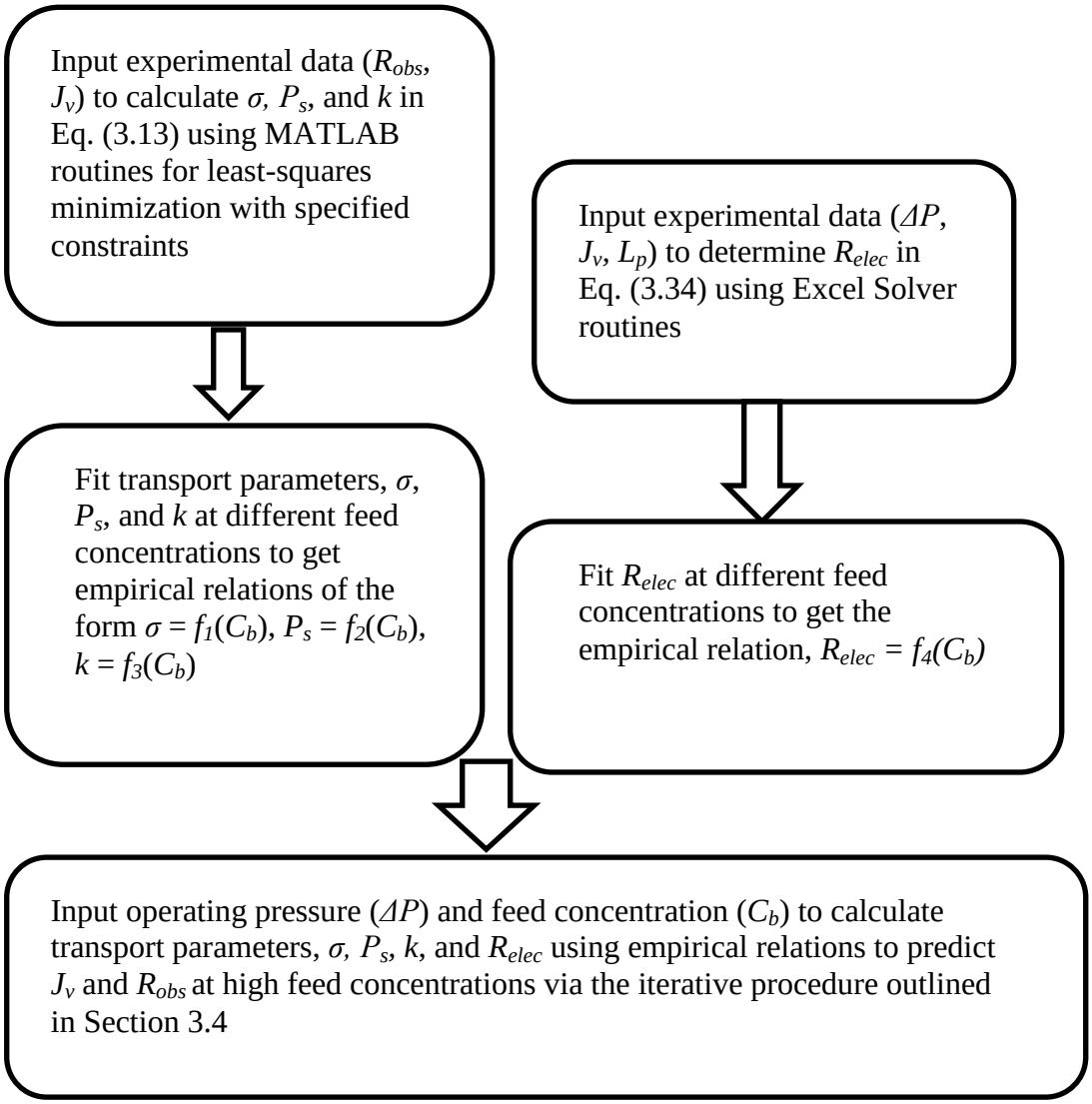

Fig. 3.4 Flow diagram of the modelling approach proposed in this work.

References

1. O. Kedem and A. Katchalsky, Permeability of composite membranes. Part 1. – Electric current, volume flow and flow of solute through membranes, Transactions of the Faraday Society 59 (1963) 1918-1930.
2. W.R. Bowen and J.S. Welfoot, Modelling the performance of membrane nanofiltration-critical assessment and model development, Chem. Engin. Sci. 57 (2002) 1121-1137.
3. M. Nystrom, L. Kaipia and S. Luque, Fouling and retention of nanofiltration membranes, Journal of membrane Science 98 (1995) 249-262.
4. A. Braghetta, F.A. DiGiano and W.P. Ball, Nanofiltration of natural organic matter: pH and ionic strength effects, Journal of Environmental Engineering 123 (1997) 628-641.
5. V. Freger, T.C. Arnot, J.A. Howell, Separation of concentrated organic/inorganic salt mixtures by nanofiltration, J.Membr.Sci. 178 (2000) 185-193.
6. W.B.S. de Lint, P.M. Biesheuvel and H. Verweij, Application of the charge regulation model to transport of ions through hydrophilic membranes: one-dimensional transport model for narrow pores (nanofiltration), Journal of Colloid and Interface Science 251 (2002) 131–142.
7. K. Boussu, Y. Zhang, J. Cocquyt, P. Van der Meeren, A. Volodin, C. Van Haesendonck, Characterization of polymeric nanofiltration membranes for systematic analysis of membrane performance, J.Membr.Sci. 278 (2006) 418-427.
8. G. Bargeman, J.M. Vollenbroek, J. Straatsma, C.G.P.H. Schroën, R.M. Boom, Nanofiltration of multi-component feeds. Interactions between neutral and charged components and their effect on retention, J.Membr.Sci. 247 (2005) 11-20.
9. V. Freger, Swelling and morphology of the skin layer of polyamide composite membranes: an atomic force microscopy study, Environ. Sci. Technol. 38 (2004) 3168-3175.
10. M. Nilsson, G. Tragardh and K. Ostergren, The influence of pH, salt and temperature on nanofiltration performance, J. Membr. Sci., 312 (2008) 97-106.
11. X. Lefebvre, J. Palmeri, P. David, Nanofiltration theory: An analytical approach for single salts, Journal of Physical Chemistry B, 108 (2004) 16811-16824.

12. A.E. Childress and M. Elimelech, Relating Nanofiltration Membrane Performance to Membrane Charge (Electrokinetic) Characteristics, Environmental Science and Technology 34 (2000) 3710-3716.
13. D. Li, Electro-viscous effects on pressure-driven liquid flow in microchannels, Colloids and Surfaces A: Physicochemical and Engineering Aspects 195 (2001) 35–57.
14. C. Rodrigues, A.I. Cavaco Morão, M.N. de Pinho, V. Geraldes, On the prediction of permeate flux for nanofiltration of concentrated aqueous solutions with thin-film composite polyamide membranes, J.Membr.Sci. 346 (2010) 1-7.
15. A.A. Merdaw, A.O. Sharif, G.A.W. Derwish, Water permeability in polymeric membranes, Part I, Desalination 260 (2010) 180-192.
16. A.A. Merdaw, A.O. Sharif, G.A.W. Derwish, Water permeability in polymeric membranes, Part II, Desalination 257 (2010) 184-194.
17. D. Bhanushali, S. Kloos, D. Bhattacharyya, Solute transport in solvent-resistant nanofiltration membranes for non-aqueous systems: experimental results and the role of solute-solvent coupling, Journal of Membrane Science 208 (2002) 343-359.
18. B. Cuartas-Uribe et al., Nanofiltration of sweet whey and prediction of lactose retention as a function of permeate flux using the Kedem-Spiegler and Donnan Steric Partioning models, Separation and Purification Technology 56 (2007) 38-46.
19. K.S. Spiegler, O. Kedem, Thermodynamics of hyperfiltration (reverse osmosis): criteria for efficient membranes, Desalination 1 (1966) 311-326.
20. S. Bason, O. Kedem, V. Freger, Determination of concentration-dependent transport coefficients in nanofiltration: Experimental evaluation of coefficients, J.Membr.Sci. 326 (2009) 197-204.
21. A. E. Yaroshchuk, Recent progress in the transport characterization of nanofiltration membranes, Desalination 149 (2002) 423-428.
22. T. Chaabane, S. Taha, R. Maachi and G. Dorange, Coupled model of film theory and the Nernst-Planck equation in nanofiltration, Desalination 206 (2007) 424-432.
23. E. Sivertsen, Membrane separation of anions in concentrated electrolytes, Norwegian University of Science and Technology, 2001. PhD Thesis.

24. E. Nagy and E. Kulcsar, The effect of the concentration polarization and the membrane layer mass transport on membrane separation, Desalination and water treatment 14 (2010) 220-226.
25. Z.V.P. Murthy and S.K. Gupta, Estimation of mass transfer coefficient using a combined nonlinear membrane transport and film theory model, Desalination 109 (1997) 39-49.
26. Z.-A. Hu, H.-Y. Wu, J.-Z. Gao, Calculation of osmotic pressure difference across membranes in hyperfiltration, Desalination 121 (1999) 131-137.
27. S. Gomes, S.A. Cavaco, M.J. Quina, L.M. Gando-Ferreira, Nanofiltration process for separating Cr(III) from acid solutions: Experimental and modelling analysis, Desalination 254 (2010) 80-89.
28. A.A. Aleksandrov, E.V. Dzhuraeva and V.F. Utenkov, Viscosity of aqueous solutions of sodium chloride, High Temperature 50 (2012) 378-383.

Chapter 4: Materials and Methods

4.1 Experimental setup

NF experiments were conducted using a flat-sheet laboratory-scale system depicted in Fig. 4.1. The system is composed of six cross-flow membrane cells in series, a feed tank, a pump, and a pressure regulator. The feed tank had a maximum volume of 4 L. The feed solution was pumped from the tank into the membrane module system as shown in Fig. 4.1. The feed temperature was maintained approximately at 25±2^{o}C and the feed flow rate was 65 L h^{-1}. The cells house circular membrane coupons with an effective filtration area of 13.2 cm^2. Although the cells are connected in series, the concentration of the feed solution did not change appreciably between the module inlet and outlet since each membrane area was small.

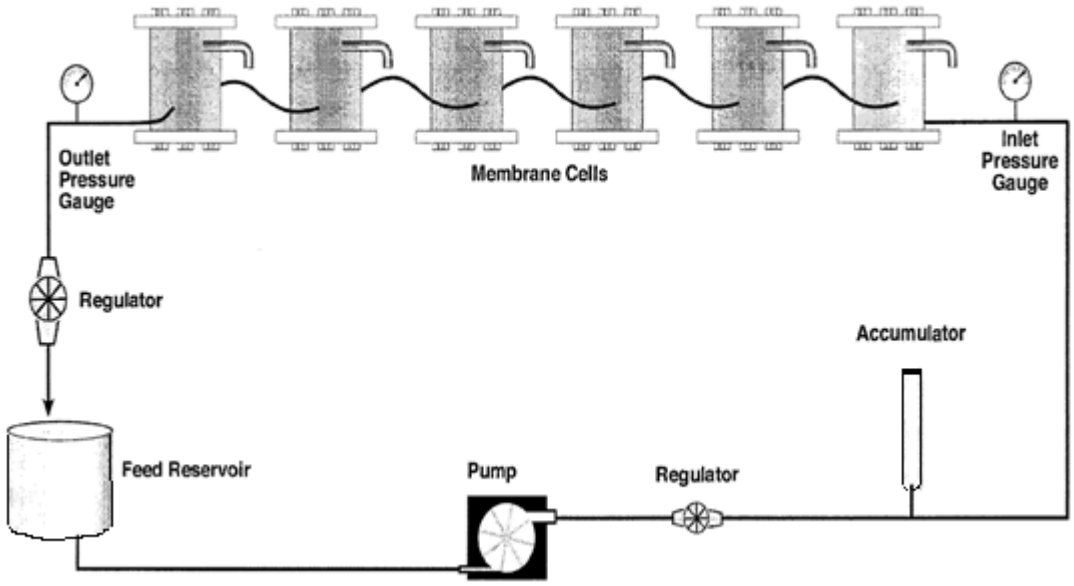

Fig. 4.1 Schematic of experimental set-up [1]

4.2 Membranes and chemicals

Two commercial thin-film polyamide NF membranes: NF270 (Dow-Filmtec) and Desal-5 DL (GE Osmonics) were tested in this work. Membrane properties as provided by the manufacturers and obtained from literature are shown in Table 4.1. Certified analytical grade sodium chloride (NaCl) salt and glucose were obtained from Fisher Scientific Canada.

Table 4.1 Properties of NF membranes tested in this work (adapted from Luo et al. [2])

Membrane	NF270	Desal-5 DL
Manufacturer	DOW-FilmTec	GE-Osmonics
Surface material	Polyamide	Proprietary polyamide
Molecular weight cut-off (Da)	150-200	150-300
Max. temperature (^{o}C)	45	50
Max. pressure (MPa)	4.1	4.0
pH range	3-10	2-11
Isoelectric point (pH)	~5.2	~4.1
Contact angle (^{o})	27[a]	41[c]
	<10[b]	

[a] Boussu et al. [3]
[b] Artuğ et al. [4]
[c] Mänttäri et al. [5]

4.3 Experimental procedure

Prior to use, fresh membrane coupons with 13.2 cm^2 effective area were soaked in deionized water overnight. The membranes were first wetted by pressurization and pre-compacted at 500 psi (~3450 kPa) for 3 hours using deionized water. Pure water flux (J_w) was then measured at various trans-membrane pressures (ranging from 100 to 450 psi or 690 to 3100 kPa) to evaluate the pure water hydraulic permeability ($L_{p,w}$).

NaCl and glucose experiments were carried out in cross-flow filtration mode with both permeate and retentate recycled to the feed tank to maintain constant feed conditions. NaCl and glucose rejections were determined for different pressure drops with the NF unit

operated for at least 45 minutes (to achieve steady state conditions) at each pressure. For each pressure, a minimum volume of the permeate solution (~10 mL) was collected in vials for subsequent analysis. Feed NaCl concentrations ranged from 0.05 to 1.96 M. Retention experiments with 1 g L^{-1} glucose solutions were performed to determine the membrane pore radius (r_p). To ensure reliability and reproducibility of the collected data, all flux and rejection measurements were performed in duplicate as a minimum.

Fresh membrane coupons were used during filtration of the more concentrated NaCl solutions (> 0.4 M) and for the glucose feed. For NaCl experiments, in-between feeds of different concentrations, the membrane unit was flushed with deionized water until at least 90% of the initial membrane permeability was obtained to maintain the membrane fouling at an acceptable level. If the $L_{p,w}$ value between experiments with different feeds decreased below 90% of the initial value, the membranes were replaced with fresh coupons.

4.4 Contact angle measurements

Contact angle measurements of the virgin membrane surfaces were performed with the sessile drop method using a VCA Optima Surface Analysis System (AST Products Inc., Billerica, MA). The top skin layer surface of sample membrane coupons was placed on a glass plate, on which a drop of deionized water (2 μL) was added using a micro syringe. The contact angles were measured at different locations on the sample coupon and the values averaged.

4.5 Analytical methods

The NaCl feed and permeate concentrations were determined from conductivity measurements via a conductivity meter (model CON 110, Oakton Instruments, Vernon Hills, IL). Glucose concentrations in the feed and permeate solutions were analyzed via a total

organic carbon (TOC) analyzer (Phoenix 8000, Rosemount Analytical Inc., Tekmar Dohrmann Division, Santa Clara, CA).

4.6 Calculations

The experimental volumetric flux, J_v, was calculated as follows:

$$J_v = \frac{V_p}{A_m t} \qquad [4.1]$$

where V_p is the volume of the permeate, t is the time, and A_m is the effective membrane area. The pure water hydraulic permeability ($L_{p,w}$) was determined using the following equation:

$$J_w = L_{p,w} \cdot \Delta P_e \qquad [4.2]$$

where $\Delta P_e = \Delta P - \Delta \pi$ is the effective pressure driving force and $L_{p,w}$ is the slope of the line fitted to the volumetric flux vs. effective pressure data.

The apparent or observed solute rejection was calculated using the following equation:

$$R_{obs}(\%) = \frac{100(C_b - C_p)}{C_b} \qquad [4.3]$$

References

1. B.J. Abu Tarboush, Preparation of thin-film-composite polyamide membranes for desalination using novel hydrophilic surface modifying macromolecules, MASc Thesis, University of Ottawa, 2008.
2. J. Luo and Y. Wan, Effect of highly concentrated salt on retention of organic solutes by nanofiltration polymeric membranes, Journal of Membrane Science 372 (2011) 145-153.
3. K. Boussu, Y. Zhang, J. Cocquyt, P. Van der Meeren, A. Volodin, C. Van Haesendonck, Characterization of polymeric nanofiltration membranes for systematic analysis of membrane performance, Journal of Membrane Science 278 (2006) 418-427.
4. G. Artug and J. Hapke, Characterization of nanofiltration membranes by their morphology, charge and filtration performace parameters, Desalination 200 (2006) 178-180.
5. M. Mänttäri, T. Pekuri and M. Nyström, NF270, a new membrane having promising characteristics and being suitable for treatment of dilute effluents from the paper industry, Journal of Membrane Science 242 (2004) 107–116.

Chapter 5: Results and Discussion

5.1 Membrane pore size

The mean pore radii (r_p) of the membranes were determined through fitting of experimental glucose retention data using a hydrodynamic model. Since the transport of uncharged solutes depends solely on the steric exclusion mechanism, a simple mathematical equation for the solute rejection can be derived based on the extended Nernst-Planck equation. Several researchers have employed this indirect method of utilizing organic solute retention for membrane pore size determination [1,2]. The experimental volumetric flux of both glucose solution and pure water for each membrane are shown as a function of the effective trans-membrane pressure (ΔP_e) in Fig 5.1. It is evident from this figure that excluding at the two highest pressures (27.5 and 31.1 bar), the volumetric flux for the glucose solution and pure water displayed a linear trend and coincided with each other, confirming that concentration polarization (CP) was not very significant over the range of pressures studied. Fig. 5.2 shows the experimental and the fitted glucose retention as a function of the volumetric flux. The glucose retentions of the NF270 membrane (>90%) are higher than those for Desal-5 DL (>86%), as expected in accordance with the MWCO values reported by the manufacturers for these membranes (Table 4.1). The calculated average pore radius of NF270 and Desal-5 DL was 0.44 and 0.52 nm, respectively. These values are in excellent agreement with literature values (Table 5.1). Slight differences between the reported values can be attributed to the different techniques employed (uncharged solute rejection vs. AFM), the molecular weight and radius of uncharged solutes used, and whether or not CP effects were taken into account.

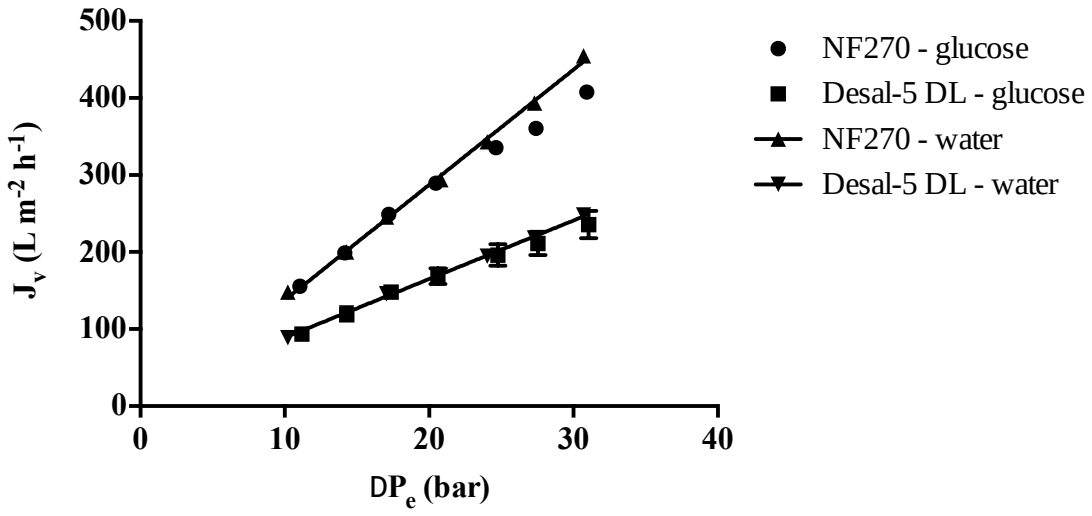

Fig. 5.1 Experimental volumetric flux as a function of the effective pressure for pure water and glucose solution (1 g L^{-1}).

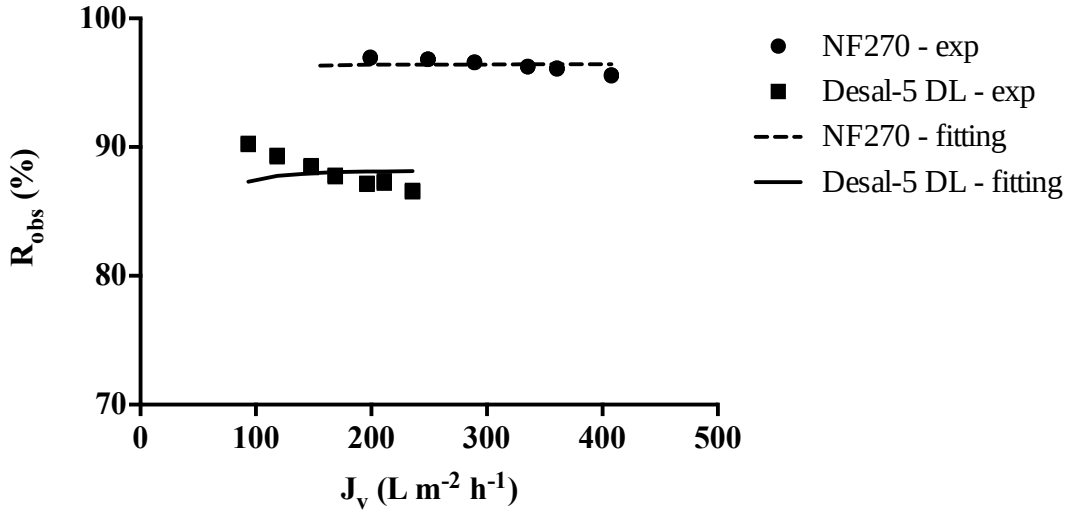

Fig 5.2 Glucose retention as a function of permeate flux for the NF270 membrane and Desal-5 DL membrane.

Table 5.1 Membrane characteristics as reported for NF270 and Desal-5 DL in literature

Membrane	Pure water permeability ($L\ m^{-2}\ h^{-1}\ bar^{-1}$)	Reference	r_p (nm)	Reference
NF270	12 - 13 (22 °C)	[31]	0.43	[1]
	13 - 14 (25 °C)	[1]	0.35[a]	[11]
	8.5 (20 °C)	[5]	0.42 ± 0.3	[28]
	13.5	[28]	0.395	[4]
	13.3 (25 °C)	[9]	0.44	This work
	17.6 (20 °C)	[4]		
	14.6 (25 °C)	This work		
Desal-5 DL	7.56	[29]	~0.51	[29]
	5.76 (20 °C)	[6]	0.45	[6]
	6 - 7 (22 °C)	[31]	0.58 ± 0.18	[30]
	5.5 - 6.5 (25 °C)	[1]	0.50	[1]
	8.8 (25 °C)	[32]	0.52	This work
	9.0	[33]		
	8.6 - 9.6 (25 °C)	This work		

5.2 Contact angle of membrane surface

Contact angle measurements via the sessile drop technique were undertaken in order to determine the degree of hydrophobicity of the two membranes. The greater the contact angle, the more hydrophobic the membrane since a hydrophobic surface is less wettable by a water droplet. From an average of thirteen angle readings, the contact angle of the Desal-5 DL membrane was estimated to be 39.9 ± 1.6 °. Mänttäri et al. [3] reported a slightly higher value (but within the 95% confidence limit of our value) of 41° for the Desal-5 DL membrane. For NF270, however, no concrete values of the contact angle could be recorded. As noted by Artuğ et al. [4], this was possibly due to the highly hydrophilic nature of this membrane and they presented an arbitrary value of less than 10° (Table 4.1). On the other hand, Boussu et al. [5] obtained a value of 27° for the same membrane (Table 4.1). Regardless of the actual value of the contact angle, it is clear that the NF270 membrane is more hydrophilic in nature.

5.3 Determination of membrane pure water permeability

The membrane permeabilities based on the pure water flux measurements obtained in this work are shown in Fig. 5.3. The pure water permeabilities ($L_{p,w}$) of NF270 and Desal-5 DL were 14.63 ± 0.14 L m^{-2} h^{-1} bar^{-1} (4.06 x 10^{-8} m^3 m^{-2} s^{-1} kPa^{-1}) and 9.12 ± 0.30 L m^{-2} h^{-1} bar^{-1} (2.53 x 10^{-8} m^3 m^{-2} s^{-1} kPa^{-1}), respectively. As expected, the pure water flux for both membranes increased linearly with the applied pressure, with the curves passing through the origin, indicating negligible osmotic pressure. The 95% confidence intervals are small and can be attributed to slight differences among the coupons that were taken from different parts of the commercial membrane sheets. Higher fluxes for NF270 are consistent with the more hydrophilic nature of the membrane (as was shown by the contact angle measurements). In spite of Desal-5 DL being the more "open" membrane (larger pore size), the pure water fluxes were considerably lower, indicating that other factors such as membrane hydrophobicity, thickness, porosity, etc. play an important role in permeate flux production. Table 5.1 lists the $L_{p,w}$ values of NF270 and Desal-5 DL as reported in literature. It can be seen that the $L_{p,w}$ determined in this study for both the membranes are reasonably concordant with those reported in literature. Possible reasons for the slight differences between the reported $L_{p,w}$ values include differences in the pre-compaction pressure used, measurement of $L_{p,w}$ at only one or two pressures by some researchers, and the module configurations used [6].

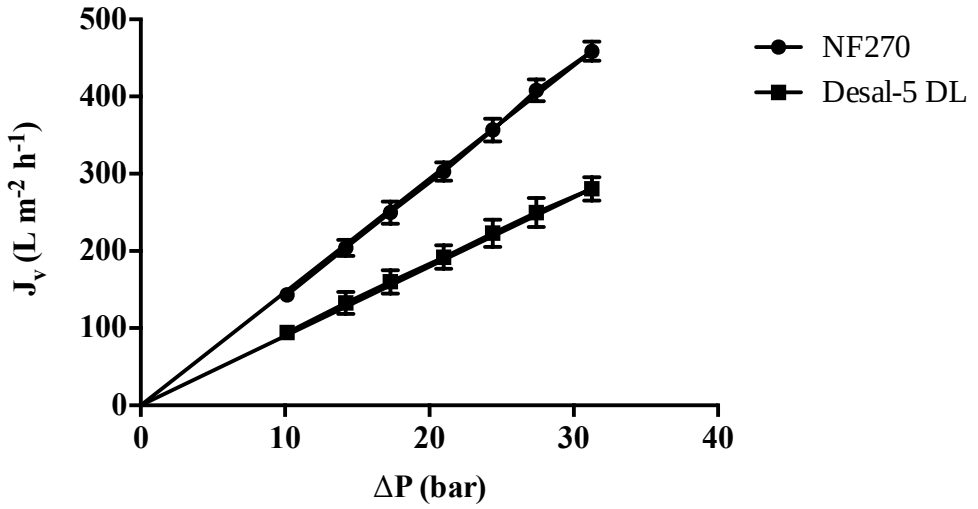

Fig. 5.3 Pure water flux as a function of the applied pressure for NF270 and Desal-5 DL membranes.

It should be pointed out that the $L_{p,w}$ of both the membranes varied between the NF experiments with the feeds of different NaCl concentrations. These observed variations were marginal, not exceeding 12%. No obvious trends were evident amongst these variations. In general, the $L_{p,w}$ of NF270 in-between experiments with different solutions was lower than the initial $L_{p,w}$. On the other hand, the $L_{p,w}$ of Desal-5 DL was slightly higher than the initial value of the virgin membrane. Rodrigues et al. [7] also reported variations in the pure water hydraulic resistance of three membranes (NF90, NF270, NF200) in between NF tests with different concentrated aqueous solutions of Na_2SO_4, glucose, and sucrose. However, in their case, the variations were as high as 25%. No apparent source of these variations could be identified. As pointed out by Rodrigues et al. [7], these deviations from the initial $L_{p,w}$ could not be attributed to irreversible fouling since deionized water and analytical grade reagents were used in all of the experiments. Structural changes in the membrane active layer or membrane swelling due to high feed salinity may possibly result in some variations [8], however, these fluctuations were also discernible at low feed concentrations. Irrespective of

the source, these variations were below 8% in most cases, and the $L_{p,w}$ measured prior to each experiment was used in the fitting procedure to minimize the impact of these inexplicable variations on transport parameter values.

5.4 Retention vs. flux of NaCl at different feed concentrations *(experimental plus fitting with combined SK/film theory model)*

Figs. 5.4 and 5.5 present the experimentally measured NaCl rejection as a function of the applied pressure for NF270 and Desal-5 DL, respectively. For both membranes, the range of observed NaCl retentions (R_{obs}) were similar to those reported by other studies [5, 9]. For NF270, Boussu et al. [5] reported a NaCl retention of 59% with a 0.05 M feed solution at a pressure of 8 bar. From Fig. 5.4a, it can be seen that at the same operating conditions, our value was approximately 60%. Understandably, at all feed concentrations, the NaCl retentions for Desal-5 DL membrane were lower than those of NF270, which can be attributed tentatively to the larger pore size of the Desal-5 DL membrane. Also evident from Fig. 5.4a, is the developing CP effects at the lower C_b resulting in the slight drop in rejection at higher applied pressures (higher fluxes). At low fluxes, the contribution of the diffusive transport of the ions through the membrane is relatively higher than the convective transport, resulting in a low rejection. With the increase in solvent flux with pressure, the convective transport dominates the ionic diffusion and rejection increases (Figs. 5.4b and 5.5). However for NF270, at lower feed concentrations, this expected trend is countered by CP and hence, the drop in rejection (Fig. 5.4a). The CP phenomenon for both the membranes is discussed in greater detail in Section 5.8. Figs. 5.6 and 5.7 illustrate the observed rejection as a function of the volumetric flux. Solid lines in Figs. 5.6 and 5.7 represent the fitted combined SK/film theory model curve (Eq. 3.13) with the regressed transport parameters (σ, P_s, and k) as input

variables. From the degree of parity evident in these figures, a good agreement between the fitted and experimental values was obtained for both membranes. The corresponding estimated transport parameters (σ and P_s) are listed in Table 5.2.

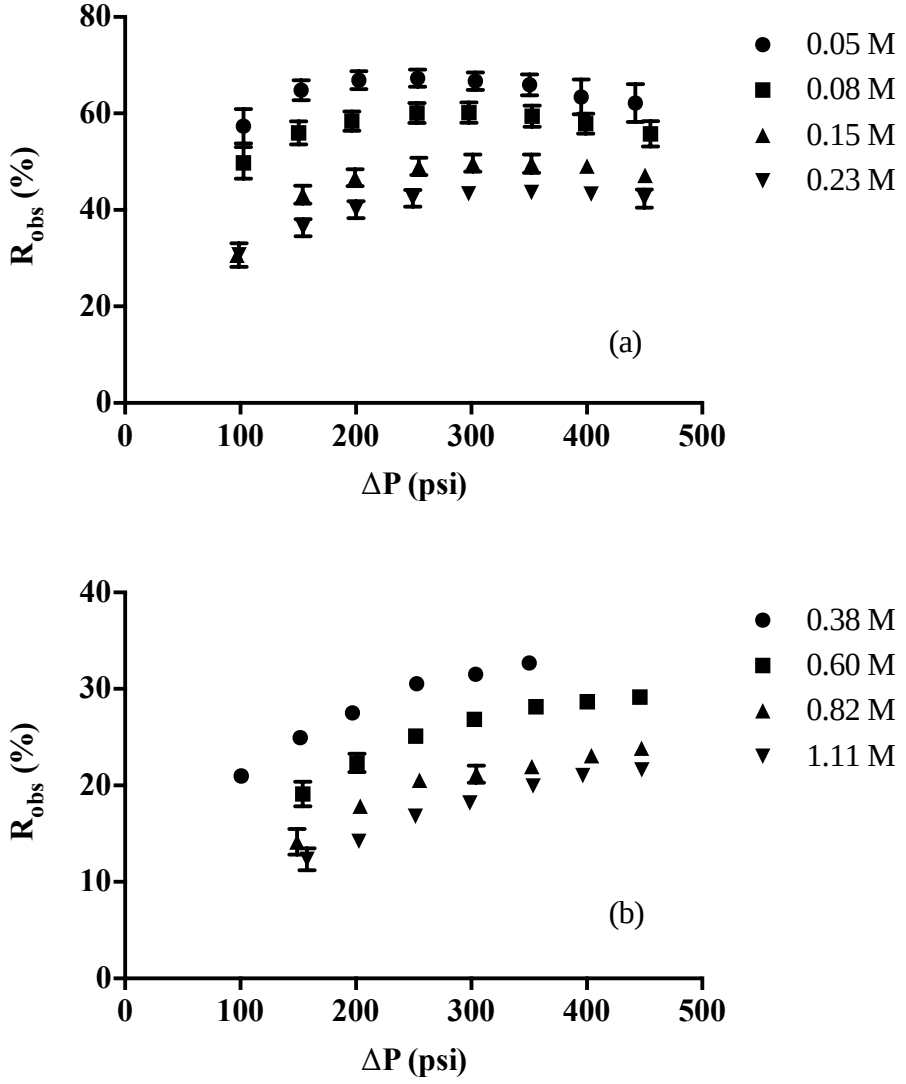

Fig. 5.4 Rejection of NaCl as a function of applied pressure for NF270 at different feed concentration ranges: a. 0.05 – 0.23 M; b. 0.38 – 1.11 M.

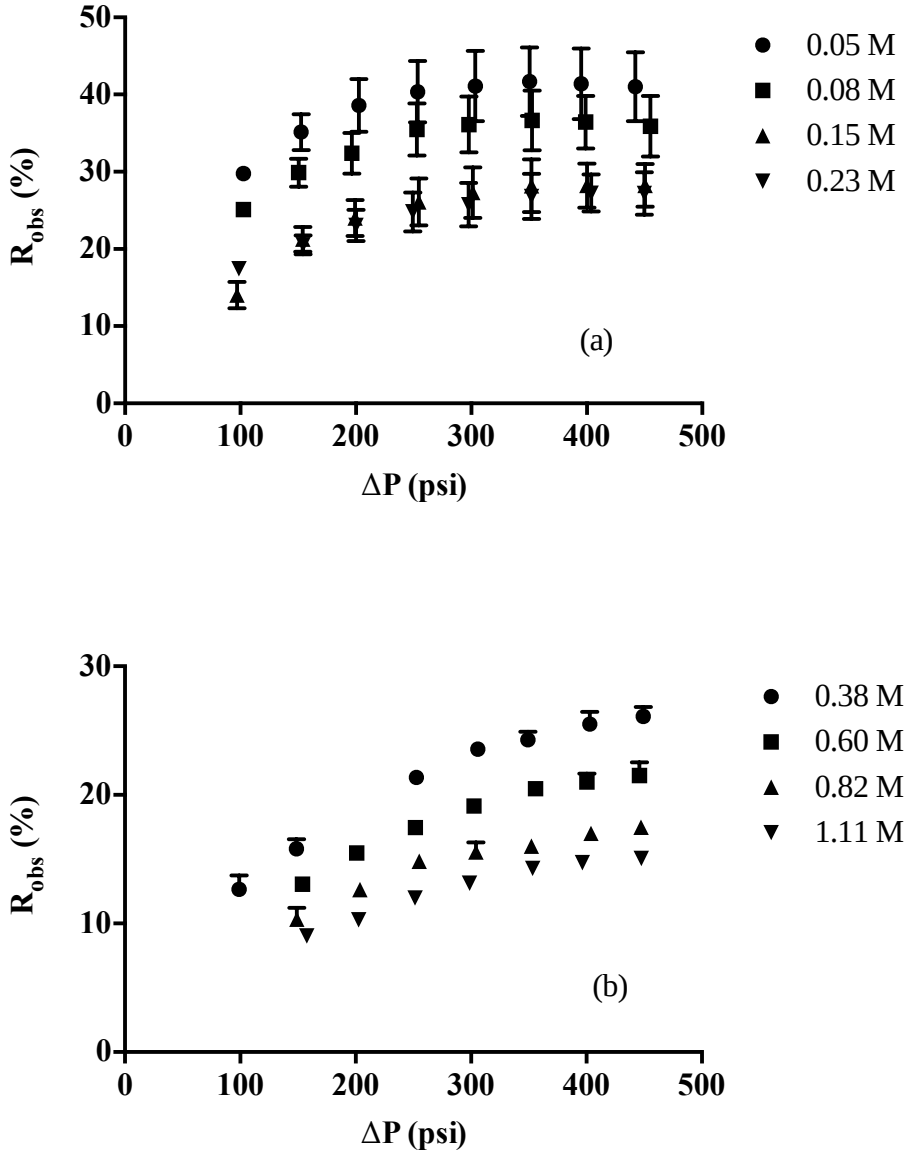

Fig. 5.5 Rejection of NaCl as a function of applied pressure for Desal-5 DL at different feed concentration ranges: a. 0.05 – 0.23 M; b. 0.38 – 1.11 M.

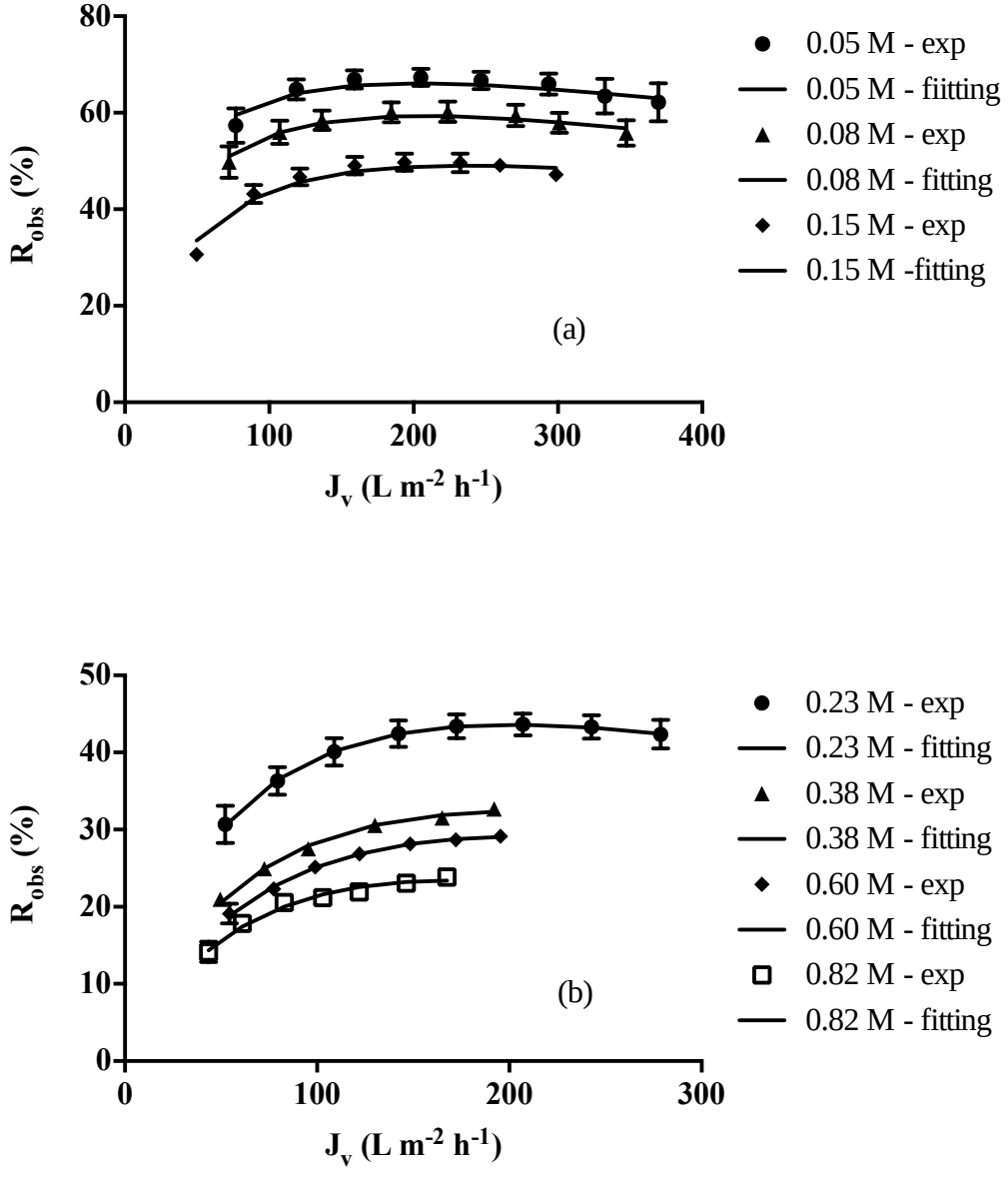

Fig. 5.6 Comparison of the experimental rejection data and best-fit curves obtained from combined SK/film theory model for NF270 at different feed concentration ranges: a. 0.05 – 0.15 M; b. 0.23 – 0.82 M.

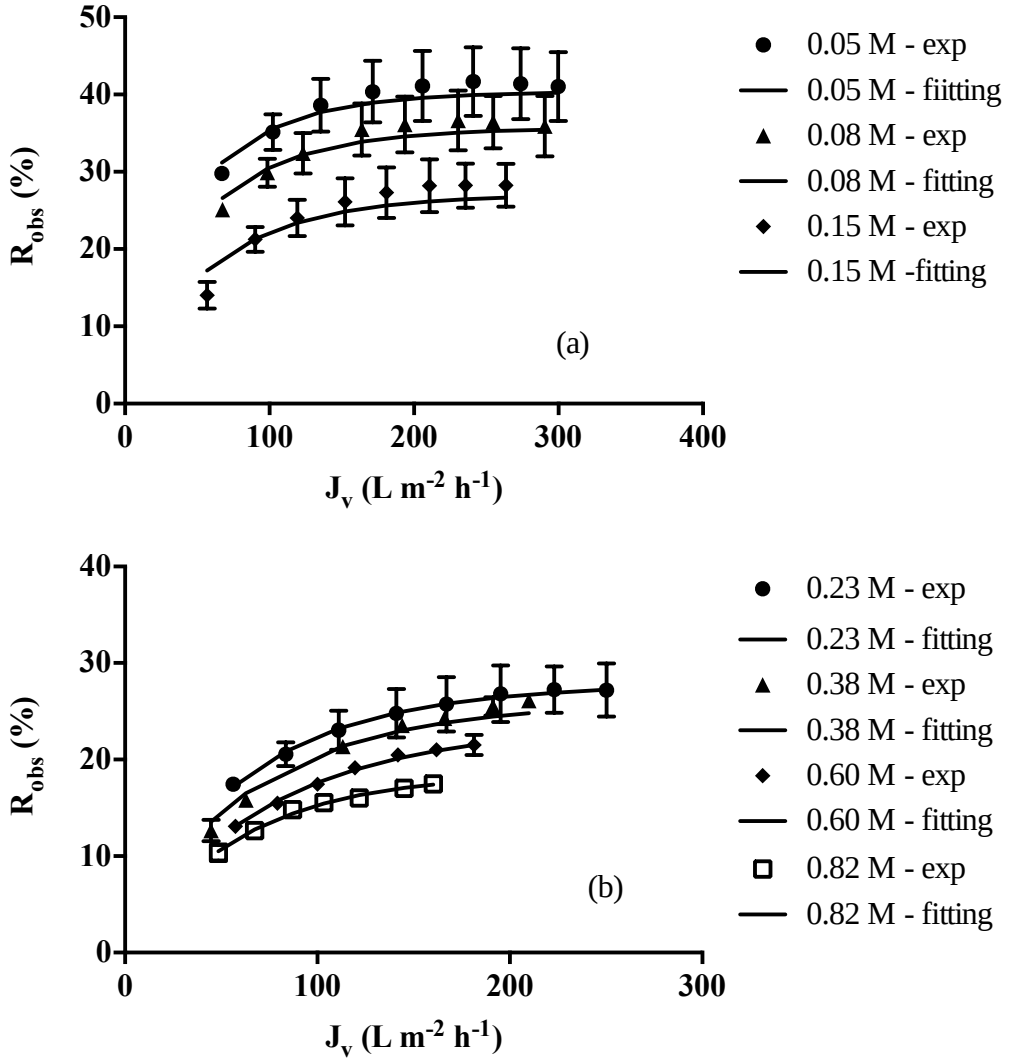

Fig. 5.7 Comparison of the experimental rejection data (dots) and best-fit curves (lines) obtained from combined SK/film theory model for Desal-5 DL at different feed concentration ranges: a. 0.05 – 0.15 M; b. 0.23 – 0.82 M.

Table 5.2 Mean reflection coefficient (σ) and solute permeability (P_s) for the studied membranes at different NaCl concentrations

Conc.	NF270		Desal-5 DL	
(M)	σ	P_s (L m^{-2} h^{-1})	σ	P_s (L m^{-2} h^{-1})
0.05	0.748	24.092	0.404	36.049
0.08	0.700	31.320	0.357	41.083
0.15	0.583	43.252	0.271	50.408
0.23	0.613	54.350	0.279	52.696
0.38	0.489	71.289	0.261	56.488
0.60	0.489	85.871	0.239	66.257
0.82	0.468	92.587	0.226	68.664

The modest NaCl rejections (30 – 50%) of the NF270 membrane indicate its applicability as a pre-treatment process for desalination purposes where the NF membrane can significantly reduce the total salinity. Both the studied membranes, in particular Desal-5 DL, are suitable for food and dairy industries where waste streams containing highly concentrated salt need simultaneous concentration of organic solutes and removal of monovalent salts [1]. It is clear from these figures that NaCl rejection decreases considerably when the feed concentration is increased. Indeed, when C_b increased twofold (from 0.60 to 1.11 M), the NaCl retention reduced by an average factor of 1.5 for both the membranes. Several authors have reported this decrease in rejection with feed concentration at a constant pH for single symmetric salts, such as NaCl or KCl [10, 11]. Numerous theories exist that explain this observed reduction in retention during nanofiltration of NaCl solutions. The pros and cons of these proposed theories will be discussed in greater detail in Chapter 6.

5.5 Correction to prediction of flux at different feed concentrations by the introduction of R_{elec}

As stated in the introduction, simultaneous prediction of NaCl rejection and permeate flux for concentrated solutions is the main focus of this work. Of particular interest is the hugely overestimated permeate flux using the original NF models, which does not account for the resistance derived from the electric interaction between membrane charges, including both surface and intrapore, and co-ions (i.e., Cl^{-1} in this study), when dealing with solutions of high ionic strengths (> 0.2 M). This is evident in Figs. 5.8a and 5.8b, which clearly show the deviations between the experimental and calculated fluxes at higher NaCl concentrations. The solid and dashed lines represent the calculated fluxes. For the sake of clarity, only the experimental data of NF270 for four concentrations (0.05, 0.23, 0.60, 0.82 M) are shown. In this case, the calculated fluxes were determined using Eq. (3.1) (see Chapter 3), which is the unmodified SK model, by utilizing the previously obtained transport parameters (Table 5.2).

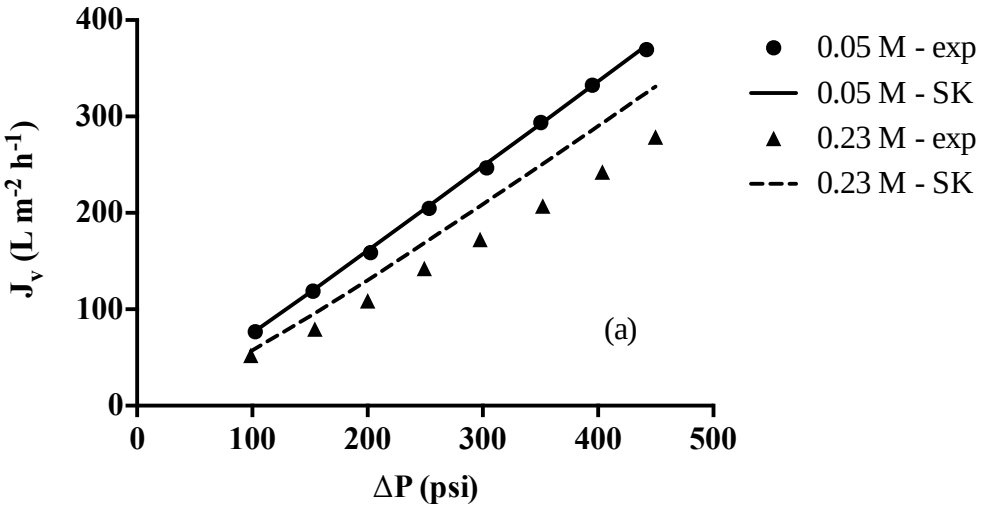

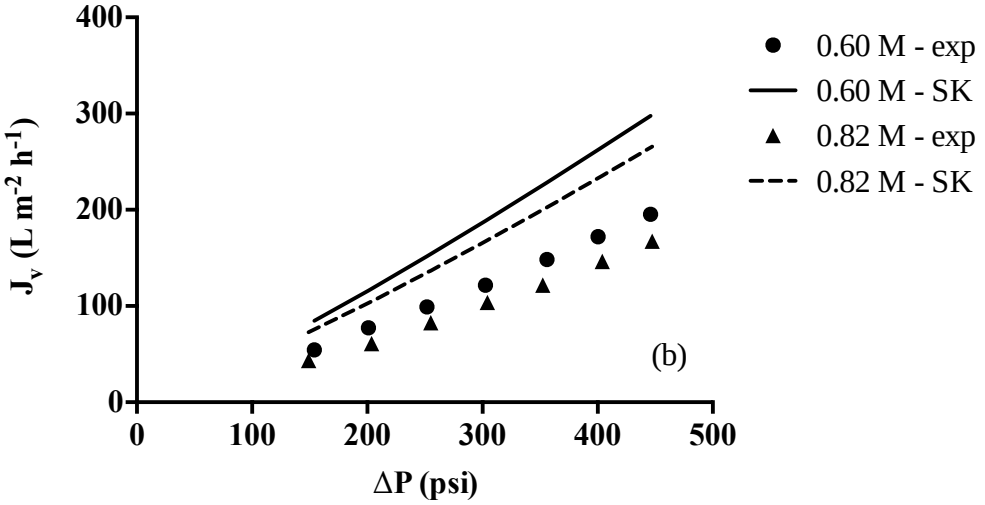

Fig. 5.8 Permeate flux vs. applied pressure for nanofiltration of NaCl solutions using NF270 at different feed concentrations: a. 0.05 M, 0.23 M; b. 0.60 M, 0.82 M, with experimental depicted by dots and modelling data by lines.

Despite accounting for the contributions of both osmotic pressure and concentration polarization in flux reduction as well as correcting for the solution viscosity with increasing NaCl concentration, the calculated fluxes still deviate from the experimentally observed ones, especially at higher feed concentrations. The magnitude of these deviations (represented by the ratio between the calculated and experimental flux) for three different NaCl feed concentrations and at three different applied pressures (low, intermediate, high) is shown in Table 5.3. For example, for a feed concentration of 0.82 M and an applied pressure of 300 psi, the ratio between the calculated and experimental flux is nearly 1.64 and 1.62 for NF270 and Desal-5 DL, respectively.

Table 5.3 Ratio between the calculated and experimental flux for the studied membranes at different NaCl concentrations

	NF270			Desal-5 DL		
ΔP (psi)	150	300	450	150	300	450
C_b (M)						
0.05	1.008	0.996	1.011	0.950	0.954	0.958
0.23	1.207	1.201	1.188	1.203	1.194	1.221
0.82	1.671	1.638	1.585	1.608	1.619	1.573

It should be stressed that these deviations cannot be due to irreversible fouling as filtered solutions contained only deionized water and analytical grade salts. Moreover, more than 90% of the initial $L_{p,w}$ was recovered after membrane usage and the $L_{p,w}$ prior to each experiment was used in the calculation. Thus, it is hypothesized that these deviations are a result of an additional hydraulic resistance due to charge effects between the ions and charges inside the nanopore that are not taken into account in the osmotic pressure model. The hydraulic resistance due to these electric charges, R_{elec}, was obtained by fitting Eq. (3.34) (Chapter 3) to the experimental data. The experimental work spans a NaCl concentration range of 0.05 to 1.96 M, however, only the data sets corresponding to C_b of up to 0.82 M was used during the fitting procedure. The estimated R_{elec} as a function of C_b for the two membranes is shown below in Fig. 5.9. Both the plots exhibit similar trends: in the concentration range examined, R_{elec} appears to increase in a linear fashion with C_b for NaCl. Surprisingly, the magnitude of this resistance factor is, on average, higher for NF270 than Desal-5 DL. The reason for this is unclear, especially given that concentration polarization (CP) was found to be negligible for the Desal-5 DL membrane. Also, Rodrigues et al. [7] found that with filtration of concentrated Na_2SO_4 solutions using different NF membranes (NF270, NF90, NF200), the magnitude of the deviations between the experimental and calculated fluxes was higher for the membrane with higher MWCO, which in their case was

NF270. Interestingly, we found the deviations i.e. R_{elec} to be similarly higher for NF270 membrane, whereas, NF270 has a lower MWCO than Desal-5 DL (Table 4.1). A possible explanation for this lies in the difference between the surface charges of the two membranes. Several works on commercial membrane characterization have shown that the NF270 membrane has a stronger negative surface charge than most membranes [9, 12]. Indeed, zeta potential measurements have shown that NF270 has a higher surface potential than NF90, NF200, and Desal-5 DL. The higher negative charge could result in these deviations being higher for NF270 regardless of the membrane MWCO, which supports our hypothesis that the differences between the calculated and experimental fluxes are a result of the electrostatic interactions between the charged nanopore and ions. In Chapter 6, we discuss the physical significance of R_{elec} in greater detail. Empirical relationships in the form of the following linear equations may be used to predict the R_{elec} and thus, the volumetric flux, J_v, at higher NaCl bulk concentrations:

R_{elec} (NF270) = $1.048C_b + 1.0136$ ($R^2 = 0.97$) [5.1a]

R_{elec} (Desal-5 DL) = $0.6816C_b + 1.0299$ ($R^2 = 0.98$) [5.1b]

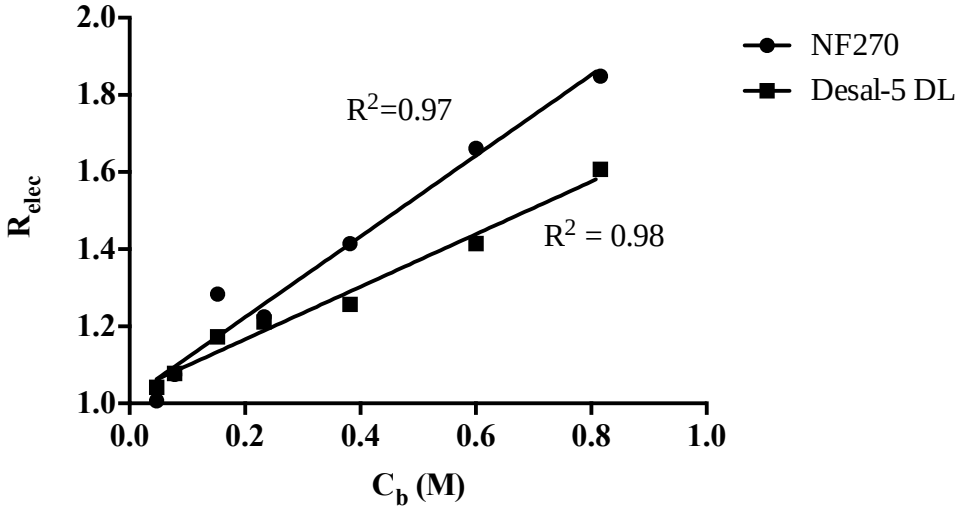

Fig. 5.9 The hydraulic resistance due to charge, R_{elec}, as a function of NaCl feed concentration for the studied membranes.

5.6 Dependence of reflection coefficient and solute permeability on bulk salt concentration

Reflection coefficient (σ) and solute permeability (P_s) were obtained for each NaCl feed concentration via the procedure outlined in Section 3.3 (Chapter 3), with relatively satisfactory regression. Theoretical salt rejections calculated using the estimated σ, P_s, and k were shown previously in Figs 5.6 and Figs. 5.7 (fitted curves) and a good agreement between the experimental and theoretical rejection data was confirmed at all feed concentrations. The values of σ and P_s for different bulk concentrations were reported previously in Table 5.2. The concentration dependence of σ and P_s for the two membranes is shown in Figs. 5.10 and 5.11, respectively. From these figures, it is clearly evident that σ decreases whereas P_s increases with increasing NaCl feed concentration. This trend is reasonable given that σ represents the limiting real rejection at infinitely high volumetric fluxes. Since with increasing C_b, a decrease in the observed and real NaCl rejections was

observed, it is expected that σ will similarly follow a decreasing trend. When feed concentrations increase, the concentration gradient increases as well, and consequently, the diffusive transport of electrolytes (characterized by P_s) across the membrane increase. However, while diffusive transport is proportional to the concentration gradient across the membrane, convection is directly proportional to the ionic concentration inside the membrane [13]. Since 1-σ characterizes the convective transport of the solute, it becomes clear that a decrease in σ with increasing C_b indicates an increase in the convective ion flow.

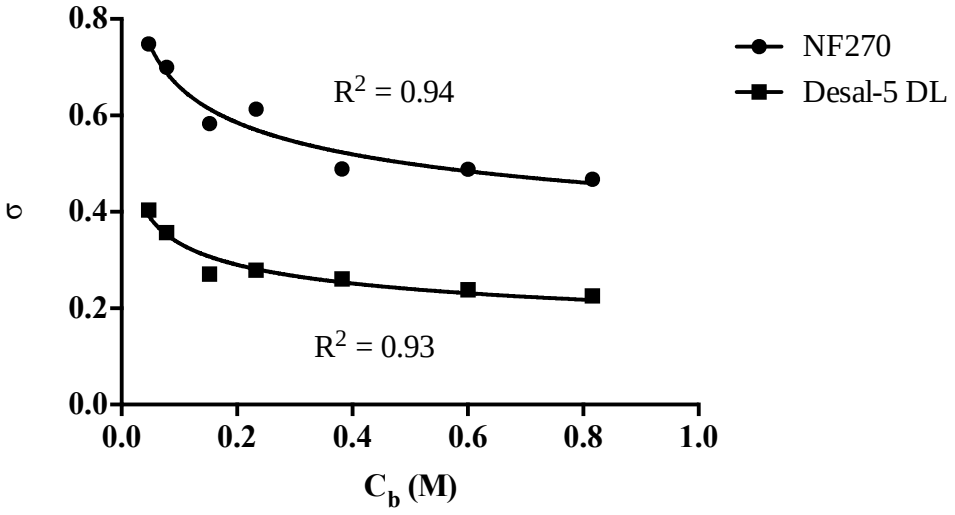

Fig. 5.10 Concentration dependency of σ.

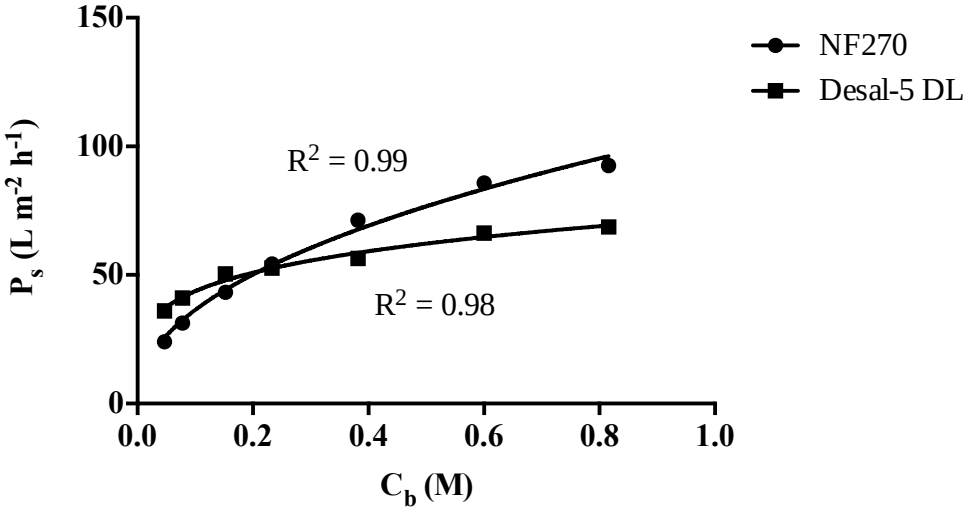

Fig. 5.11 Concentration dependency of P_s.

These findings corroborate those from an earlier study by Wang et al. [14] regarding the NaCl concentration dependency of σ. In spite of the numerous works dealing with SK modelling of NF separation of univalent electrolytes, few conduct an in-depth study of the concentration dependency of the transport parameters. For practical predictive purposes, it becomes necessary to assess how both σ and P_s change with the bulk concentration. Kovacs et al. [15] noted that no definite conclusion could be drawn from existing literature concerning the dependency of these transport parameters on feed concentration. Indeed, while several authors have attained constant parameters [16,17], others have found them to strongly depend on the feed concentration [11,14]. Gupta et al. [17] suggested that inaccurate characterization of concentration polarization (CP) phenomena forced transport parameters to be concentration dependent. They showed it was possible to describe both the R_i and J_v of different salt systems ($MgSO_4$, NaCl, Na_2SO_4, $MgCl_2$) over a range of feed concentrations, feed flow rates, and trans-membrane pressures using constant values of the parameters. However, it is worth pointing out that in their study, the highest NaCl concentration studied was less than 0.2 M and thus their results cannot be reasonably extended to concentrations 1

M or higher. Chaabane et al. [18] studied the transfer mechanism of calcium salts through NF membranes at different feed concentrations; however, relationships between the transport parameters (σ and P_s) and C_b were not addressed. In a study similar to ours, Hilal et al. [11] used the SK model to predict NF270 performance with NaCl solutions up to 25,000 ppm (~0.43 M), a salinity level comparable to that of seawater. Over the studied concentration range (0.09 – 0.43 M), P_s was found to increase linearly with C_b whereas σ remained relatively constant. However, it is worth mentioning that their modelling work did not include the contribution of CP.

A majority of the aforementioned modelling endeavours deal with low salt concentrations, limiting the practical applicability of these research findings since concentrated salt solutions are largely involved in industrial separation processes. Also, few focus on establishing well-defined relations between the transport coefficients and feed concentration in the form of mathematical expressions. Based on experiments performed with 0.1 M NaCl solutions, Koter et al. [19] assumed the following functional relations between transport parameters and the concentration: $\sigma = 1\text{-}b(C/C^*)^n$ and $P_s = a(C/C^*)^m$, where a, b, m, and n are empirical constants and C^* was arbitrarily chosen to be 1 mol/m^3. For their NF experiments with NaCl and NaBr at different feed concentrations (0.0001 – 0.1 M), Bason et al. [8] found the following function best described the concentration dependence of P_s: $P_s = a_1 C^a{}_2 + a_3$, where a_1, a_2, and a_3 are fitted parameters. Based on the data obtained in this study, the following empirical power functions best described the concentration dependency of the transport parameters and may be used to predict their values at higher concentrations:

$$\sigma(\text{NF270}) = 0.4437 C_b^{-0.172} \qquad (R^2 = 0.94) \qquad [5.2a]$$

σ (Desal-5 DL) = $0.2121C_b^{-0.195}$ (R^2 = 0.93) [5.2b]

P_s (NF270) = $108.34C_b^{0.4861}$ (R^2 = 0.99) [5.3a]

P_s (Desal-5 DL) = $72.741C_b^{0.2229}$ (R^2 = 0.98) [5.3b]

It should be mentioned that the choice of the function to fit the concentration dependence of the transport parameters is not critical and other fitting equations are also possible. The above power functions had the highest coefficient of determination (R^2) values and moreover, they resemble the functional relations suggested by Bason et al. [8] and Koter et al. [19].

5.7 The "constrained" fitting approach for estimation of transport parameters

In their recent works, Bason et al. [8,20] have criticized what they termed as the "constant" method of evaluating the dependence of σ and P_s on solute concentration. The underlying assumption of this conventional approach is that σ and P_s vary with concentration yet are constant for each flux-rejection curve, i.e. for a given feed. This requires Eq. (3.13) (Section 3.2.2 of Chapter 3) to be independently fitted to each set of experimentally obtained R_{obs} vs J_v data corresponding to a given feed solution, which then yields the transport coefficients specific to that feed concentration. Once the parameters are acquired for several feeds, a plot of the parameters versus the feed concentration may be constructed to reveal the concentration dependence. However, this widely used simplified approach has several drawbacks: (a) it ignores the fact that salt concentration undergoes a large change across the membrane thickness in each single experiment, (b) it ignores the fact the CP-corrected concentration (C_m) varies with flux within the same flux-rejection curve despite the feed solution being constant, and (c) imposes no restriction on the relation between the σ and P_s

[8]. Concerning the last point, Kedem and Freger [21] and Yaroshchuk [22] emphasized that both transport coefficients, *1- σ* and P_s, should have similar concentration dependence, allowing their ratio, denoted by the parameter A ($A = [1-\sigma]/P_s$), to be relatively concentration-independent. Following this general assumption, they proposed a new phenomenological "variable" approach to determine the coefficients that involves numerical integration of the SK equation with variable coefficients. The discrepancy between the approaches in terms of the obtained values of σ and P_s is shown in Fig. 5.12.

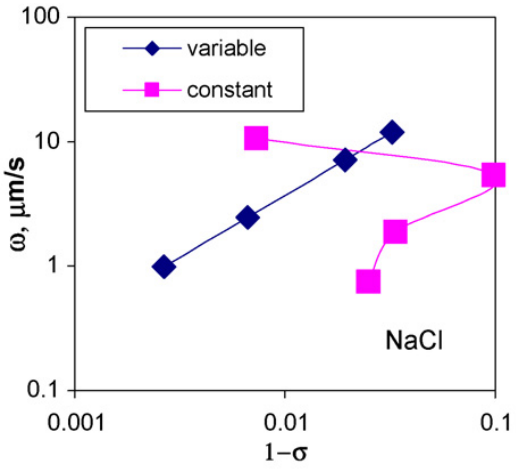

Fig. 5.12 Correlation between the parameters *1- σ* and P_s evaluated via the two different procedures for four different concentrations of NaCl (0.001, 0.01, 0.05, and 0.1 M) [8].

This prior discussion on the so-called "constant" approach was necessary since we have employed this approach in our study for assessing the concentration dependency of σ and P_s (as outlined in Section 3.3 of Chapter 3). However, placing the following constraint on σ in the parameter estimation problem overcomes one of the aforementioned weaknesses of the "constant" approach by taking into account the variation of the CP-correction concentration with flux:

$$\left|\frac{\sigma_{fit}-\sigma_{calc}}{\sigma_{fit}}\right| \leq 0.01 \qquad \text{[Constraint \#2]}$$

where σ_{calc} was calculated by the following equation (Sections 3.2.3 and 3.3)

$$\sigma_{calc} = \frac{\sum_{i=1}^{n}\left[\frac{\Delta P_i(1-\frac{C_{p,i}}{C_{m,i}})}{(\Delta P_i-\Delta\pi_i\frac{C_{p,i}}{C_{m,i}})}\right]}{n} \qquad [3.33]$$

Commonly, due to physical limitations, σ is constrained between an upper bound of 1 and a lower bound of 0 ($0 < \sigma < 1$); however, the additional constraint imposed in this study ensures that changes in σ with applied pressure i.e. the flux is accounted for. As evident from Eq. (3.33), σ_{calc} is essentially the arithmetic average over the data set of the σ values calculated at different applied pressures for a given feed concentration. The constraint forces the estimated/fitted σ to be within a specified tolerance of σ_{calc}, thereby placing a restriction on the acceptable values of the estimated σ. The parameter estimation algorithm implemented in MATLAB ensures that the constraint is satisfied to within the specified value of the tolerance i.e. 0.01. It should be highlighted that this additional constraint (Eq. 3.33) is not an arbitrary one; instead, it is based on the analytical expression for σ (see Section 3.2.3 for complete derivation), which we developed by means of an alternative interpretation of the physical meaning of the reflection coefficient.

Besides accounting for the variation of σ with flux, there are several other advantages offered by our proposed method of estimating the transport parameters and their concentration dependency. Firstly, the benefit of our proposed constrained method can be appreciated when comparing the parameter values obtained via our approach with the corresponding values estimated via the non-constrained method, especially at low NaCl concentrations (Table 5.4). At feed concentrations of 0.08 and 0.15 M, it is surprising that for

Desal-5 DL with very low R_{obs} (~ 14 - 36%), σ estimated via the non-constrained is so contradictorily high (~ 1.000). Moreover, it will be shown in the following section (Section 5.8) that for Desal-5 DL, concentration polarization (CP) was negligible over this pressure and concentration range and the real or intrinsic retention (*R)* should be fairly close to the values of R_{obs}, which is not the case when the non-constrained method is used. It should be mentioned here that despite the unreasonable values, transport parameters obtained using the non-constrained method resulted in a slightly better fit of the experimental J_v - R_{obs} data at low C_b. However, this implies that multiple sets of transport parameters may succeed in fitting any experimental data and caution must be exercised when selecting a set of parameters by taking prior process knowledge and common sense into consideration. In fact, our proposed approach considerably reduces this ambiguity when searching for a set of coefficients that fit the experimental data, ensuring that that the regressed value of σ is the mean value over the studied pressure range.

Table 5.4 Comparison of the reflection coefficient estimation using the conventional approach and our proposed constrained approach

Conc. (M)	σ (NF270)		σ (Desal-5 DL)	
	Conventional approach	"Constrained" approach	Conventional approach	"Constrained" approach
0.05	0.999	0.748	0.583	0.404
0.08	0.998	0.700	1.000	0.357
0.15	0.996	0.583	1.000	0.271
0.23	0.625	0.613	0.281	0.279

An unexpected outcome of the constrained method can be seen in Fig 5.13 where the P_s values are plotted against 1-σ. The observed linear trend (R^2 > 0.90) is similar to one attained by Bason et al. [8] as shown previously in Fig. 5.12. This indicates that the ratio of the two parameters ($A = [1-\sigma]/P_s$) is indeed relatively constant over the studied concentration

range, as assumed by Bason et al. [8]. However, this linearity between the parameters was not anticipated in our study since unlike the work referred to here, our approach was not derived based on a constant *A* assumption and our studied NaCl concentrations were significantly higher (by a factor of 8). Interestingly, this not only justifies our implementation of the alternative expression of σ (i.e. the second constraint) but also, confirms the results obtained by other works.

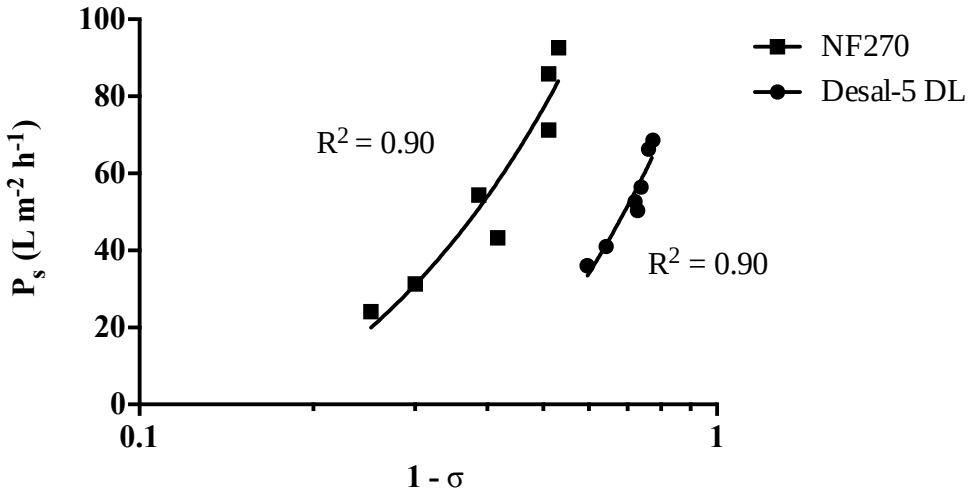

Fig. 5.13 Relation between the parameters *1-* σ and P_s evaluated via the constrained method of parameter estimation.

In summary, our constrained nonlinear parameter estimation procedure has several merits over the traditional approach: (a) takes into account the variation of σ with applied pressure i.e. flux by essentially searching for the mean value of σ over the pressure range, (b) produces a unique set of values for the transport coefficients (σ, P_s, and k) which are reasonable, (c) confirms a linear correlation between 1-σ and P_s as hypothesized previously by other researchers. Our mathematically simple yet practical constrained fitting procedure

for transport parameter estimation can be easily applied at higher NaCl concentrations, and should be a very useful contribution originating from this study.

5.8 Dependence of mass transfer coefficient on feed concentration

Given that the real or intrinsic rejection, *R*, depends on the solute concentration near the membrane surface (C_m), it becomes important to incorporate the concentration polarization (CP) phenomena into a membrane transport model by determining the mass transfer coefficient (*k*). Moreover, since resistance due to CP directly influences osmotic pressure effects and consequently, the pressure driving force across the membrane and the resultant volumetric flux; reliable prediction of the permeate flux demands accurate estimation of *k* values. However, currently, no reliable direct method exists that allows accurate prediction of *k* and hence, CP [23].

Using the combined SK/film theory (CFSK) approach outlined in Section 3.3, the mass transfer coefficient was determined for both membranes alongside σ and P_s. The *k* values reported in this study (Fig 5.14) are much higher than those commonly found in literature, which are in the order of 10^2 L m^{-2} h^{-1}. This is especially evident in the case of the Desal-5 DL membrane. The remarkably high *k* values for the Desal-5 DL membrane indicate negligible or a very weak CP over the concentration range studied i.e. C_m was essentially equal to C_b, and as a result, the intrinsic retention (*R*) was equal to the observed retention (R_{obs}). It should be noted that the in the case of Desal-5 DL membrane, the *k* values were found to be highly sensitive to the initial values of the transport parameters supplied for the fitting procedure.

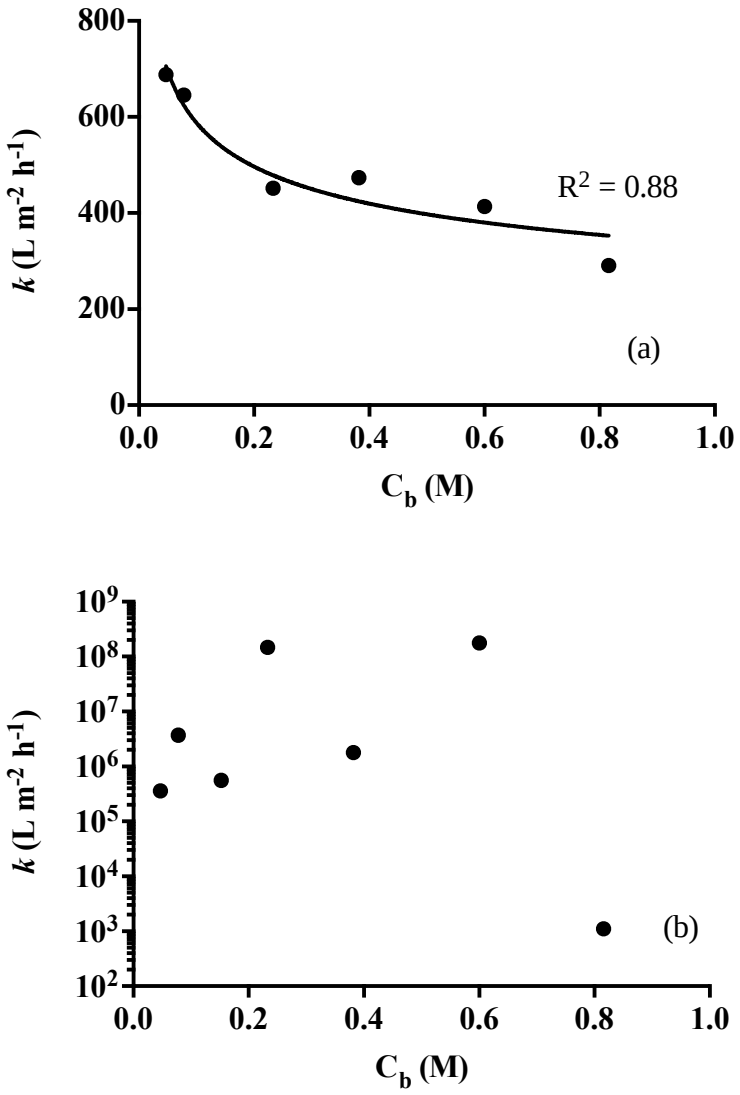

Fig. 5.14 Mass transfer coefficient as a function of bulk NaCl concentration for: a. NF270; b. Desal-5 DL.

Several theories are offered and discussed in this section to elucidate the discrepancies between the literature and our *k* values. Early modelling efforts by Murthy and Gupta [24] on RO membranes adopted the combined SK/film theory (CFSK) approach used in this study and reported similarly high *k* values. For NaCl-water and ethylene glycol-water systems, they compared two membrane transport models for mass transfer coefficient estimation, and found the CFSK model yielded *k* values nearly 5 to 15 times higher. This

considerable difference in k values was attributed to the presence of a reflection coefficient in the CFSK model, signifying that the mass transfer coefficient determination depends on the choice of the transport model used in the analysis. Moreover, they recommended the use of the CFSK approach for NF membranes over other existing models since for these membranes, σ is far from unity and cannot be ignored.

Another possible explanation lies in the alternative expression of the mass transfer coefficient, $k = D/\delta$, where D is the solute diffusivity and δ is the CP boundary layer thickness. Since the CP layer is formed by the accumulation of the retained solutes, it is fairly reasonable to assume that the k value will depend on the membrane salt retention characteristics. Koter et al. [19] found a strong relation between the thickness of the polarization layer (δ) and the observed retention, R_{obs}: the higher the R_{obs}, the thicker δ. Accordingly, the low retention characteristics observed for Desal-5 DL over our studied NaCl concentration range (R_{obs} ~ 9 - 40%), allows limited solute accumulation near the membrane surface and consequently, a thinner δ and a higher k value. Moreover, Koter et al. [19] concluded that generalized correlations based on heat transfer processes, although widely employed by modelling studies [7, 25], are unsuitable for the estimation of k as they do not take membrane properties into account. These ready Sherwood correlations consider only the solute diffusivity, experimental system geometry, and cross-flow velocity, disregarding the impact of individual membrane characteristics on k estimation. Therefore, it becomes doubtful whether the comparisons between our k values and the literature values are justified in the first place.

Although these explanations can sufficiently justify the high k values obtained in this study, their accuracy still remains questionable, especially for Desal-5 DL. Moreover, for

this membrane a clear trend between k and the feed concentration, C_b, is not evident, making the prediction of k values at higher NaCl concentrations quite difficult (Fig. 5.14b). Also, it is known that the mass transfer coefficient is a function of the feed flow rate, with higher feed flow rates greatly increasing the k value. In our case, all experiments were conducted under the variable applied pressure and constant feed flow rate conditions, however, there were slight fluctuations in the feed flow rate with the change in pressure. The presence of these variations may also result in decreased accuracy of k determination. From Fig 5.14a, for NF270, the k values appear to decrease in a nonlinear fashion with bulk concentration. A power function was found to best fit the experimental data empirically and maybe used to predict the mass transfer coefficient at higher C_b for NF270:

$$k = 325.37 C_b^{-0.259} \qquad [5.4]$$

Similarly for NF of concentrated glucose solutions, Wang et al. [26] found k to decrease with increasing C_b and determined a power relation best fit their experimental data.

A noteworthy point is the dependence of k on the membrane itself. Our work clearly show that despite the module configuration and operating conditions being the same, the estimated k values differ significantly between the two membranes and thus, membrane properties indeed play an important role in determination of transport parameter values and should not be neglected. Clearly, there is a need for CP-based models that take these factors into account, allowing for a more reliable estimation of k.

5.9 Verification of MSK model at high NaCl concentrations.

In order to validate the developed modified SK (MSK) model and the above correlations for the transport parameters (Eqs. 5.1-5.4), the salt rejection and volumetric flux of NF270 were predicted for the highest three NaCl concentrations (1.11, 1.53, and 1.96 M)

via the procedure outlined in Section 3.4 of Chapter 3. The empirical correlations were used to determine σ, P_s, k, and R_{elec} for higher C_b. Although $L_{p.w}$ values prior to each experiment deviated to some extent from the initial $L_{p,w}$ of the fresh, clean membrane; the original $L_{p,w}$ values corrected for viscosity were used in the model predictions. After characterizing the membrane in terms of these parameters, the set of nonlinear equations were solved for C_m, C_p, J_v, and R_{obs} using the numerical method (Section 3.4), which involves iterating on the volumetric flux as it appears on both sides of the equation. An arbitrary stop criterion of < 0.001 was assumed for the difference between the initial guess and new values of J_v. To the best of our knowledge, this approach based on the combined SK/film theory has not been used for simultaneous prediction of the salt rejection and permeate flux in the open literature. Based on the large number of modelling papers reviewed, Hu et al. [27] determined the volume flux and rejection for hyperfiltration of concentrated NaCl and $MgCl_2$ solutions employing a numerical calculation similar to ours. The transport parameters (σ, and P_s) employed in their model calculations were those obtained from fitting of the experimental data. On the contrary, to avoid too much dependence on the experimental fitting, data sets for the concentration range 0.05 to 0.82 M were used for parameter determination whereas data sets corresponding to concentrations higher than 0.82 M were used for model validation.

Figs. 5.15 and 5.16 depict the volumetric flux and observed rejection predictions of NF270, respectively. As clear from the figures, incorporation of R_{elec} significantly improves the flux predictions. Reasonably good agreement is also obtained between the experimental and predicted R_{obs} values. For all cases concerned, an average percentage deviation of less than 12% between the predicted and experimental NaCl rejection was observed.

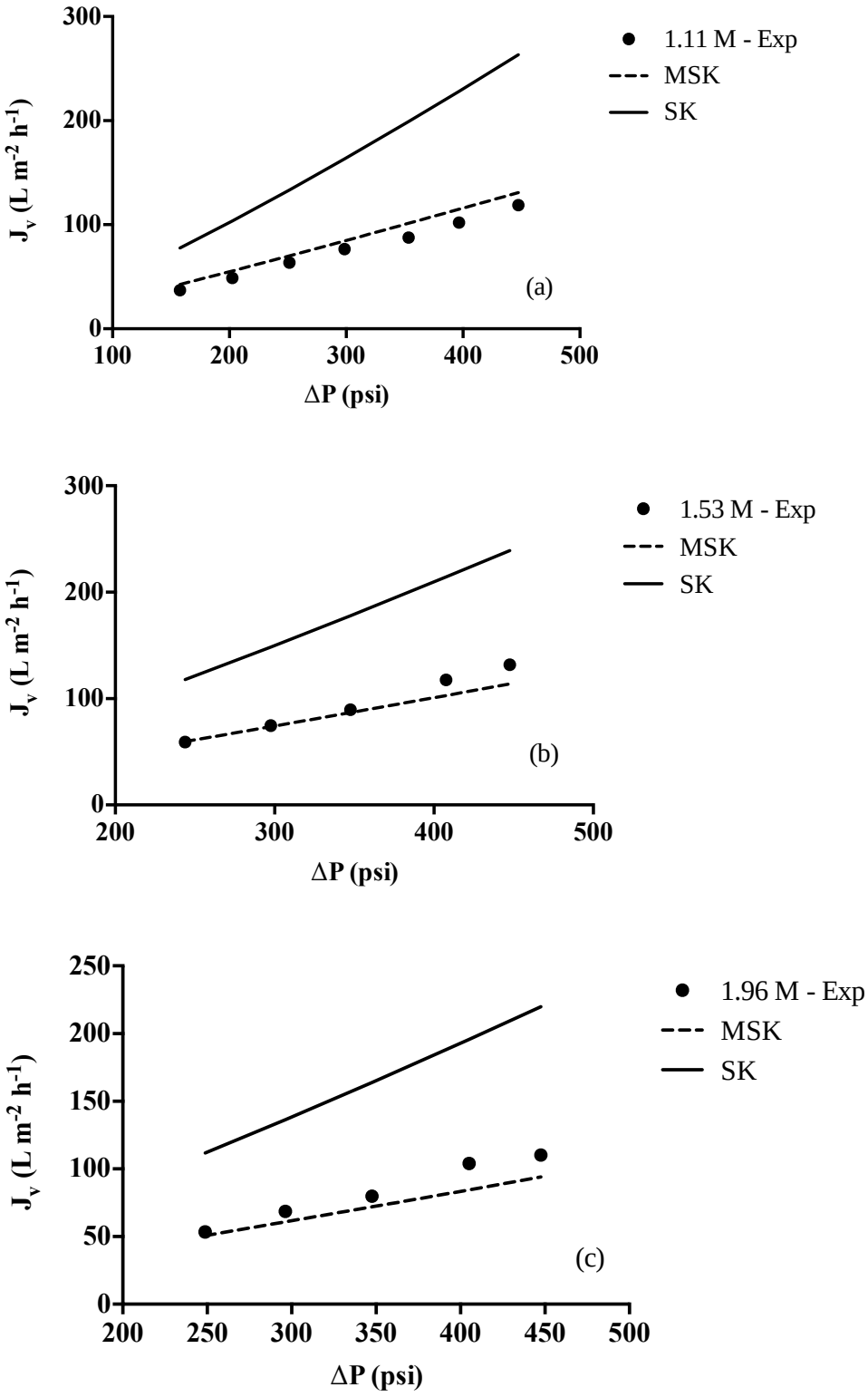

Fig. 5.15 Comparison between our model predictions and experimental fluxes for NF270 at high NaCl bulk concentrations: a. 1.11 M; b. 1.53 M; c. 1.96 M.

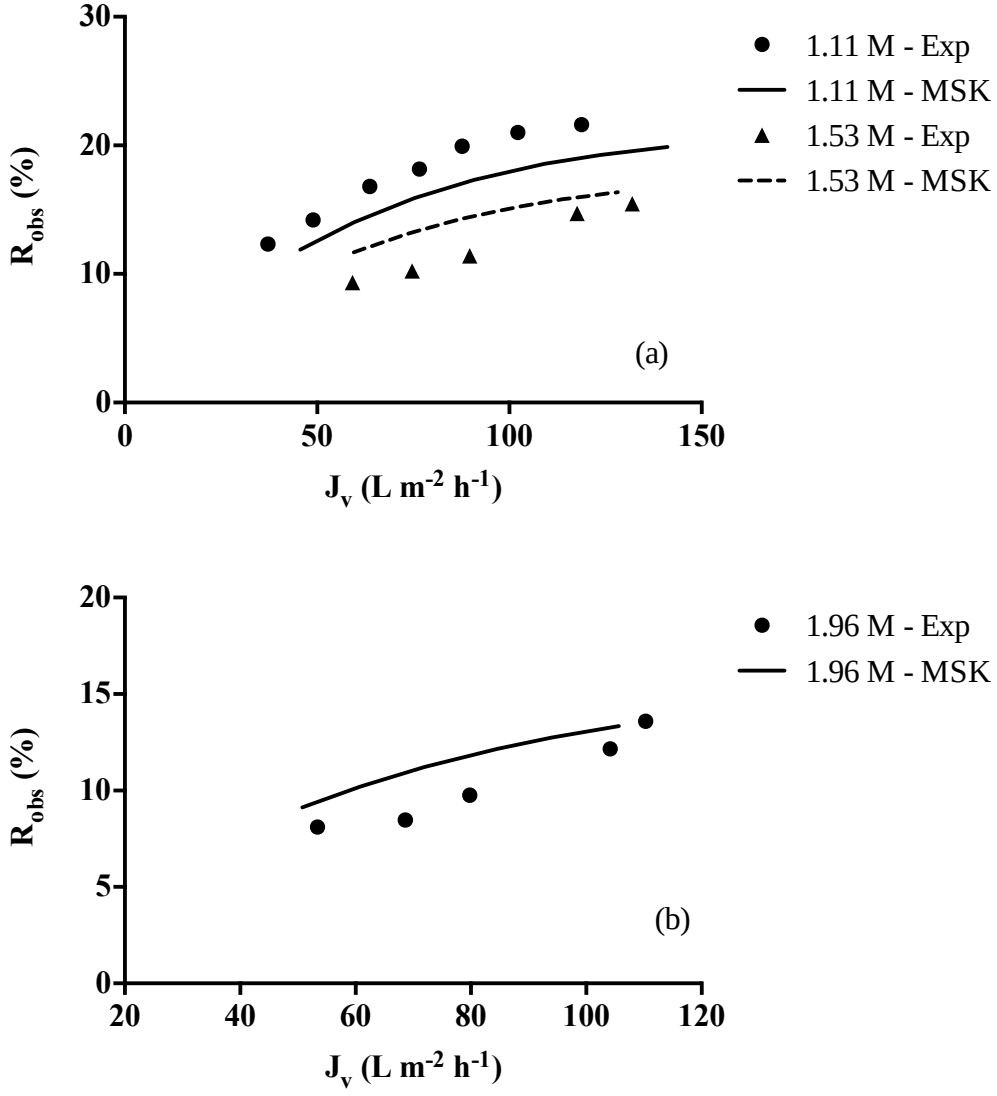

Fig. 5.16 Comparison between predictions and experimental rejections for NF270 at high NaCl bulk concentrations: a. 1.11 and 1.53 M; b. 1.96 M.

It is clear from the above figures that our model allows for reasonably good predictions of both volumetric flux and observed rejections simultaneously for higher NaCl concentrations not used in model fitting and transport parameter determination. This justifies the applicability of the empirical correlations obtained for σ, P_s, k, and R_{elec} at higher C_b and moreover, establishes the need for R_{elec} in flux predictions.

References

1. J. Luo, Y. Wan, Effect of highly concentrated salt on retention of organic solutes by nanofiltration polymeric membranes, J.Membr.Sci. 372 (2011) 145-153.
2. S. Gomes, S.A. Cavaco, M.J. Quina, L.M. Gando-Ferreira, Nanofiltration process for separating Cr(III) from acid solutions: Experimental and modelling analysis, Desalination 254 (2010) 80-89.
3. M. Mänttäri, T. Pekuri and M. Nyström, NF270, a new membrane having promising characteristics and being suitable for treatment of dilute effluents from the paper industry, Journal of Membrane Science 242 (2004) 107–116.
4. G. Artug and J. Hapke, Characterization of nanofiltration membranes by their morphology, charge and filtration performace parameters, Desalination 200 (2006) 178-180.
5. K. Boussu, Y. Zhang, J. Cocquyt, P. Van der Meeren, A. Volodin, C. Van Haesendonck, et al., Characterization of polymeric nanofiltration membranes for systematic analysis of membrane performance, J.Membr.Sci. 278 (2006) 418-427.
6. G. Bargeman, J.M. Vollenbroek, J. Straatsma, C.G.P.H. Schroën, R.M. Boom, Nanofiltration of multi-component feeds. Interactions between neutral and charged components and their effect on retention, J.Membr.Sci. 247 (2005) 11-20.
7. C. Rodrigues, A.I. Cavaco Morão, M.N. de Pinho, V. Geraldes, On the prediction of permeate flux for nanofiltration of concentrated aqueous solutions with thin-film composite polyamide membranes, J.Membr.Sci. 346 (2010) 1-7.
8. S. Bason, O. Kedem, V. Freger, Determination of concentration-dependent transport coefficients in nanofiltration: Experimental evaluation of coefficients, J.Membr.Sci. 326 (2009) 197-204.
9. J. Tanninen, M. Mänttäri, M. Nyström, Effect of salt mixture concentration on fractionation with NF membranes, J.Membr.Sci. 283 (2006) 57-64.
10. C. Mazzoni, S. Bandini, The role of the electrolyte on polyamide NF membranes performances: experimental analysis with NaCl and CaCl2 solutions, Desalination 200 (2006) 135-137.

11. N. Hilal, H. Al-Zoubi, A.W. Mohammad and N.A. Darwish, Nanofiltration of highly concentrated salt solutions up to seawater salinity, Desalination 184 (2005) 315–326.
12. K. Boussu, J. De Baerdemaeker, C. Dauwe, M. Weber, K.G. Lynn, D. Depla, et al., Physico-chemical characterization of nanofiltration membranes, ChemPhysChem. 8 (2007) 370-379.
13. A. Szymczyk and P. Fievet, Investigating transport properties of nanofiltration membranes by means of a steric, electric and dielectric exclusion model, Journal of Membrane Science 252 (2005) 77–88.
14. X.-L. Wang, T. Tsuru, S. Kimura, Evaluation of pore structure and electrical properties of nanofiltration membranes, Journal of Chemical Engineering of Japan 28 (1995) 186-192.
15. Z. Kovacs, M. Discacciati and W. Samhaber, Modeling of amino acid nanofiltration by irreversible thermodynamics, Journal of membrane science 332 (2009) 38-49.
16. K.S. Spiegler, O. Kedem, Thermodynamics of hyperfiltration (reverse osmosis): criteria for efficient membranes, Desalination 1 (1966) 311-326.
17. V. Gupta, S.T.-Hwang, W.B. Krantz and A.R. Greenberg, Characterization of nanofiltration and reverse osmosis membrane performance for aqueous and salt solutions using irreversible thermodynamics, Desalination 208 (2007) 1-18.
18. T. Chaabane, S. Taha, N. Ameraoui, G. Dorange, R. Maachi, Contribution to the comprehension of the calcium ions transfer phenomena through a nanofiltration spiral wound membrane, Desalination 167 (2004) 361-368.
19. S. Koter, Determination of the parameters of the Spiegler–Kedem– Katchalsky model for nanofiltration of single electrolyte solutions, Desalination 198 (2006) 335-345.
20. S. Bason, Y. Kaufman and V. Freger, Analysis of ion transport in nanofiltration using phenomenological coefficients and structural characteristics, The Journal of Physical Chemistry B 114 (2010) 3510-3517.
21. O. Kedem, V. Freger, Determination of concentration-dependent transport coefficients in nanofiltration: Defining an optimal set of coefficients, Journal of Membrane Science 310 (2008) 586-593.
22. A. E. Yaroshchuk, Recent progress in the transport characterisation of nanofiltration membranes, Desalination 149 (2002) 423-428.

23. E. Sivertsen, Membrane separation of anions in concentrated electrolytes, Norwegian University of Science and Technology, 2001. PhD Thesis.
24. Z.V.P. Murthy and S.K. Gupta, Estimation of mass transfer coefficient using a combined nonlinear membrane transport and film theory model, Desalination 109 (1997) 39-49.
25. V. Silva, V. Geraldes, A.M. Brites Alves, L. Palacio, P. Prádanos, A. Hernández, Multi-ionic nanofiltration of highly concentrated salt mixtures in the seawater range, Desalination 277 (2011) 29-39.
26. R. Wang, Y. Li, J. Wang, G. You, C. Cai, B.H. Chen, Modeling the permeate flux and rejection of nanofiltration membrane separation with high concentration uncharged aqueous solutions, Desalination 299 (2012) 44-49.
27. Z.-A. Hu, H-.Y. Wu, J.-Z. Gao, Calculation of osmotic pressure difference across membranes in hyperfiltration, Desalination 121 (1999) 131-137.
28. L.D. Nghiem, Removal of emerging trace organic contaminants by nanofiltration and reverse osmosis, University of Wollongong, 2005. PhD Thesis.
29. W. R. Bowen and A. W. Mohammad, Diafiltration by nanofiltration: prediction and optimization, AIChE Journal, 44 (1998) 1799–1812.
30. K. Hu and J. M. Dickson, Nanofiltration membrane performance on fluoride removal from water, Journal of Membrane Science 279 (2006) 529–538.
31. J. Luo, L. Ding, X. Chen, Y. Wan, Desalination of soy sauce by nanofiltration, Separation and Purification Technology 66 (2009) 429-437.
32. P. Religa, A. Kowalik, P. Gierycz, Effect of membrane properties on chromium(III) recirculation from concentrate salt mixture solution by nanofiltration, Desalination 274 (2011) 164-170.
33. B. Van der Bruggen, M. Manttari and M. Nystrom, Drawbacks of applying nanofiltration and how to avoid them: A review, Separation and Purification Technology 63 (2008) 251-263.

Chapter 6: Physical significance of the electric resistance constant, R_{elec}

In this work, the electric resistance constant, R_{elec}, which is defined as the hydraulic resistance due to electrostatic interactions between the charged NF membrane and co-ions, was introduced to account for the reduction in volumetric flux with feed concentration during NF of NaCl solutions. The intrinsic membrane permeability present in the volumetric flux equation of the classical Spiegler-Kedem model was modified to include an additional correction factor or R_{elec}, which was calculated as a fitting parameter from relevant NF experimental data. For predictive purposes, empirical correlations of R_{elec} as a function of the bulk NaCl concentration were obtained. The data presented in Chapter 5 demonstrated that the inclusion of R_{elec} drastically improved the precision of the prediction of both the permeate flux and salt rejection at high salt concentration. In this chapter, we strive to provide in-depth analysis on the physical meaning of this newly introduced parameter.

6.1 Charge-shielding, the electrical double layer theory

As summarized in Chapter 2, despite the extensive studies of scientists in this field, existing models have largely failed in predicting simultaneously the permeate fluxes and salt rejection of NF processes at high salt concentration. This problem, has been demonstrated in Chapter 5 and has been remedied to a large extent by the MSK model, which introduced an additional constant, R_{elec}**,** to account for the resistance stemming from the electric interactions between the co-ions and the membrane charges, both on the membrane surface and the inside the nanoscale membrane pores. A well-documented experimental observation that cannot be explained by the existing theories is the reduction in salt retention and permeate flux with the increase of salt concentration in feed.

A theory widely quoted for the explanation of the aforementioned observation, i.e., the reduction of both salt rejection and permeate flux with salt concentration in feed, is the electric double layer (EDL) hypothesis. According to EDL, when a charged surface of a solid object is placed into an electrolyte solution, an electrical double layer (EDL) composed of oppositely charged counter-ions forms at the solid-liquid interface. This EDL effectively "screens" or "shields" the net charge on the surface i.e. neutralizes it. For example, if a surface is negatively charged, the concentration of cations in the EDL will be higher than that of the anions. An in-depth discussion of the different models of EDL description (Helmholtz, Gouy-Chapman, Stern) is beyond the scope of this work. For the purposes of our discussion, it is sufficient to know that the electrical potential at the charged surface decays exponentially to the bulk solution value of zero (due to electroneutral conditions) over a characteristic distance given by the so-called Debye length, λ, which corresponds to the thickness of the EDL [1]. The widely adopted Poisson-Boltzmann equation is used to describe the distribution of ions surrounding the solid-water interface under the influence of the electrical field induced by the surface charge [2].

One may argue that the EDL hypothesis can also be applied to account for the reduced resistance of the intrapore charges to co-ions. However, in such a scenario, when a charged nanopore is placed in an electrolyte solution, EDL developed from each pore wall would result in a high concentration of counter-ions inside the nanopore. According to Fig. 6.1 and Table 6.1, the Debye length is an inverse function of the bulk ionic concentration. At high concentrations, the Debye length is much smaller, the potential decays fast and the EDLs are close to the pore walls. Conversely, at low ionic strengths, the thickness of the EDL is larger and the potential does not reach zero in the nanopore.

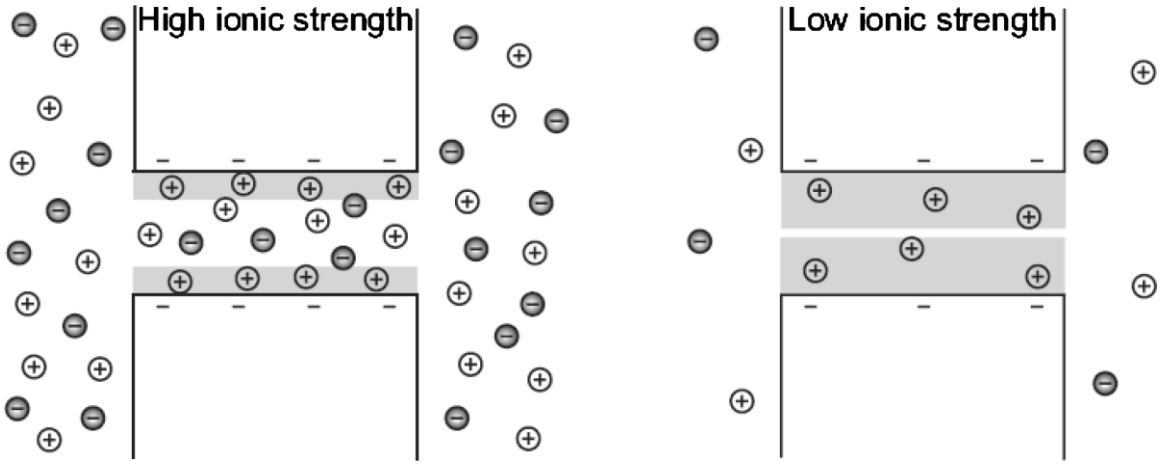

Fig. 6.1 EDL formation at different ionic concentrations in a nanochannel [1].

It is important to realize that this dependency of the Debye length on the ionic concentration is the basis behind most theories in the existing literature explaining the reduction of NaCl retention with increasing salt concentration during NF processes. Boussu et al. [3] explained that the retention of NaCl decreases with increasing concentration because the EDL of the NF membrane becomes thinner and charge no longer plays a significant role in ion exclusion (the electric potential is zero in most of the nanopore allowing co-ions and counter-ions to pass through). Garcia-Aleman and Dickson [4] similarly explained that compression of the EDL with increasing concentration, allows co-ions to penetrate the membrane more easily compared to lower concentrations. Others hypothesized that at high salt concentrations, membrane charge is effectively screened by counter-ions, facilitating the diffusive transport of ions across the membrane.

Table 6.1 EDL thickness (Debye length, λ) for typical NaCl concentrations at 25^{o}C [1]

Concentration (M)	Debye length λ (nm)
1.0	0.3
0.1	1.0
0.01	3.1
0.001	9.6

It should be emphasized, however, the widely-accepted EDL theory as the mechanism for the explanation of the decreasing role of charge as an exclusion mechanism with increasing salt concentration fails to predict both retention and permeate fluxes in NF processes at high salt concentration. The aforementioned works can be largely classified into two groups. For one group, the authors discuss retention only but ignore the variation of permeate flux with salt concentration. The other group of research reported their attempt to model both retention and flux but all come up with significant over-prediction of permeate fluxes except in cases, when the authors treated the hydraulic permeability (L_p) as a variable that depends on salt concentration [5]. Apparently, the EDL theory is flawed at least partially in this case and new mechanisms need to be established to better explain the observed phenomenon.

6.2 The point-size assumption

Several works in the field of nanofluidic devices have stressed the importance of the complex electrostatic interactions between charged nanopores and ions in ion transport and partitioning. According to Cervera et al. [6], atomistic details should be significant as the nanopore radius becomes comparable to the ionic radius. The author noted that hydrated

ionic radius is the more important quantity in aqueous solutions because the small ions move together with a water layer [6]. However, from Table 3.2 (Section 3.2.4), it can be seen that the hydrated ion radii of chloride ions (0.33 nm) is nearly of the same size as the membrane pore radius (0.42 nm). In fact, several authors have noted that ion dehydration is an important barrier to pore transport in NF membranes [7,8]. The fact that ions need to undergo partial dehydration during transport through nanopores makes shielding of the pore charges highly unlikely.

It is important to realize that charges exist both on the external surface of the membrane and inside the nano-dimensional membrane pores. Saliha et al. [9] showed that the assumption considering that the surface charge density inside the nanodimensional pores is the same as that on the external surface is only a rough approximation. Although counter-ions may effectively "screen" the external surface charges at high ion concentrations, given the same-scale sizes of the ions and the membrane pore, complete shielding of the charges inside the nanopores seems highly unlikely. To illustrate this concept, it is worth mentioning that the Poisson-Boltzmann theory predicts unrealistic counter-ion concentrations at the pore surface due to the point-size assumption, which assumes the dimension of the ions to be dimensionless points. On the contrary, Cervera et al. [6] noted that the size of the ions could not be ignored because they occupy a significant fraction of the pore. As noted by Kralchevsky et al. [10], when the finite size of the ions is taken into account, it results in a lower counter-ion concentration near a charged surface and a weaker Debye screening (in comparison with the point-ion model).

6.3 The membrane charge density: surface charges vs. intrapore charges

Also of particular interest is the theory that the membrane charge density (X_d) increases with bulk concentration due to co-ion adsorption. In the case of NaCl filtration, several authors have indicated that chloride adsorption at high feed concentrations leads to increased volumetric charge of the membrane [11-13]. Bruni and Bandini [11] modelled surface charge owing to co-ion (anions in the case of negatively charged membranes) adsorption on the hydrophobic functional groups of the membrane. According to Lefebvre et al. [14], although the magnitude of X_d increases with C_b, the normalized charge density ($\xi = X_d/C_b$) decreases with concentration, resulting in decreased rejection. Hu and Dickinson [15], on the other hand, hypothesized that the effective pore radii of NF membranes should be larger in lower concentration solutions due to decreased effect of adsorption. As such, chloride adsorption at high concentrations should decrease the membrane pore size and consequently, increase the NaCl retention, which is contrary to what is observed during NF experiments.

6.4 Dependency of the electric resistance on salt concentration in feed: reduced permeate flux

As discussed in Chapter 5, the MSK predicts that both the permeate flux and the salt retention in NF would decrease with salt concentration in the feed (i.e., C_b). The reduction of permeate flux could be explained by the increase of R_{elec} with C_b. This can be tentatively explained as follows.

The electric resistance generated by the expelling of co-ions (e.g., anions in our study) by the charges in membrane pores (i.e., negative charges in this study) would serve as resistance to slow down anion diffusion inside the pores. The membrane properties,

including the pore size and intrapore charge density, are constants in a NF, the increase of salt concentration would result in the increase of the concentration of co-ions in membrane pores. In other words, larger portion of the particles (e.g., water molecules, cations, ions, and other molecules) approaching the intraporous charges would be co-ions that would experiencing repelling force from the membrane charge at higher salt concentration. This, in combination with the increase intraporous viscosity, and the steric hindrance of rejected co-ions to water molecules and other particles, would cause the increase of R_{elec} and therefore reduce the overall permeate flux.

6.5 Driving force for salt passage over NF membrane: reduction of salt rejection with increase of salt concentration in feed

As mentioned previously in Chapter 3, the resistance to the diffusion of anions through a membrane pore depends on four factors, i.e., the energy barriers for ion transport through membrane pores during NF of salt solutions depend on the pore size, ion type (charge and size), and membrane surface charge. All these four factors are constants for a given membrane and anion pair. However, the driving force of anions diffusion is the concentration gradient across the membrane, which increases with the salt concentration in the feed. On the other hand, the retention is the ratio of anions retained versus the total anion concentration at the membrane surface, which is given by the following equation if concentration polarization is neglected for simplicity:

$$R = \frac{C_b - C_P}{C_b}$$

An increase in feed brine salt concentration would cause the increase of C_p due to the increased driving force, i.e., the concentration gradient across the membrane. As a result, the

increase of C_b-C_p would be smaller than the increase of C_b as it is balanced by the increase of C_p. Therefore, retention decreases with feed salt concentration.

In this work, it is hypothesized that due to the nanometer scales involved, the electrostatic interactions between the in-pore charges and the co-ions would be significant enough to slow down the anion diffusion across the membrane. With an increase in bulk concentration, a larger number of slow-moving co-ions would decrease the overall movement of ions and water molecules through the membrane pore. This retardation of hydraulic flow across them membrane as a result of nanopore charge is quantified using the R_{elec} parameter. Experimental work in this area appears to validate the existence of this additional hydraulic resistance factor.

6.6 Conclusions

The MSK model, which is in essence the SK model enhanced by the introduction of a new resistance correction factor, the electric resistance constant (R_{elec}), can be used for the prediction of permeate flux and salt rejection of NF at both low and high salt concentrations. The existence of R_{elec} highlights the significance of the resistance imposed to the passage of co-ions through the charge nano-dimensional pores across the membrane, which is amplified by the fact that the radius of co-ions are not significantly (0.1-0.3 nm) smaller than that of the nano-pores (1-2 nm). The introduction of the electric resistance constant, especially the consideration of the interaction of ions inside the membrane pores with intrapore charges, offers reasonable explanations to two widely observed phenomena, i.e., both the permeate flux and salt rejection decrease with the increase of salt concentration in feed.

References

1. R.B. Schoch, J. Han and P. Renaud, Transport phenomena in nanofluidics, Reviews of modern physics 80 (2008) 839-883.
2. J.-H. Tay, J. Liu, D. Delai Sun, Effect of solution physic-chemistry on the charge property of nanofiltration membranes, Water Research 36 (2002) 585-598.
3. K. Boussu, Y. Zhang, J. Cocquyt, P. Van der Meeren, A. Volodin, C. Van Haesendonck, J.A. Martens and B. Van der Bruggen, Characterization of polymeric membranes for systematic analysis of membrane performance, Journal of Membrane Science 278 (2006) 418–427.
4. J. Garcia-Aleman and J. M. Dickson, Mathematical modeling of nanofiltration membranes with mixed electrolyte solutions, Journal of Membrane Science 235 (2004) 1–13.
5. V. Gupta, S.T.-Hwang, W.B. Krantz and A.R. Greenberg, Characterization of nanofiltration and reverse osmosis membrane performance for aqueous and salt solutions using irreversible thermodynamics, Desalination 208 (2007) 1-18.
6. J. Cervera, P. Ramirez, J. A. Manzanares and S. Mafe, Incorporating ionic size in the transport equations for charged nanopores, Microfluid Nanofluid, 9 (2010) 41-53.
7. A.A. Merdaw, A.O. Sharif, G.A.W. Derwish, Water permeability in polymeric membranes, Part II, Desalination 257 (2010) 184-194.
8. L. A. Richards, A.I. Schafer, B.S. Richards and B. Corry, The importance of dehydration in determining ion transport in narrow pores, Small 8 (2012) 1701-1709.
9. B. Saliha, F. Patrick and S. Anthony, Investigating nanofiltration of multi-ionic solutions using the steric, electric, dielectric exclusion model, Chemical Engineering Science 64 (2009) 3789—3798.
10. P.A. Krachevsky, K.D. Danov, E.S. Basheva, Hydration force due to the reduced screening of the electrostatic repulsion in few-nanometer thick films, Current Opinion in Colloid & Interface Science 16 (2011) 517–524.
11. L. Bruni, S. Bandini, The role of the electrolyte on the mechanism of charge formation in polyamide nanofiltration membranes, J.Membr.Sci. 308 (2008) 136-151.

12. A.W. Mohammad, N. Hilal, H. Al-Zoubi and N.A. Darwish, Prediction of permeate fluxes and rejections of highly concentrated salts in nanofiltration membranes, Journal of membrane science 289 (2007) 40-50.
13. S. Gomes, S.A. Cavaco, M.J. Quina, L.M. Gando-Ferreira, Nanofiltration process for separating Cr(III) from acid solutions: Experimental and modelling analysis, Desalination 254 (2010) 80-89.
14. X. Lefebvre, J. Palmeri, P. David, Nanofiltration theory: An analytical approach for single salts, Journal of Physical Chemistry B 108 (2004) 16811-16824.
15. K. Hu and J. M. Dickson, Nanofiltration membrane performance on fluoride removal from water, Journal of Membrane Science 279 (2006) 529–538.

Chapter 7: Conclusions and Recommendations

Separation performance (rejection and flux) of aqueous solutions of sodium chloride was investigated using two different commercial membranes. It was demonstrated that the application of the classical SK model with concentration polarization effects and solution viscosity taken into account, the permeate flux predictions were significantly higher than the experimental observations. A modified SK model (MSK), which is based on the introduction of an additional resistance factor, electric resistance factor (R_{elec}), to the classic SK, was developed and verified. The MSK model allowed for the first time simultaneous simulation of flux and salt rejection in NF at high salt concentration. In summary, the following could be concluded from the results of this study.

1. A MSK model was developed and verified for simultaneous prediction of permeate flux and salt rejection in NF for NaCl solutions;
2. Introduced a new parameter, the electric resistance (R_{elec}), based on our deepened understanding to the mechanisms of salt rejection of NF;
3. Provided a better explanation for the widely observed reduction in permeate flux and salt rejection with increase of salt concentration in feed;
4. A mathematical correlation was developed to describe the reflection coefficient, σ, which provided a better understanding to the physical meaning of this important parameter;
5. A constrained fitting approach was proposed and implemented to eliminate ambiguity in the process of fitting model equations with experimental data in searching for transport parameters of the model.

Many important applications of NF deal with high salt concentration brines. Therefore, the result of this research presents an important step toward the development of a realistic model for design, optimization, and scale-up of laboratory and industrial NF processes. Nevertheless, this study only tested pure NaCl solutions with two commercial membranes. To establish the model as a reliable tool for different systems, the following studies are recommended:

1. Test the MSK model with pure solutions of other electrolytes;
2. Extension of the MSK model to multi-electrolytic brines;
3. Better the understanding of the electric interaction inside the nanoscale membrane pores between ions and membrane charges;
4. Investigate the distribution of membrane charges on membrane surface and pores and its effects on NF flux and rejection;
5. Study the effects of membrane properties (e.g., pore size and charge density) on R_{elec}, rejection, and flux;
6. Study the effects of co-ion properties (e.g., ion radius, charge density) on R_{elec}, rejection, and flux;
7. Study the effects of counter-ion properties (e.g., ion radius, charge density) on R_{elec}, rejection, and flux;
8. Develop application software for simulation, design, optimization, and scale-up of NF processes in industry.